# A Development of Partial Surfaces Ion Balance Analyzer

**Sayan  Plong-ngooluam**

**A Thesis Submitted in Fulfillment of the Requirements for the
Degree of Doctor of Philosophy in Electrical Engineering
Prince of Songkla University
2017**

**A Development of Partial Surfaces Ion Balance Analyzer**

**Sayan Plong-ngooluam**

**A Thesis Submitted in Fulfillment of the Requirements for the
Degree of Doctor of Philosophy in Electrical Engineering
Prince of Songkla University
2017**

**Thesis Title**     A Development of Partial Surfaces Ion Balance Analyzer
**Author**          Mr. Sayan Plong-ngooluam
**Major Program**  Electrical Engineering

_____

| **Major Advisor** | **Examining Committee:** |
|---|---|
| …………………………….. | …………………………....Chairperson |
| (Assoc. Prof. Dr. Nattha Jindapetch) | (Assist. Prof. Dr. Anan Kruesubthaworn) |
| | …………………………....Committee |
| | (Assoc. Prof. Dr. Krerkchai Thongnoo) |
| **Co-advisors** | |
| …………………………….. | …………………………....Committee |
| (Dr. Phairote Wounchoum) | (Assoc. Prof. Dr. Nattha Jindapetch) |
| …………………………….. | …………………………....Committee |
| (Dr. Duangporn Sompongse) | (Dr. Phairote Wounchoum) |
| | …………………………....Committee |
| | (Dr. Warit Wichakool) |

      The Graduate School, Prince of Songkla University, has approved this thesis as fulfillment of the requirements for the Doctor of Philosophy Degree in Electrical Engineering.

…………………………………….
(Assoc. Prof. Dr. Teerapol Srichana)
Dean of Graduate School

This is to certify that the work here submitted is the result of the candidate's own investigations. Due acknowledgement has been made of any assistance received.

…………………………...Signature
(Assoc. Prof. Dr. Nattha Jindapetch)
Major Advisor

…………………………...Signature
(Mr. Sayan Plong-ngooluam)
Candidate

I hereby certify that this work has not been accepted in substance for any degree, and is not being currently submitted in candidature for any degree.

…………………………...Signature
(Mr. Sayan Plong-ngooluam)
Candidate

ชื่อวิทยานิพนธ์     การพัฒนาหน่วยวิเคราะห์ความสมดุลย์ของอิออนบนพื้นผิวย่อย
ผู้เขียน           นายสายัณห์ ปล้องงูเหลือม
สาขาวิชา        ปรัชญาดุษฎีบัณฑิต สาขาวิศวกรรมไฟฟ้า
ปีการศึกษา      2559

# บทคัดย่อ

ในการรักษาความสมดุลย์ของอิออนในสภาพแวดล้อมที่จำเป็นต้องควบคุมไฟฟ้าสถิตอย่างเคร่งครัดเพื่อให้อยู่ในระดับที่ต่ำกว่า 1 โวลต์นั้นต้องวิเคราะห์ด้วยพื้นผิวย่อย มาตรฐานการทดสอบ ANSI/ESD STM3.1-2014 ได้กำหนดค่าความสมดุลย์ของอิออนด้วยค่าของศักย์ไฟฟ้าสถิตบนแผ่นตัวนำแยกโดดรูปสี่เหลี่ยมจัตุรัสขนาด 15 เซนติเมตร×15 เซนติเมตร เรียกว่าจานรับประจุมาตรฐาน ซึ่งเป็นขนาดที่ไม่เหมาะสมกับชิ้นส่วนอิเล็กทรอนิกส์ในปัจจุบันซึ่งมีขนาดเล็กกว่าจานประจุขนาดมาตรฐานนี้อย่างมาก ด้วยเหตุดังกล่าว งานวิจัยนี้จึงมีความมุ่งหมายที่จะทำการพัฒนาหน่วยวิเคราะห์ความสมดุลย์ของอิออนบนพื้นผิวย่อยด้วยเทคนิคการวัดหลาย ๆ แผ่น โดยได้พิจารณารูปร่างและขนาดของจานรับประจุซึ่งสามารถที่จะส่งผลกระทบต่อความเที่ยงตรงในการวัดความสมดุลย์ของอิออนได้ด้วยการวิเคราะห์แบบไฟไนต์เอลิเมนต์ ซึ่งผลการวิเคราะห์นั้นถูกนำไปใช้ในการเลือกแบบจานรับประจุที่เหมาะสมเพื่อที่จะได้ผลลัพธ์ที่มีรายละเอียดเพิ่มขึ้น ผลการวิเคราะห์ได้ชี้ชัดว่าเมื่อจานรับประจุถูกแบ่งย่อยมากขึ้นก็จะให้ผลการวัดที่มีรายละเอียดเพิ่มขึ้น ทั้งนี้แผ่นรับประจุรูปวงกลมสามารถให้ผลที่ยอมรับได้โดยการแบ่งอย่างน้อยที่สุด 9 แผ่น ส่วนแผ่นรับประจุแบบรูปสี่เหลี่ยมนั้นจะให้ผลที่ยอมรับได้โดยการแบ่งอย่างน้อยที่สุด 16 แผ่น งานวิจัยนี้ได้เลือกสร้างจานรับประจุแบบสี่เหลี่ยมที่ถูกแบ่งเป็น 25 แผ่น และใช้วงจรวัดประจุชักนำแบบความต้านทานขาเข้าสูงยิ่งยวดในการวัดศักย์ไฟฟ้าสถิตบนจานรับประจุหลาย ๆ แผ่น หน่วยประมวลผลแบบฝังตัวถูกใช้ในการประมวลผลสัญญาณเชิงอนุมานอย่างพร้อมเพรียงและทำการแสดงผลเชิงกราฟ การประมาณค่าช่วงแบบน้ำหนักและระยะผกผันสามารถช่วยเพิ่มรายละเอียดของผลการวัดแบบหลายจานได้มากขึ้น หน่วยวิเคราะห์ที่ได้ทำการพัฒนาขึ้นนี้มีความเหมาะสมที่จะนำไปใช้ในการวิเคราะห์ความสมดุลย์ของอิออนในพื้นที่ควบคุมไฟฟ้าสถิตที่ต้องรองรับชิ้นงานขนาดเล็ก เช่น วงจรรวม หรือ ชิ้นส่วนหัวอ่านในฮาร์ดดิสก์เป็นต้น

**Thesis Title**       A Development of Partial Surfaces Ion Balance Analyzer

**Author**             Mr. Sayan Plong-ngooluam

**Major Program**      Degree of Doctor of Philosophy in Electrical Engineering

**Academic Year**      2016

# ABSTRACT

A sub-1V ion balance in the tightly ionized environment raises the requirement of the partial surfaces ion balance analysis. According to ANSI/ESD STM3.1-2014, the ion balance is defined by the resultant of voltage on standard charged plate with the floated 15 cm×15 cm square shape conductive exposure surface. The size of this plate does not suit with the present devices which are very much smaller than the standard charged plate. Therefore, this research aims to develop the partial surfaces ion balance analyzer using the multi-plate sensor. The finite element analysis of shape and size of the receiving plates which could affect the precision of ion balance measurement has been done. The results can be used for selecting the suitable plate for improving the measurement resolution. Then, the analysis revealed that the measurement resolution could be proportionally increased with the number of partial segments. Furthermore, the minimum partial segment number of the circular and square shape plates are 9-segment and 16-segment, respectively. Eventually, the proposed analyzer was designed by using the 25-segment square plates with the ultra-high input impedance charge induced meter to measure the electrostatic potential on the multi-plate sensor. The embedded microcontroller processes the multi-channel analogue signals synchronously, then presents the results in a graphical display. The inverse distance weighting interpolation enables the higher resolution results beyond the physically data from the multi-plate sensor. This developed analyzer is suitable for ion balance measurement in the electrostatic controlled areas where the small footprint devices such as an integrated circuit, or the head gimbals assembly of a hard disk drive are placing.

# ACKNOWLEDGEMENT

# CONTENTS

# CONTENTS (CONT.)

# LIST OF TABLES

# LIST OF FIGURES

# LIST OF FIGURES (CONT.)

# Table of Nomenclature

| Symbol | Descriptions | SI Unit | Abbreviation |
|---|---|---|---|
| $CIV$ | Critical Inception Voltage | Volt | V |
| $F$ | Force | newton | N |
| $Q$ | Charge | coulomb | C |
| $r, R$ | Distance | meter | m |
| $\varepsilon_0, \varepsilon_r$ | Dielectric permittivity | farad/meter | F/m |
| $\mathbf{E}$ | Electric field intensity | volt/meter | V/m |
| $\rho_v$ | Volume charge density | coulomb/meter$^3$ | C/m$^3$ |
| $\rho_S$ | Surface charge density | coulomb/meter$^2$ | C/m$^2$ |
| $\rho_L$ | Linear charge density | coulomb/meter | C/m |
| $\psi$ | Electric flux | coulomb | C |
| $D$ | Electric flux density | coulomb/meter$^2$ | C/m$^2$ |
| $V$ | Scalar potential | Volt | V |
| u | Fluid, air velocity | meter/second | m/s |
| v$_d$ | Electron drift velocity | meter/second | m/s |
| $\rho_{air}$ | Air density | kilogram/merter$^3$ | kg/m$^3$ |
| $\rho_{ion}$ | Space charge density | coulomb/meter$^3$ | C/m$^3$ |
| $P$ | Static air pressure | pascal | Pa |
| $\mu_{air}$ | Air dynamic viscosity | pascal-second | Pa·s |
| $D_p, D_n$ | Positive, negative, ion diffusion coefficient | meter$^2$/second | m$^2$/s |
| $\mu_E, \mu_p, \mu_n$ | Ion, positive ion, negative mobility | meter$^2$/volt-second | m$^2$/V·s |
| $I, i$ | Electric current, Ion current | Ampere | A |
| $J$ | Electric current density | ampere/meter$^2$ | A/m$^2$ |
| $\sigma$ | Conductivity | mho/meter | ʊ/m |

# List of Published Papers and Proceedings

1. S. Plong-ngooluam, N. Jindapetch, P. Wounchoum and D. Sompongse, "3-D Computational Simulations of Electrostatic Potential in Partial Surfaces towards the Precision of Ion Balance Analysis," *Applied Mechanics and Materials*, vol. 781, pp.308-311, April, 2015.

2. S. Plong-ngooluam, N. Jindapetch, P. Wounchoum and D. Sompongse, "Partial Measurement of Planar Surface Ion Balance Analysis," *Pertanika Journal of Science and Technology*, to be published.

3. S. Plong-ngooluam, N. Jindapetch, P. Wounchoum and D. Sompongse, "A Feasibility Study of Ion Balance Measurement by Partial Surfaces," *Procedia Computer Science*, vol. 86, pp. 164-167, 2016.

4. Plong-ngooluam, N. Jindapetch, P. Wounchoum and D. Sompongse, "A Finite Element Analysis of Multiple Ion Receiving Plates for Ionizer Balance Monitoring," *J. Electrostatics,* vol. 86, pp. 50-58, 2017.

5. S. Plong-ngooluam, N. Jindapetch, P. Wounchoum and D. Sompongse, "A Proof-of-concept Study Demonstrating a Multi-Plate Ion Balance Analyzer," *J. Sensors and Actuators A: Physical,* to be published.

# Permission from the Publishers

## Paper A1 Permission

Copyright
Clearance
Center

**MONOGRAPHIC SERIES**

| | | | |
|---|---|---|---|
| **ISSN:** | 1660-9336 | **Language:** | English |
| **Publication year(s):** | 2004 – present | **Country of publication:** | Switzerland |
| **Author/Editor:** | Scitec Publications | | |
| **Publisher**: | Trans Tech Publications | | |
| **Rightsholder**: | TRANS TECH PUBLICATIONS, LTD | | |

## Academic

**Photocopy or share content electronically**

> **LICENSE COVERAGE**
>
> **Annual Copyright License for Academic Institutions**
>
> This permission type is covered. The Annual Copyright License authorizes the licensee's faculty, staff, students, and other authorized users to distribute print and electronic copies of copyrighted content within your institution through:
>
> - Print or electronic coursepacks
> - Classroom handouts
> - Electronic reserves
> - Institution Intranets
> - Course/Learning Management systems CMS/LMS)
> - CD-ROM/DVD
> - Other internal academic uses

The description above is provided for summary purposes only. Please refer to your institution's Annual Copyright License for the complete terms and conditions and scope of coverage of the license.

Covered by CCC Annual License – Academic

## Paper A2 Permission

**PART I:** *Publishing Agreement—* *(to be completed by the Main or **Corresponding** Author)*

| | |
|---|---|
| **PUBLISHER:** | **UPM PRESS** |
| **PUBLICATION:** | **Pertanika Journal of Science and Technology** |
| **MANUSCRIPT TITLE:** | Partial measurement of planar surface ion balance analysis |
| **AGREEMENT DATE:** | 16/07/2016 *(in dd/mm/yyyy format or as per your PC's settings)* |

**AUTHOR(S) PARTICULARS:** *Name(s) & contact details [address, telephone number, email address] of all Author(s):*

**AUTHOR 1:** *(Name in full as in IC/Passport)* — **I/C / PASSPORT NO.**

**SAYAN PLONG-NGOOLUAM** — AA6392307

CURRENT MAILING ADDRESS:

400/347 Moo 8, Wangthongthani Village, Kookote, Lamlookka, Pathumthani, 12130 ,Thailand.

EMAIL(S): — TEL: *(with country/area IDD codes)*

Primary: Sayan.Plong-ngoolaum@wdc.com — Office Tel: ( 66 ) - 35,278,772

Alternate: sayanplo@hotmail.com — Mobile: ( 66 ) - 875,233,406

**AUTHOR 2:** *(Name in full as in IC/Passport)* — **I/C / PASSPORT NO.**

**NATTHA JINDAPETCH** — AA1439651

CURRENT MAILING ADDRESS:

Department of Electrical Engineering, Faculty of Engineering, Prince of Songkla University, Hat Yai, Songkhla, 90112, Thailand.

EMAIL(S): — TEL: *(with country/area IDD codes)*

Primary: Nattha.s@psu.ac.th — Office Tel: ( 66 ) - 74,287,045

Alternate: — Mobile: ( 66 ) - 869,605,394

**AUTHOR 3:** *(Name in full as in IC/Passport)* — **I/C / PASSPORT NO.**

**Phairote Wounchoum** —

CURRENT MAILING ADDRESS:

Department of Electrical Engineering, Faculty of Engineering, Prince of Songkla University, Hat Yai, Songkhla, 90112, Thailand.

EMAIL(S): — TEL: *(with country/area IDD codes)*

Primary: Phairote.w@psu.ac.th — Office Tel: ( 66 ) - 74,287,045

Alternate: — Mobile: ( 66 ) - 865,088,185

**AUTHOR 4:** *(Name in full as in IC/Passport)* — **I/C / PASSPORT NO.**

**Duangporn Sompongse** — AA5567937

CURRENT MAILING ADDRESS:

21/28 Ladprao 8, Chompol, Chatuchak, Bangkok,10900, Thailand.

EMAIL(S): — TEL: *(with country/area IDD codes)*

Primary: Duangporn.Sompongse@wdc.com — Office Tel: ( 66 ) - 35,278,760

Alternate: — Mobile: ( 66 ) - 818,485,719

**NOTE**: Use next page if more than four.

**THIS PUBLISHING AGREEMENT** ("Agreement") is entered into by and between Universiti Putra Malaysia ("UPM Press") and the Author(s) specified above ("Author(s)") as of the Contract Date specified above.

**WHEREAS**, UPM Press is in the business of publishing journals and wishes to procure a licence to publish the Author's Manuscript,

**WHEREAS**, the Author(s) wish(es) to publish the Author(s) original work ("Manuscript") in the **Pertanika Journal of Tropical Agricultural Science** (JTAS),

**NOW, THEREFORE**, in light of the premises and the mutual promises contained herein, the receipt and sufficiency of which are hereby acknowledged, the parties agree as follows:

## Section 1: *Licence to Publish*

**1.      LICENCE TO PUBLISH**
The Author(s) hereby grant(s) to **UPM Press** an exclusive, royalty-free, worldwide licence to:

1.1.      publish, reproduce, store, distribute, transmit and communicate to the public, the Manuscript and any supplemental material in whole or in part, in print and/or digital form, whether or not in combination with the works of others, under The Copyright Act 1987 (see http://www.agc.gov.my/Akta/Vol.%207/Act%20332.pdf );

1.2.      create adaptations, summaries or extracts of the Manuscript and any supplemental material or other derivative works based on the Manuscript and any supplemental material and exercise all of the rights in such adaptations, summaries, extracts and derivative works;

1.3.      include the Manuscript and any supplemental material, in whole or in part, in a computerised database and to make this database available to third parties;

1.4.      include the Manuscript and any supplemental material, in whole or in part, in a reader or compilation; and

1.5.      rent or lend the Manuscript and any supplemental material to third parties.

## Section 2: *Copyright Ownership*

**2.      COPYRIGHT OWNERSHIP**

2.1.      Subject to the licence grant in 1 above, the Author(s) shall retain all copyright rights held by the Author in the Manuscript.

2.2.      This Agreement shall have no bearing on the moral rights of the Author(s) in the Manuscript, i.e. the right to be identified as the author and the right to object to derogatory treatment of the Manuscript.

2.3.      Notwithstanding the copyright ownership set out in this clause, the Parties agree that third parties shall attribute the Pertanika Journal of Tropical Agricultural Science when reproducing or otherwise using the Manuscript.

## Section 3: *Representations and Warranties*

**3.      REPRESENTATIONS AND WARRANTIES**

3.1      The Author(s) represent(s) and warrant(s) that:

3.1.1      The Manuscript is original and has not been published before in its current or a substantially similar form in another publication, i.e. the publication in the Pertanika Journal of Tropical Agricultural Science shall be the first publication of the Manuscript. For the avoidance of doubt, theses and manuscripts that have been presented with only abstracts at conference(s) do not qualify as "another publication";

3.1.2      The tables, figures and images have not been previously published or adapted from previous publication without written permission from the original source unless a written permission has been obtained and is submitted to Pertanika Journal of Tropical Agricultural Science;

3.1.3      The Manuscript is not under consideration for publication by another Publisher;

3.1.4      The Manuscript does not contain any unlawful statements or content and does not infringe any existing third party copyright, moral right or other intellectual property rights;

3.1.5      The Manuscript does not contain any defamatory material, is not in violation of any rights of privacy or any other rights of third persons, and does not violate any existing common law or statutory copyrights.

3.1.6      The Author(s) possess(es) all rights in the Manuscript necessary to grant the license set out in clause 1;

3.1.7      Where the Manuscripts reports on research involving human or non-human vertebrates, the research meets the highest reporting standards and has been approved by an institutional ethics committee;

3.1.8      "Proof of consent" has been obtained for studies of named organisations and people;

3.1.9      All Author(s) have received a final version of the Manuscript, have reviewed its content and agree(s) to its publication and the order of the Authors as listed;

3.1.10      Any person that has made a significant contribution to the research and the paper has been listed as an author and that minor contributors and works of others mentioned in the Manuscript have been appropriately attributed in the Manuscript;

3.1.11      The Author(s) has/have disclosed any potential conflict of interest in the research and that any support from a third party has been noted in the Acknowledgements.

## PART II: *Author Confirmation*

**(a) ALL AUTHORS**: *[Part (a) should either be signed by <u>all authors</u>, OR **Part (b)** below **must** be signed by the **MAIN author**].*

**Author 1:**
**Name:** SAYAN PLONG-NGOOLUAM                    SIGNATURE:
Signed at          on this          day of          20     .

**Author 2:**
**Name:** NATTHA JINDAPETCH                    SIGNATURE:
Signed at          on this          day of          20     .

**Author 3:**
**Name:** Phairote Wounchoum                    SIGNATURE:
Signed at          on this          day of          20     .

**Author 4:**
**Name:** Duangporn Sompongse                    SIGNATURE:
Signed at          on this          day of          20     .

**Author 5:**
**Name:**                    SIGNATURE:
Signed at          on this          day of          20     .

**Author 6:**
**Name:**                    SIGNATURE:
Signed at          on this          day of          20     .

**Author 7:**
**Name:**                    SIGNATURE:
Signed at          on this          day of          20     .

**Author 8:**
**Name:**                    SIGNATURE:
Signed at          on this          day of          20     .

**Author 9:**
**Name:**                    SIGNATURE:
Signed at          on this          day of          20     .

## OR

**(b) MAIN AUTHOR**:
*\*(By signing below, I take responsibility that all authors listed in this article have approved the paper for release and are aware of it being submitted to Pertanika).*

### Signature of Main Author and on behalf of other Author(s):

**Name:** Sayan P.                    SIGNATURE: Sayan Plong-ngooluam | Digitally signed by Sayan Plong-ngooluam Date: 2016.11.17 13:56:04 +07'00'
Signed at          on this          day of          20     .

# Paper A3 Permission

## Academic

**Photocopy or share content electronically**

    **LICENSE COVERAGE**

    **Annual Copyright License for Academic Institutions**

    This permission type is covered. The Annual Copyright License authorizes the licensee's faculty, staff, students, and other authorized users to distribute print and electronic copies of copyrighted content within your institution through:

- Print or electronic coursepacks
- Course/Learning Management systems CMS/LMS)
- Classroom handouts
- CD-ROM/DVD
- Electronic reserves
- Other internal academic uses
- Institution Intranets

The description above is provided for summary purposes only. Please refer to your institution's Annual Copyright License for the complete terms and conditions and scope of coverage of the license.

Covered by CCC Annual License – Academic

# Paper A4 Permission

**Copyright Clearance Center**

**JOURNAL**

| | | | |
|---|---|---|---|
| **ISSN:** | 0304-3886 | **Language:** | English |
| **Publication year(s):** | 1974 – present | **Country of publication:** | Netherlands |
| **Author/Editor:** | HORENSTEIN, M | | |
| **Publisher:** | ELSEVIER BV | | |
| **Rightsholder:** | ELSEVIER SCIENCE & TECHNOLOGY JOURNALS | | |

## Academic

**Photocopy or share content electronically**

### LICENSE COVERAGE

**Annual Copyright License for Academic Institutions**

This permission type is covered. The Annual Copyright License authorizes the licensee's faculty, staff, students, and other authorized users to distribute print and electronic copies of copyrighted content within your institution through:

- Print or electronic coursepacks
- Classroom handouts
- Electronic reserves
- Institution Intranets
- Course/Learning Management systems CMS/LMS)
- CD-ROM/DVD
- Other internal academic uses

The description above is provided for summary purposes only. Please refer to your institution's Annual Copyright License for the complete terms and conditions and scope of coverage of the license.

Covered by CCC Annual License – Academic

# Paper A5 Permission

## Academic

**Photocopy or share content electronically**

**LICENSE COVERAGE**

**Annual Copyright License for Academic Institutions**

This permission type is covered. The Annual Copyright License authorizes the licensee's faculty, staff, students, and other authorized users to distribute print and electronic copies of copyrighted content within your institution through:

- Print or electronic coursepacks
- Course/Learning Management systems CMS/LMS)
- Classroom handouts
- CD-ROM/DVD
- Electronic reserves
- Other internal academic uses
- Institution Intranets

The description above is provided for summary purposes only. Please refer to your institution's Annual Copyright License for the complete terms and conditions and scope of coverage of the license.

Covered by CCC Annual License – Academic

# CHAPTER 1

# INTRODUCTION

This chapter introduces the background of electrostatic discharge problem and the use of ionizer to eliminate the electrostatic charges. Then, the literature review and problem statement are reviewed. These are important guides to describe the reasonable gap of research of this thesis. Finally, the left of this chapter briefly describes the thesis overview which contains the five works [A1-A5]. These works are the steps to meet the development objectives based on measurable boundaries to be described in the next chapter.

## 1.1 Background

The electrostatic is a physical phenomenon related to the interaction between stationary electric charges or charge distributions in a finite space with stationary boundaries [1]. Electrostatic field is an electric field which is produced by static electric charges [1-5]. These static charges are stating in the sense of amount charges which are constant in time and positions in space. The electrostatic field and the electrostatic force have been observed a long time ago. Since the ancient Greeks found a strange property of amber that attracts small and light pieces of matter in its vicinity certain conditions [1], this phenomenon has been studied and explained as an effect of the electrostatic field.

An electrostatic charge could be built up on the object surface by the tribocharging, electrostatic field inducing, ion collecting, or direct charging. When the differently-charged objects are brought close or contacted together, the electric current will rapidly flow between these objects. This event is called

"electrostatic discharge (ESD)." The ESD event could be caused by contacting, electrically bridging, or dielectric breakdown. It became a problem in the electronics industry since 1970s [6], and caused device failures, manufacturing yield losses and system interference. After this phenomenon was understood, devices were designed to improve the robustness and processes were designed to improve the device handling capability.

In general, the ground connecting is a method for ESD protection. However, it is less effective for eliminating the static charges from the insulative surfaces or isolated conductive materials. The air ionization is a widely used technique for eliminating the electrostatic charges from the insulator surfaces, the particles or the tiny conductive objects which are unable to apply the ground wiring. Ionizers are the most necessary equipment to eliminate the unnecessary electrostatic charges in the production line of electrostatic discharge sensitive (ESDS) devices. The ionizer performance is determined in two parameters: ion balance and decay time. The ion balance is defined by the resultant of voltage on a floated 15 cm×15 cm conductive surface. The appearance of that voltage is caused by an accumulation of charges when the surface is exposed to the electric field. The decay time is the time duration which is necessary for the ionizer to neutralize the charges on the floating plate from an initial voltage to the desired stop voltage. Typically, +/-1000 V is for the initial voltage and +/-100V is for the ended voltage.

Since the smaller plate reports an ion balance voltage result less than a larger plate [21], the ion balance measured by the 15 cm×15 cm surface is insufficient resolution for many electronics manufacturers, which are working on tiny devices such as the magneto resistive heads. They might concern to the precision of ion balance measurement because the actual devices are much smaller than the measurement plate.

This insufficient measurement also has been mentioned in [22]. Maintaining of sub-1V ion balance in the tight ionized environment raises the requirement of a precise ion balance analysis and recommends the miniaturized sensor to measure the ion balance of an ionizer. Then the miniaturized ion balance analyzers were launched to serve the sub-1V measurement such as the ionizer controller of US patent US 7,522,402 B2 [23] and biased-plate monitor [24]. However, these analyzers do not characterize the ion balance on the whole area as the conventional plate measurement. Their results are given in a single point at a time. They are still insufficient, because the ion distribution in the transport region depends many factors according to the electrohydrodynamics theory investigated by the Ohsawa's ionizer models [10-13]. These investigations explained that ions have particularly distribution characteristic which depends on the air velocity, ion mobility, diffusion, and ion-ion recombination factors.

To correct this insufficiency, the measurement based on multiple ion receiving plates is required for characterizing the ion balance on the surface to be neutralized. These multiple plates should be synchronously measured, and provide the mapping result likes surface potential measurement (SPM), and the wafer surface charge monitor (CHARM). These are conventional tools used in the wafer fabrication processes to characterize the charges built up on the wafer surface [17-20].

Therefore, this thesis aimed to develop a partial surface ion balance analyzer by using the multi-plate sensor which could measure the ion balance on the multiple segment plates synchronously, and illustrate the fine-grained results like the CHARM. Moreover, the data interpolation was used to estimate values at points within the range of the measured points. This interpolation enhanced the resolution of the ion balance distribution on the surface to be neutralized.

## 1.2 Literature Review

To describe how the ionizer works and the reason of insufficiency, this section reviews the related theory, ionizer and ion balance, standard test method of ion balance measurement, and the related works which are conventional system for characterizing the charges on the wafer processes.

### 1.2.1 Electrohydrodynamics Theory

The ionization is explained by the electrohydrodynamics theory (EHD) which consists of electrostatic and fluid dynamic theories. EHD is the dynamics of electrical charged fluids. It is the study of the motions of ionized particles or molecules and their interactions with electrostatic field and the surrounding fluid [7]. The phenomena of corona discharge associated with the ion drift from emitter towards the collector electrodes. The corona discharge occurs while the voltage is increased above a critical inception voltage (CIV), and a visual corona will appear as the first evidence of stress in the air [8]. It will be sparking between the electrodes if the electric field with a voltage exceeds the air breakdown level. The ratio between the air gap and the radius of the wire is important because a critical value exists where a spark that bridges the electrodes can occur before the corona discharge phenomenon appears [9]. The Peek's breakdown criterion [8] is used to calculate the CIV as

$$CIV = E_i r \ln(\frac{d}{r}),\qquad(1.1)$$

where

$$E_i = E_0 \delta (1 + \frac{\gamma}{\sqrt{r}}),\qquad(1.2)$$

when    $E_i$    Electric field strength to produce corona discharge (V/m)

$E_0$     Electric field strength to break down air, $3.37 \times 10^5$ V/m for positive ion and $3.10 \times 10^5$ V/m negative ion

$\gamma$     Peek's value from table [8], $0.0301 \sqrt{m}$

$r$     Radius of corona electrode (m)

$d$     Distance between positive and negative electrodes (m)

$\delta$     Air density factor, where

$$\delta = \frac{3.92 \times barometiricpressure \quad (cm)}{273 + temperature(^\circ C)} .$$

Then, the ion density at the source $n$ described on [10] can be expressed as

$$n = \begin{cases} \dfrac{4\pi\varepsilon_0}{ed^2}|V - V_c|, & |V| > |V_c|, \\ 0, & |V| < |V_c|. \end{cases} \quad (1.3)$$

where $V_c$ is CIV calculated by (1.1), $n$ is ion density, $e$ is an elementary charge and $\varepsilon_0$ is the permittivity of free space.

The motions of positive ion $n_p$ and negative ion $n_n$ depend on the air velocity which could be described by the continuity equations [10-13] as

$$\frac{\partial n_p}{\partial t} + \nabla \cdot (n_p \mathbf{u}_p) - D_p \nabla^2 n_p = -\beta n_p n_n \qquad Positive, \quad (1.4)$$

$$\frac{\partial n_n}{\partial t} + \nabla \cdot (n_n \mathbf{u}_n) - D_n \nabla^2 n_n = -\beta n_p n_n \qquad Negative, \quad (1.5)$$

where $\mathbf{u}_p$ and $\mathbf{u}_n$ are air velocities consisting of positive and negative ion mobilities, $D_p$ and $D_n$ are positive and negative ion diffusion coefficients, and $\beta$ is the ion-ion recombination coefficient.

Then, ion balance can be described by the electrostatic potential $V$ which depends on positive ion density $n_p$ and negative ion density $n_n$ as

$$\nabla^2 V = \frac{-e(n_p - n_n)}{\varepsilon_0}.$$ (1.6)

The electric potential of (1.6) can be used to obtain the electric field $\mathbf{E}$ as

$$\mathbf{E} = -\nabla V.$$ (1.7)

The volume charge $\rho_v$ depends on the elementary charge $e$ and the balance of positive ion density $n_p$ and negative ion density $n_n$. Then, we can obtain the Poisson's equation (1.6) as

$$\nabla^2 V = -\frac{\rho_v}{\varepsilon_0}.$$ (1.8)

The ion charges are accelerated by the Coulomb force and move towards the object to be neutralized. This charge drift creates an electric current density [14] which can be defined as

$$\mathbf{J} = \mu_E \rho_v \mathbf{E} + \rho_v \mathbf{u} - D\nabla \rho_v,$$ (1.9)

where $\mu_E$ is ion mobility, $D$ is a diffusion coefficient and $\mathbf{u}$ is air velocity field.

The first term of right hand side is the electric current caused by the drift velocity, the second term is the current convection caused a system volume velocity, and the third term is diffusion current which depends on the differential of the amount of charge in each volume. This means the ion current comprises of three currents: drift, convection and diffusion currents.

### 1.2.2 Ionizer and Ion Balance Measurement

The ionizers are the equipment used for removing the undesirable electrostatic charges. They provide either positive or negative air ions to neutralize the electrostatic charges on the insulative surface or a tiny object. The typical corona ionizers generate the ions by collisions between neutral molecules and electrons which are accelerated by an electric field which exceeds the inception level described by the electrohydrodynamics theory [10]. They could be the bipolar DC, AC, or pulse-DC ionizers, with or without an air-blower, depend on the applications.

The ion balance is defined by the electrostatic potential $V$ on the plate caused by an accumulation of positive and negative ions described in (1.6). This electrostatic potential can be expressed by the ratio of the amount of charge $Q$ which has accumulated on that plate with capacitance $C$ as

$$V = \frac{Q}{C}. \tag{1.10}$$

Assume charge on the ion receiving surface and electrostatic field are uniformly distributed, then the amount charge $Q$ can be defined as

$$Q = \rho_S A, \tag{1.11}$$

where the $\rho_S$ is the density of charge on the ion receiving surface $A$.

This charge density is the ion balance term of (1.6) which can be defined as

$$\rho_S = e(n_p - n_n). \tag{1.12}$$

By the substitution (1.11) and (1.12) to (1.10), the electrostatic potential on the ion receiving plate $V_P$ can be expressed as

$$V_P = \frac{e(n_p - n_n)A}{C}.$$ 

(1.13)

Thus, the electrostatic potential on the plate proportionally depends on the receiving surface area and the ion balance.

### 1.2.3  Standard Test Method of Ion Balance Measurement

In order to characterize the ionizer, ANSI/ESD STM3.1-2015 [15] and IEC 61340-4-7 [16] constitute a standard test method (STM) for evaluation and selection of ionizers. The STM defines ion balance and decay time measurements as follows.

The STM defines the ion balance as electrostatic potential appeared on the 15 cm×15 cm square shape conductive plate with 20 pF capacitance as shown in Fig.1, called charged plate monitor (CPM). A non-contact voltmeter is used for measuring the voltage on the floated conductive plate. If a CPM is placed in an ionized environment, the ion balance is determined by the recording of voltage on the plate that is induced by an electric field during one minute.
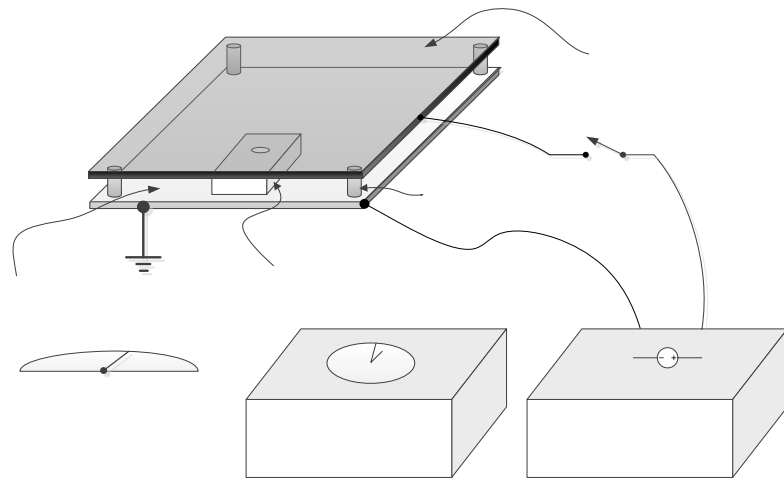


**Figure 1.** ANSI/ESD STM3.1 charged plate monitor apparatus.

The DC voltage power supply is used to simulate the charge on the plate for characterizing the rate of neutralization called discharge time or decay time. The STM recommends the discharge timer to capture the decay time, which is initiated at 1000 V then ends the capturing when the plate voltage is decreased to 100 V. The decay time test needs to perform with the both positive and negative polarities.

### 1.2.4  Ion Balance Measurement In Wafer Fabrication Process

The ion balance in a closed chamber of the wafer fabricates processes also needs the air ionization to neutralize the charges that are built up on the wafer surfaces. The paper [17] reports the 2-D measurement of the charged particles diffusing from the DC corona ionizer operated in air and nitrogen atmosphere. The measurement has been done by using the small movable probe to monitor a surface voltage on the silicon wafer downstream of the DC corona ionizer. Thus, the wafer fabricates processes need a small array sensor to characterize the charges which are built up on the wafer surface.

To characterize the electrostatic potential of the wafer surface, the surface potential measurement is developed for characterizing the electrostatic potential on the wafer surface. The SPM is a family of micro electrochemical imaging and spectroscopy techniques based on the scanning of a physical sensing probe over the surface of the sample under test likes an atomic force microscopy (AFM). The SPM result is the mapping of the electrostatic potential on the wafer surface under test. It has been widely used in mapping surface potential distribution at the micrometre scale. The surface potential image from SPM is finer than CHARM but coarser than AFM.

A wafer surface charge monitor (CHARM) has been developed for measuring the charges that are built up on the wafer surface [17]. It comprises of

many EEPROM transistors which are collecting the charges on the exposed gate area of transistors. It is a fabricated wafer which provides electrical contacts to source and drain circuit for reading and erasing. The latest development of the CHARM system is the CHARM-2 system which is modular and capable of 1 mm spatial resolution [19]. The result from CHARM-2 wafer can be mapped to the wafer as shown in Fig. 2. This is an example of the surface potential mapping results imaged the top view of the 15 cm CHRAM-2 wafer. The value of each segment is the peak potential read from each floating gate transistor.

CHARM and SPM are used in the different purposes. CHARM is used for characterizing the process, but SPM is used for characterizing the product (wafer). Then, the work [20] compared the surface potential mapping between the SPM image of the 1000Å thermal oxide wafer and the CHARM-2 data taken from the same process. The results proved that SPM and CHARM-2 data can be correlated for single plasma charging step process. However, SPM can explain only the last event of the wafer surface that may not correlate to device damage results.
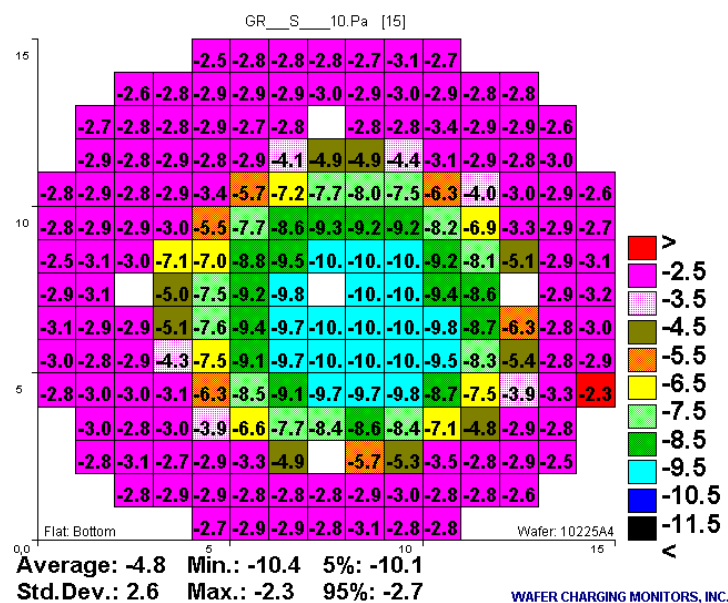


**Figure 2.** The surface potential mapping read from the CHARM-2 wafer.

On the other hand, CHARM-2 is able to record the charging current to identify the charging source and evaluate the potential damage in the multiple processes characterization. These systems are used in wafer processes such as ion implanters, resist ashers, polysilicon etchers, metal etchers, oxide etchers, sputter cleaners, oxide depositions and metal depositions.

## 1.3 Problem Statement

The size of CPM was selected because it was similar to a typical silicon wafer at the time of drafting the standard in the late 1980s [21]. In the current situation, the electronics manufacturers that produce a miniaturized devices such as an integrated circuit or magneto resistive head. These devices are sensitive to ESD damage at low voltage levels, so the ionizer balance must be less than ±1V or even better. The sub-1V ion balance environment requires the sufficient resolution and accuracy to measure ionizer balance [22]. The standard CPM has insufficient resolution in ion balance measurement, because the measurement plate is larger than the devices to be treated.

The small size ion balance analyzers have been launched to serve that requirement such as the ionizer controller on US patent number US 7,522,402 B2 [23] and biased-plate monitor [24]. However, their results are reported in the single point at a time, and they could not measure the ion balance of the 15 cm× 15 cm area to satisfy the STM's requirement.

The electrostatic potential measurement using the multiple plates was simulated on [A1] and revealed that the measurement resolution could be enhanced by this concept. Then the concept had been validated by the study on [A2, A3]. The 25-segment conductive plates were exposed under ionized air and measured the electrostatic potential by the high resistance electrostatic voltmeter. The fine-grained levels over the conductive plates had been indicated and proved that concept. However, the results were regulatory measured in the different

times. This could not be explaining the right pattern of the ion balance distribution along the 15 cm×15 cm surface.

## 1.4 Gap of Research

From the insufficient measurement of prior arts, this research aims to develop a partial surface ion balance analyzer using the multi-plate sensing technique which could measure the ion balance on the multiple segment plates synchronously.

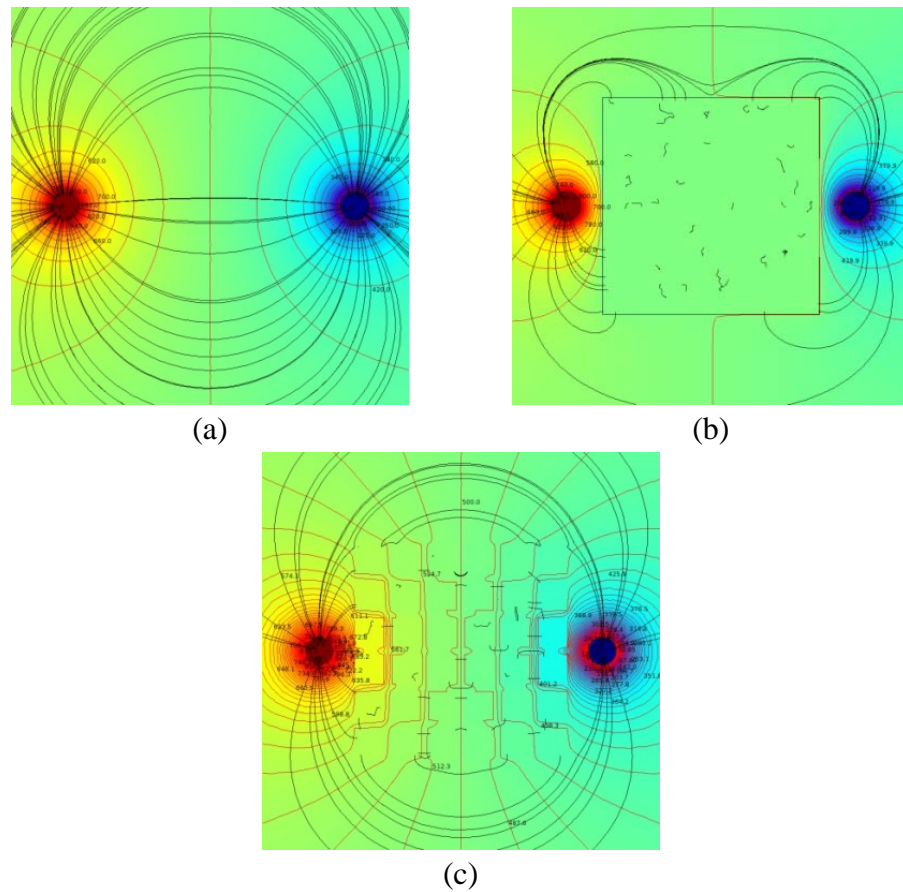

(a)                                        (b)

(c)

**Figure 3.** The illustrations of electrostatic potential and electrostatic flux uniformity changes due to ion balance measurement plates.

a) A normal uniformity of electric potential and flux.

b) A uniformity deformed after measured by the CPM.

c) The partial surfaces to correct the uniformity deformation.

To minimize the number of prototypes and experiments, the finite element analysis (FEA) of electrostatic modeling is used to validate the topology selection and optimization of the reasonable number of segments, shape, and size of the multi-plate sensor.

Moreover, the interpolation is used to construct the approximated data points within the range of measured data points for enhancing the resolution beyond the physical measurement. The interpolated results could estimate the ion balance on the surface to be neutralized like the estimation of the spatial distribution within the focal area such as the climate change, rainfall mapping or the distribution of pollution levels. Furthermore, the measurement results from this analyzer can image the ion balance distribution such as contour and surface plots as shown in Fig. 3.

## 1.5 Thesis Overview

The thesis was developed in four key processes: conceptual design, feasibility study, detail design and prototype design as shown in Fig. 4. The problem statement and literature review provided the gap of research that the standard CPM with the 15 cm×15 cm plate size has limitation in the ion balance measurement resolution. This motivated the conceptual design partial surface ion balance analyzer using the multi-plate sensing technique as follows.

The conceptual design was validated by feasibility studies [A1-A3]. The computational simulation [A1] proved that the ion balance measurement resolution could be enhanced by partial surfaces analysis. The FEA results indicated the fine-grained levels while the segment number of partial surface were increasing. However, these FEA results needed the field measurement to validate these results as tangible.
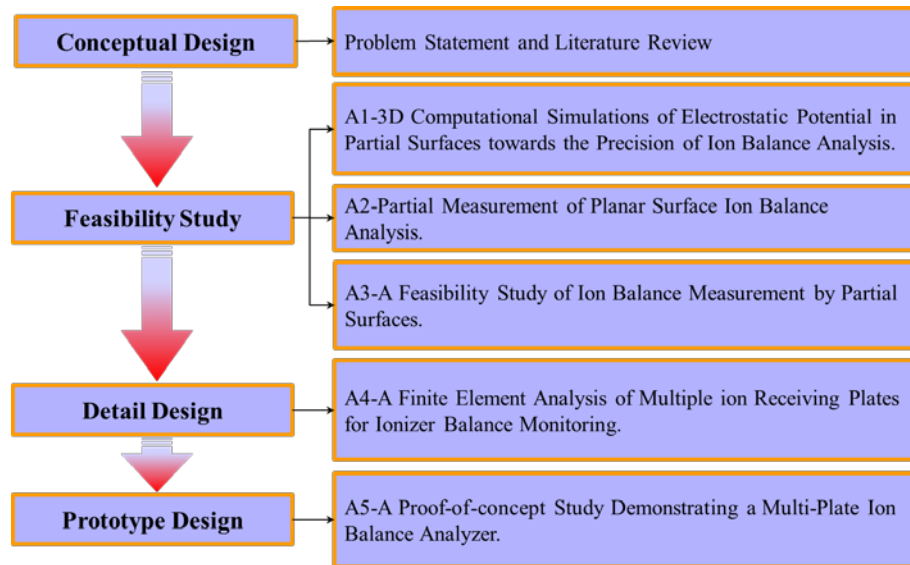
**Figure 4**. The development methodologies and research papers mapping.

Then, the partial measurement [A2] has been evaluated by using the 2.54 cm$\times$2.54 cm plate to measure the ion balance from ionizer on the planar surface at the same area as the standard CPM placement. The experimental results indicated the spatial variation of ion balance levels on each location. These variation were moving around -0.5 V, $\pm$0.3 V and $\pm$0.5 V while the ionizer balance was adjusted at -1.0 V, 0.0 V and +1.0 V, respectively. At this point, the partial measurement results proved that ion balance measured by the standard CPM is losing the fine-grained levels on that planar surface because the given result is the summation of all ions which are collected from the whole surface.

The relationship between the ion balances measured by the standard CPM and the partial surfaces plate has been investigated in the feasibility study [A3]. This study revealed that the average ion balance from all segments of the partial surfaces plate correlated to the standard CPM result.

At this point, the feasibility studies results from [A1-A3] have been proved that the ion balance measurement resolution can be enhanced by the partial surfaces method as tangible, and correlated to standard CPM. However,

these results did not suggest the suitable shape, and the segment number of plates which are met the minimum acceptation described by the measurement error approximation.

The shape and the segment number of partial surface plates have been investigated by the detail design [A4]. The FEA which was the same as method in [A1] was used to model various plates in the both square and circular shapes. The potential distributions from each model was further analyzed by the SLR to provide the qualitative results of the approximated measurement error. The results concluded that the finer segment plates provided the finer-grained results and the minimum acceptance was 9-segment for the circular plates and 16-segment for the square plates. At this point, the selection of the suitable shape and the segment number have been made with the 25-segment square plates. This selection was based on the minimum acceptance and the fabrication technology which could be done at the laboratory level.

Finally, the laboratory prototype of the partial surface ion balance analyzer has been built, demonstrated, and reported in [A5]. This prototype analyzer was developed based on the suitable plate selecting in [A4]. However, the proposed design provided the discrete results individually, based on the physical plate segments. These discrete results need the data interpolation to construct the new data points between these discrete results for the resolution enhancement beyond the physical measurement. Then, the IDW interpolation has been implemented and demonstrated in the data interpolation mode.

# CHAPTER 2

# OBJECTIVES

From the research gap mentioned in the previous chapter, the key processes including conceptual design, feasibility study, detail design, and prototype design are needed to develop the partial surface ion balance analyzer for the higher measurement resolution. The objectives and the scopes of each key process are given as follows.

## 2.1 Development Objectives

The thesis aims to develop the new ion balance analyzer which can improve the ion balance measurement resolution. The development objectives are settled corresponding to the key processes as the objectives mapping shown in Fig. 5. The objective descriptions are listed items below:

2.1.1   To perform FEA of electrostatic potential characteristics of the partial planar surfaces in the ionized environment.

2.1.2   To perform the feasibility study of the partial surfaces ion balance measurement based on the field evaluation.

2.1.3   To perform the side effects study of the segment number, size and shape of the multi-plate sensor for the partial surfaces ion balance analyzer.

2.1.4   To develop the prototype of a partial surfaces ion balance analyzer for improving the ion balance measurement resolution.
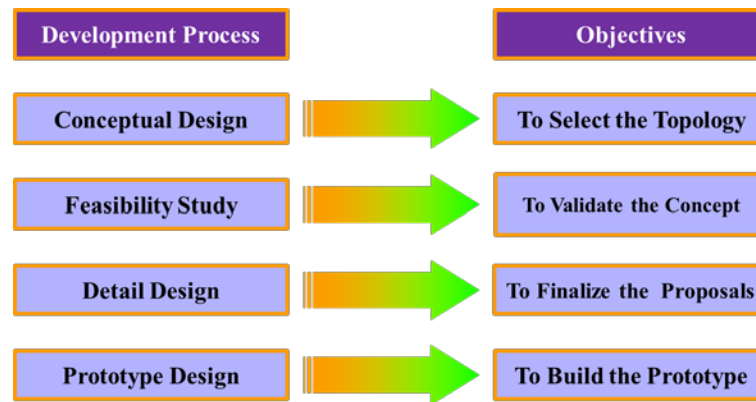
**Figure 5.** The key development processes and the objectives mapping.

## 2.2 Development Scopes

The suitable shape, and the segment number of the multi-plate sensor are the objectives based on the measurement error approximation. The development scopes are aligned with the development boundaries listed and summarized in Table 1.

2.2.1 The FEA results should validate the possibility of measurement resolution increasing by the partial surfaces ion balance measurement method.

2.2.2 The evaluation results should be based on the physical plate measurement, and validate the FEA result as tangible. The field evaluation should also prove the correlation with STM result.

2.2.3 The segment number and shape of the new ion receiving plates should be analyzed and approximated measurement errors qualitatively.

2.2.4 The laboratory prototype of a partial surfaces ion balance analyzer should demonstrate with the improvement of measurement resolution, and image the ion balance distribution on 15 cm×15 cm planar surface as in the CHARM-2 data mapping.

Table 1. The mapping of development objectives and development scopes.

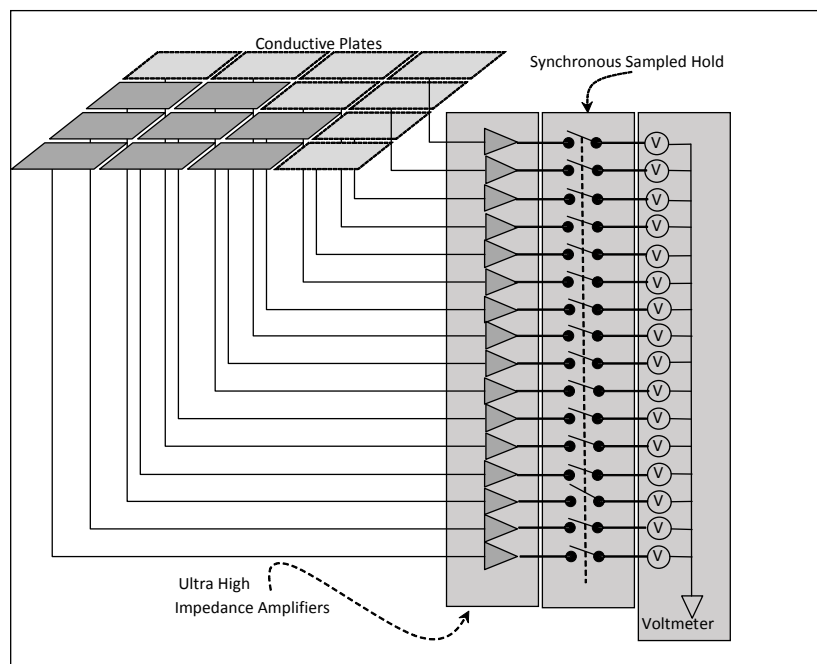| Development Objectives | Development Scopes |
|---|---|
| To select the topology | • Validating the possibility of measurement resolution enhancement by a partial surfaces technique using FEA. |
| To validate the concept | • Validating the FEA result as tangible.<br>• Proving the correlation with STM. |
| To finalize the proposals | • Selecting the suitable number of plates, size, and shape by considering the measurement error approximation. |
| To build the prototype | • Demonstrating the laboratory prototype analyzer.<br>• Imaging the ion balance distribution on the 15 cm×15 cm planar surface. |



**Figure 6**. The conceptual diagram of the partial surfaces ion balance analyzer.

## 2.3 Feasibility Study

From the development objectives and scopes, the thesis aims to create the new ion balance analyzer by dividing the 15 cm×15 cm plate into the small array segments. These segments are independently buffered by the ultra-high impedance amplifiers as the charged induced meter [8, 25-29] with the synchronously sampled-hold measurement as shown in Fig. 6. Then, the ion balance distribution is imaged as in the CHARM-2 system.

The feasibility study contains two parts: computer simulation, and field measurement evaluation. The computer simulation aims to simulate the electrostatic potential uniformity change caused by the placement of the ion balance measurement plate. In addition, the results could be exported for the statistical analysis for estimating the errors and providing the qualitative results in the detail design process. The field measurement evaluation aims to validate the computer simulation results practically, and compare with the STM result to describe the correlation. This research had done one computer simulation and two field measurement evaluations in this feasibility study step.

### 2.3.1 3-D Computational Simulations of Electrostatic Potential in Partial Surfaces towards the Precision of Ion Balance Analysis

The work [A1] aims to simulate the electrostatic potential uniformity that has been changed by the placing of various measurement plates. The modeling is guided by the study of ionized fields in DC electrostatic precipitator in [30].  In addition, the partial surfaces that are divided from the conventional plate into 4, 9 and 16 segments are analyzed for validating the feasibility of measurement error reduction by the partial surfaces ion balance analysis.

### 2.3.2 Partial Measurement of Planar Surface Ion Balance Analysis

To validate the computer simulation [A1], the work [A2] evaluated the partial surface ion balance measurement on the 15 cm×15 cm square planar surface by the miniaturized 2.54 cm×2.54 cm charged plate, which was ordinary arranged as the same area as the standard charged plate measurement. The partial results were imaged by the surface plots to express the ion balance distribution along the 15 cm×15 cm planar square shape surface which was neutralized by the ionized air from the DC corona ionizer.

### 2.3.3 A Feasibility Study of Ion Balance Measurement by Partial Surfaces

The work [A3] aims to study the feasibility of the resolution enhancement by the partial surfaces technique which is described in [A1-A2]. The 25-segment partial surfaces have been assembled over the 15 cm×15 cm on the insulative base. It is exposed below the DC corona ionizer which is used as the adjustable ion source. The apparent voltage on each plate is measured by the high impedance electrostatic voltmeter. The experimental results would be tangible validation of the partial surfaces measurement topology.

### 2.4 Detail Design

The detail design aims to understand the side effects of the segment number, size and shape of the multi-plate sensor. The work [A4] analyzed the multiple plates using the FEA and the statistical method to define the change of the electrostatic potential in the quantitative results. The simple linear regression (SLR) is used to compare and approximate the gain and offset error with the goodness of fit to prove the confidence level of the linear regression results. Furthermore, circular and square plates are modeled and compared for investigating the curvature effect.

## 2.5 Prototype Design

The work [A5] aims to report a new ion balance measurement method using the multi-plate sensor, which could measure the ion balance on the multiple segment plates synchronously, and to illustrate the fine-grained results. Moreover, IDW interpolation was used to estimate values at the unknown data points within the range of the measured points. This interpolation enhanced the resolution of the ion balance distribution on the surface to be measured.

# CHAPTER 3

# RESULTS AN DISCUSSIONS

This chapter summarized and discussed the results of papers [A1-A5] which had described the feasibility study, detail design and the prototype design in the previous chapter. These results are discussed at the end of the chapter and concluded in the next chapter.

## 3.1 The Feasibility Study Results

Three steps of feasibility study has been perform to support the conceptual design from simulation to real measurement. Firstly, the computer simulation [A1] of the partial surfaces measurement has been done to compare the fine-grained level of electrostatic potentials on the multiple conductive plates. Then, the field measurement [A2] has been performed by using the miniaturized 2.54 cm×2.54 cm standard charged plate analyzer to measure the ion balance from the DC corona ionizer which was installed over the non-obstructive workstation. Finally, the 25-segment receiving plates have been developed by 25 pieces of aluminium sheets [A3] to measure the ion balance in the same condition as [A2]. The detailed results of each step are as follows.

The computer simulation [A1] explains the electrostatic field in free space could change when the conductive plates were placed in the simulated electrostatic field. Fig. 7 images the electrostatic potential in free space caused by ground and source electrodes. The red tip is the highest electrostatic potential at the source electrode. The blue tip is the lowest electrostatic potential at the ground electrode. The colour legend is unit in volt (V).
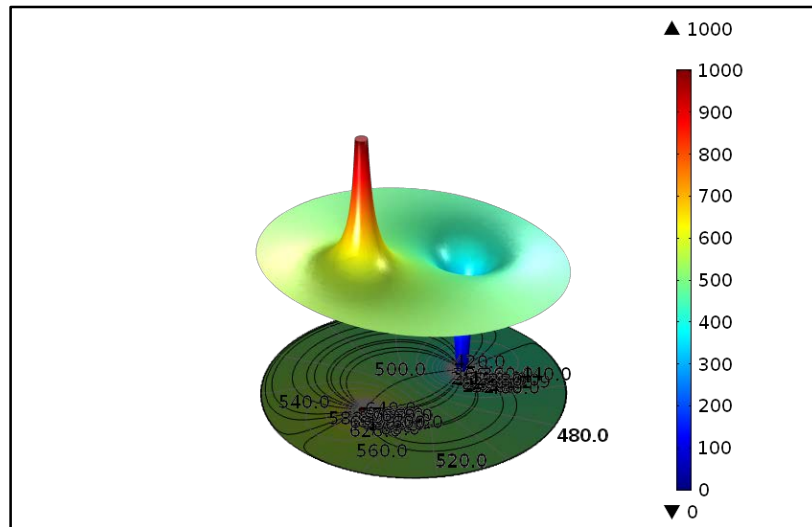
**Figure 7.** The 2-D surface, contour and isosurface of electrostatic potential plots from the free space model without the measurement plate.

The 15 cm×15 cm conductive plate model shows the rough-grained result as the single yard between the electrodes as shown in Fig. 8. Then, the grain of images are finer after replacing the single 15 cm×15 cm conductive plate by 4-segment, 9-segment and 16-segment plates. Fig.9 images the electrostatic potential from the 16-segment plate model which expresses the finer-grained result, improved from the single plate model result in Fig. 8.
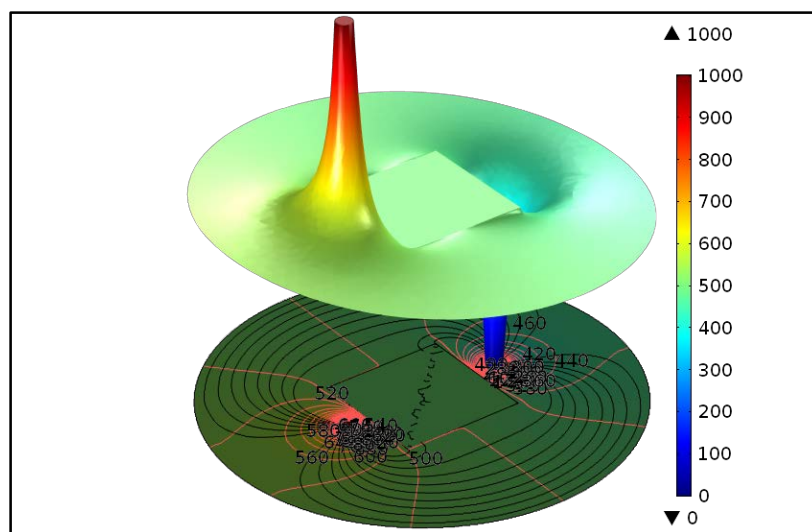


**Figure 8.** The 2-D surface, contour and isosurface of electrostatic potential plots from the 15 cm×15 cm conductive plate measurement model.
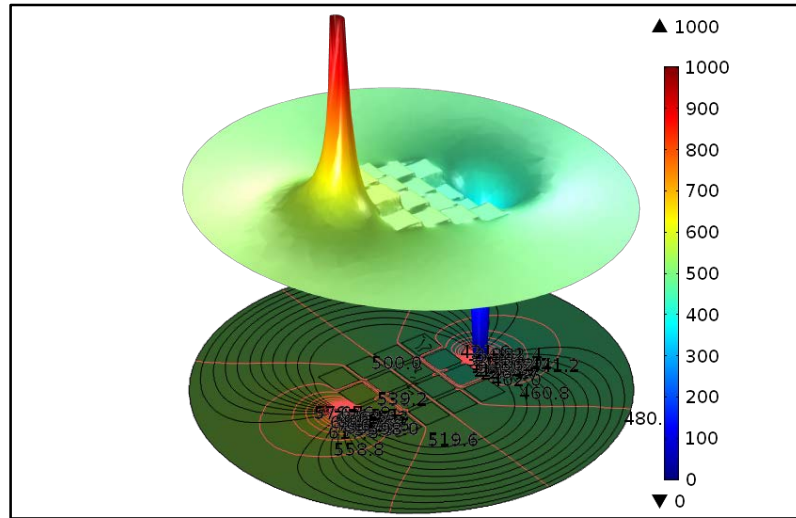
**Figure 9.** The 2-D surface, contour and isosurface of electrostatic potential plots from the 16-segment conductive plate measurement model.

To validate the simulation in [A1], the partial measurement [A2] has been evaluated by using the standard CPM to measure the ion balance from the DC corona ionizer which was installed over the non-obstructive workstation with a grounded surface. Then, the 36-segment partial surface measurement was performed by using the 2.54 cm×2.54 cm plate ordinary arranged over the standard CPM as shown in Fig. 10.
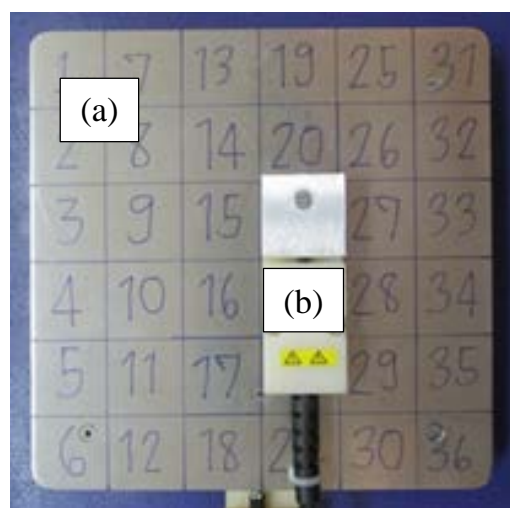


**Figure 10.** The 36-segment partial measurement point arranging on the planar surface; (a) The standard charged plate, and (b) the 2.54 cm×2.54 cm plate.

The evaluation results were reported in the six rows and six columns with the x-y axis intersections with the unit in inch. The ion balance distributions have been analyzed and imaged by the wireframe plot with the 50×50 mesh interpolation using distance method by MiniTab [31]. The evaluation revealed that the partial measurement could indicate the various results of the ion balance on each plate. The measurement results were closing to the ionizer adjusted point which was measured by the standard CPM as the reference. For example, the ion balance distribution image in Fig. 11 expressed the fine-grained levels which vary around ±0.3V from the settled point (0.0V). This fine-grained results proved that the ion balance measurement resolution could be improved by the partial surfaces measurement.

Then, the relationship between the ionizer's settled points measured by the standard CPM and the ion balance which were collected by the partial surfaces has been investigated by using of the isolated plates. The feasibility study [A3] evaluated the 25-segment partial surfaces ion collecting by the multiple plates as shown in Fig. 12. The plates were made of 25 pieces of aluminium sheets assembled on the acrylic base.
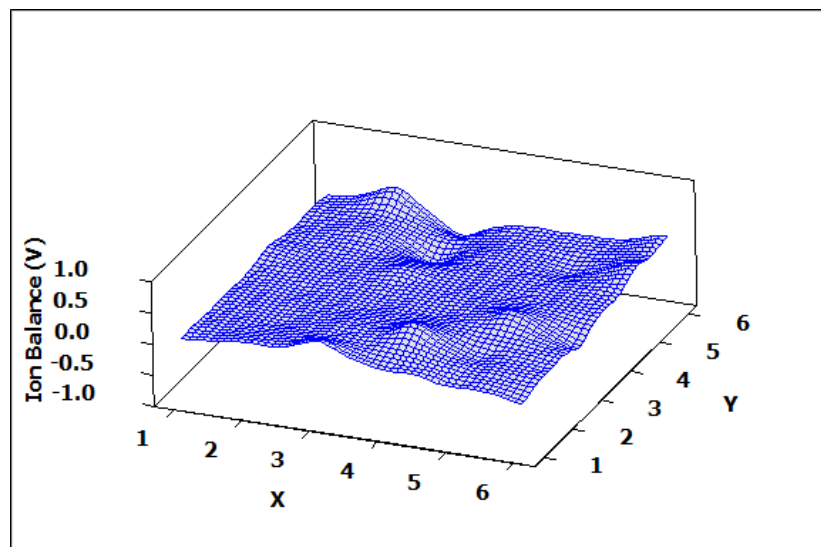


**Figure 11.** The ion balance distribution image with 0.0V ionizer adjustment.
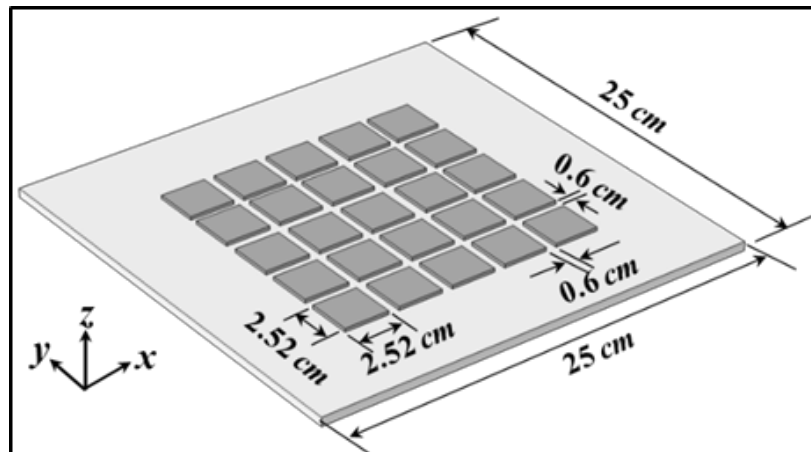
**Figure 12.** The geometrical illustration of 25-segment partial surfaces plate.

The evaluation revealed that the average voltage of the 25-segment plates correlated with the results from the standard CPM as a scattering plot in Fig. 13. The first order linear equation shows 0.904 of the slope, 0.275 V of the offset, with 0.996 of $R^2$. This relationship is the guidance of the correlation method between the proposed analyzer and the conventional analyzer.

Overall, the feasibility study results [A1-A3] proved that ion balance measurement resolution could be improved by the partial surfaces technique as tangible. Moreover, it also correlated with the standard CPM result.
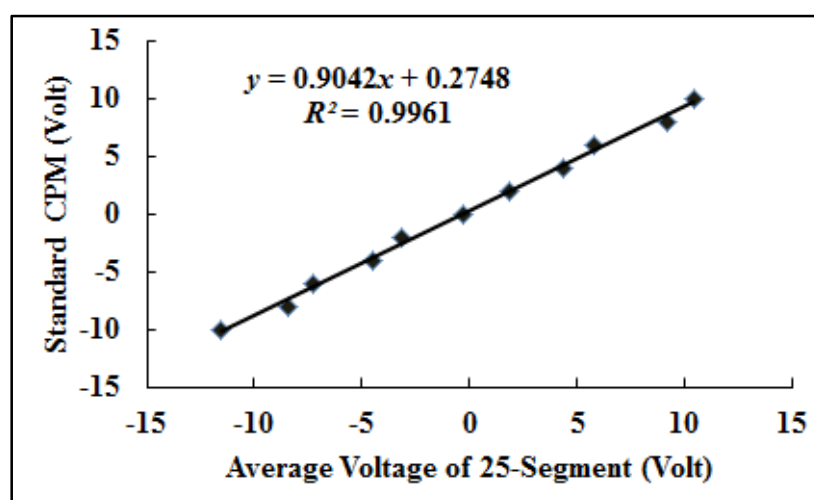


**Figure 13.** The scattering plot of the average ion balance of the 25-segment partial surfaces plate versus the standard CPM results.

## 3.2 Detail Design Results

The computational simulation has been re-investigated in the work [A4] to define the suitable plates. The curvature, shape and size of the multiple plates were considered in the FEA and the statistical method to define the minimum acceptance plates. The one millimetre thick square aluminium plates which are the 15 cm×15 cm square plate and its divided by 4, 9, 16 25 and 36-segment plates were simulated as the ion receiving plates. Similarly, the circular plates, including the single 16.9 cm circular plate and its divided by 4, 9, 16, 25, 36-segment plates were also simulated in the same manner.

The simple linear regression (SLR) was used to compare and approximate gain and offset errors. The goodness of fit ($R^2$) was used to prove the confidence level of the error approximated results. The analysis results which are summarized in Table 2 could explain the comparison in qualitative number clearly. The linear regression from the single plate models does not fit as shown in Fig. 14. The $R^2$ and the gain are close to zero with the high offset error. It means that all measurement points on this plate are equal to 499.83 V.
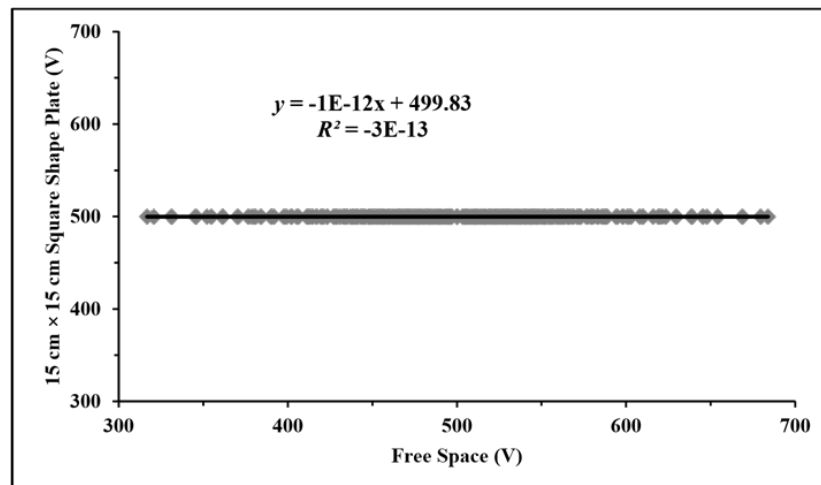


**Figure 14.** The scattering plot of electrostatic potential from the 15 cm×15 cm square plate model versus the free space model

**Figure 15.** The scattering plot of electrostatic potential from 36-segment square plate model versus the free space model.

The results in Table 2 indicate that the offset errors are decreasing exponentially as the increasing of number of segments increasing. The scattering plots in Fig.15 and Fig. 16 show the best fitting results of the square and the circular shape plates, respectively. The $R^2$ are close to 0.99, the gains are close to unity with lowest offset error.



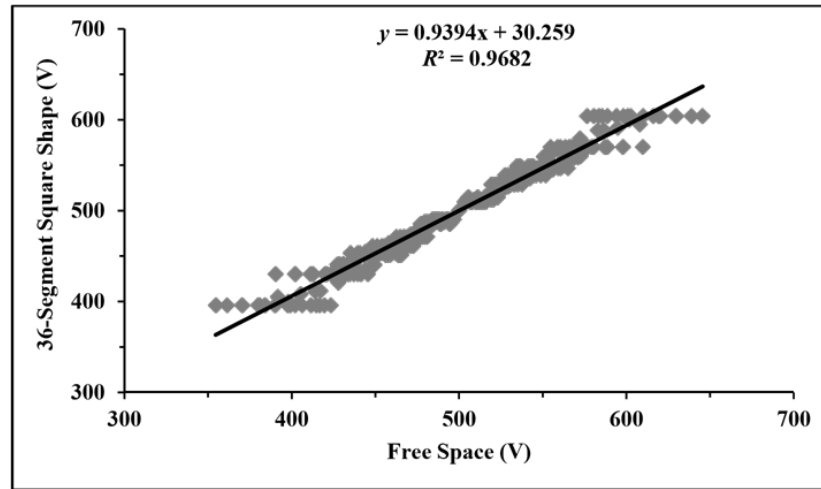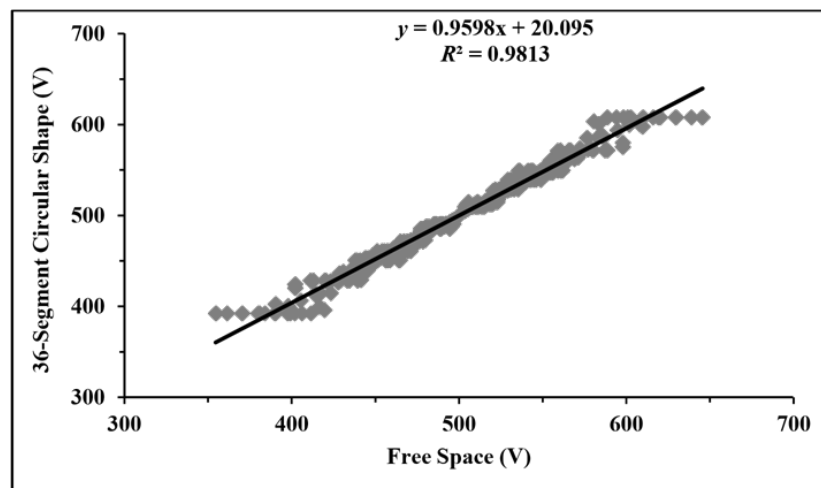**Figure 16.** The scattering plot of electrostatic potential from 36-segment circular plate model versus the free space model.

Table 2 Summarization of SLR analysis results.

| Measurement Plate | Parameters | | |
|---|---|---|---|
| | $R^2$ | Gain | Offset error (V) |
| 15 cm×15 cm (Square) | <0.01 | <0.01 | 499.83 |
| 4-Segment (Square) | 0.757 | 0.520 | 240.05 |
| 9-Segment (Square) | 0.870 | 0.752 | 123.68 |
| 16-Segment (Square) | 0.923 | 0.841 | 79.32 |
| 25-Segment (Square) | 0.948 | 0.885 | 57.12 |
| 36-Segment (Square) | 0.968 | 0.939 | 30.26 |
| 16.9 cm (Circular) | <0.01 | <0.01 | 500.17 |
| 4-Segment (Circular) | 0.762 | 0.589 | 205.28 |
| 9-Segment (Circular) | 0.912 | 0.838 | 80.79 |
| 16-Segment (Circular) | 0.942 | 0.856 | 71.88 |
| 25-Segment (Circular) | 0.968 | 0.929 | 35.18 |
| 36-Segment (Circular) | 0.981 | 0.960 | 20.10 |

Generally, the minimum acceptance of $R^2$ is 0.9. Thus, the minimum segment numbers are 16- and the 9-segment for the square and the circular plates, respectively.

In addition, the significant difference between the results from square and circular plates advocates that the electrostatic field uniformity could also be distorted by the curvature effects because the square shape is consisting of the convex corners which could create the electrostatic field strength variation. However, this development satisfied with the 25-segment square plate based on the available fabrication process at the laboratory level and met the minimum acceptance which is requiring 16 or higher segments for the square plate.

**Figure 17.** The laboratory prototype multi-plate ion balance analyzer.

## 3.3 Prototype Design Results

This laboratory prototype unit of the partial surfaces ion balance analyzer has been built and demonstrated as the multi-plate ion balance analyzer described in [A5] based on the experimental results and conclusions in the feasibility study and detail design. The photograph of the proposed prototype analyzer is shown in Fig.17. For the ion balance measurement purpose, the multi-plate sensor was installed on the top side for receiving ions from an ionizer.
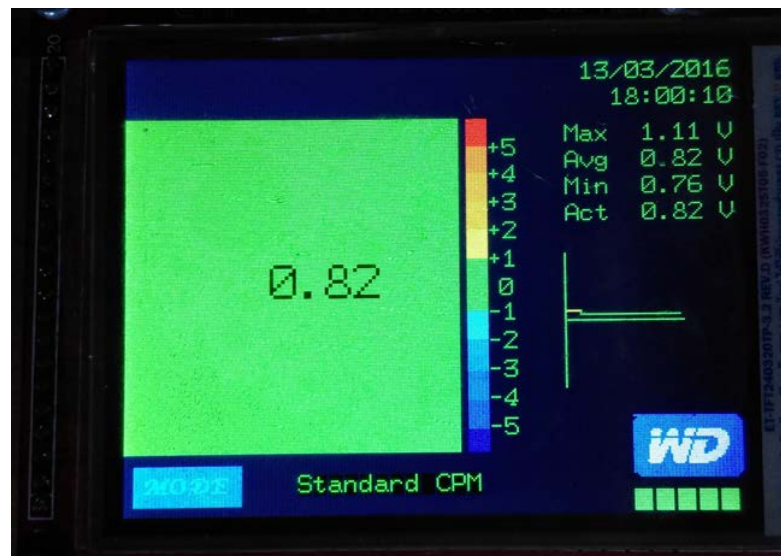


**Figure 18**. The display of the average voltage when the prototype analyzer was measuring the ion balance at zero volt ionizer adjustment.

The prototype analyzer was evaluated for analyzing the ionizer balance with the same configuration as the feasibility study [A3]. At the zero volt ionizer adjustment measured by the standard CPM, the proposed analyzer described the averaged ion balance from all 25 segments as 0.82V offset in the standard CPM mode as shown in Fig. 18. This different offset was suspected to repeatability issue. Then, the correlation in Fig. 19 was re-evaluated for validating the repeatability purpose. This scatter plot is not the same correlation plot as shown in Fig. 12 of [A5] due to the ten times repetition. The ionizer measurement apparatus were prepared in the same configuration as [A2]. The ionizer was adjusted to have the settled point of ion balance from -7.0 V to +7.0 V measured by the standard CPM. The ion balance was analyzed by the proposed analyzer operating in the standard CPM mode with repetition of ten times. Fig. 19 indicates the maximum variation about ±1 V at 5 V and 6 V. Thus, the observed results from the proposed analyzer could be different from the reading from the standard CPM ± 1 V freely. However, this correlation could be accepted due to the gain is close to unity, the offset error is close to zero and $R^2$ is higher than 0.9.
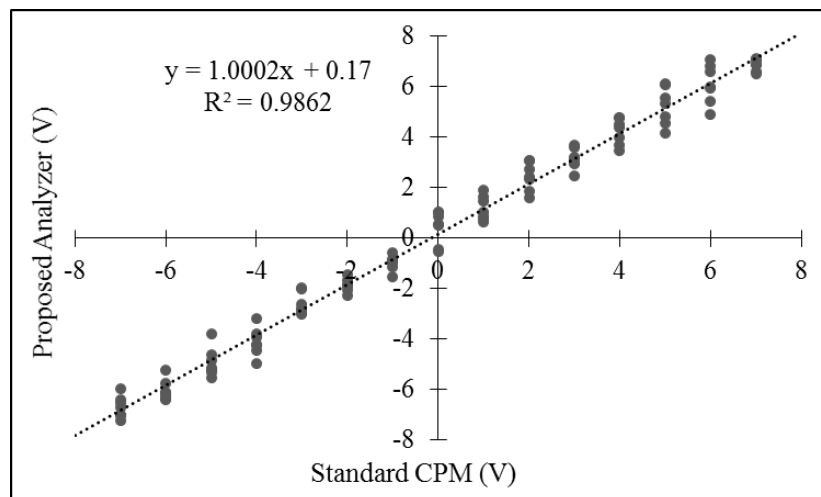


**Figure 19.** The correlation between the prototype analyzer (standard CPM mode) and the standard CPM.

In the partial surfaces analysis mode, the proposed analyzer could show the electrostatic potential on each segment as shown in Fig. 20. This result was measured by the zero volt ionizer adjustment condition. It shows the large non-uniformity of ion balance distribution along sensing area, but the averaging result shows 0.82V. The partial surfaces measurement could show the finer-grained levels which could not be indicated by the single plate measurement. This non-uniformity suspected to the fluctuation of the air velocity, which was transporting the positive and the negative ions from emitter pins to the plate explained by the divergence terms in (1.4) and (1.5).

This non-uniformity was unrepeatable because the air velocity at the measured surface always varied due to the turbulent flowing and its reflecting after reached the rigid surface. This makes the variation of ion balance in each measurement surface. This variation could be eliminated by reducing air velocity or using the laminar air instead of the axial fan. Fig. 21 is an overall correlation between the proposed analyzer and the conventional electrostatic voltmeter. This is the extended work from [A5] for validating the accuracy of the measurement voltage of the individual plate.
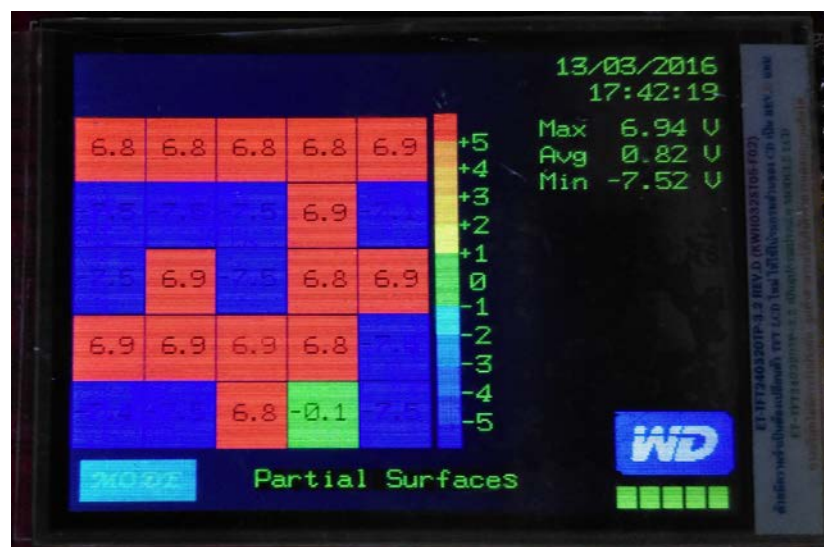


**Figure 20.** The ion balance showed large non-uniformity when viewed at the resolution of the partial surfaces analysis mode.
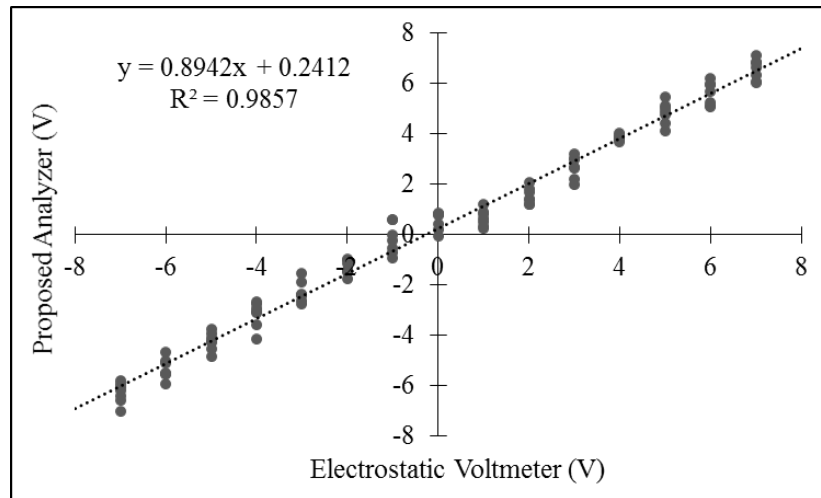
**Figure 21.** The overall correlation between the prototype analyzer operated in partial surfaces analysis mode and electrostatic voltmeter.

The evaluation was prepared in the same configuration as [A2] but the plate was measured by the electrostatic voltmeter which was used in [A3]. The linear equation shows good correlation with the gain which is close to unity, the offset error which is close to zero and $R^2$ which is higher than 0.9. Thus, this linear equation proved that each segment of the proposed analyzer could provide the accurate results compared to the conventional electrostatic voltmeter which is used to probe the electrostatic potential on the floating conductive sheet.

From the partial surfaces ion balance analysis result, the IDW data interpolation provides the finer-grained images of ion balance distribution like the heat map as shown in Fig. 22. The interpolation was calculated for the unknown data points from the 25-segment measured points in Fig. 20 based on (5) in [A5] with the exponent $n=1$. However, the IDW interpolation will not remove the large voltage variations in the multi-plate measurement. It only estimates the unknown data points within the range of measured points and keeps the values which were measured by the 25-segment multi-plate sensor.
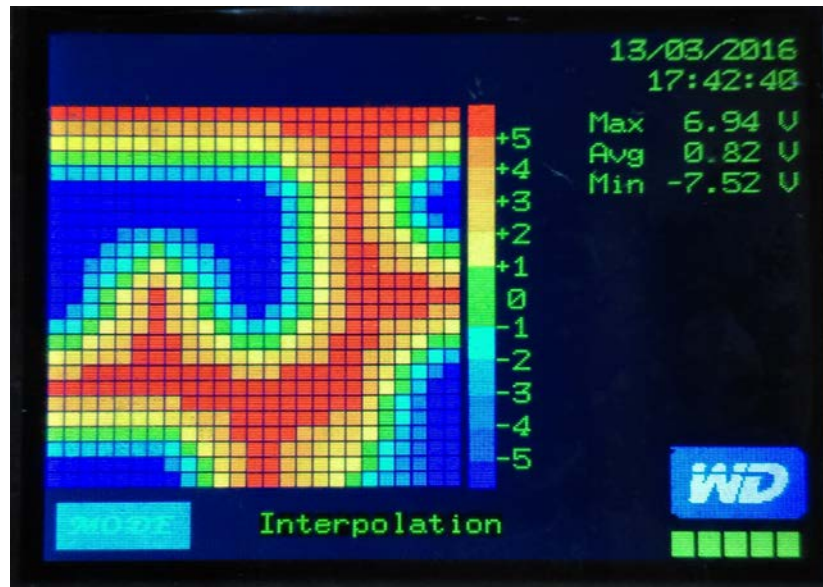
**Figure 22.** The ion balance distribution imaged as the heat map of Fig. 20 refined by proposed analyzer with IDW interpolation.

At this moment, there is no conventional equipment which can provide fine-grained result for comparing with the results interpolated by the partial surfaces analyzer. However, the verification could be done by using the data in Fig. 20 to interpolate by an external program. Fig. 23-26 are extended works for validating data interpolation purpose. The 25-segment results data in Fig. 20 were further used to image the ion balance distribution as the heat map in Fig. 23 and the surface plots with contour lines in Fig. 24 by the Gnuplot [31] which is an open-source plotting program.

The heat map of ion balance distribution image of the proposed analyzer in Fig. 22 shows the same trend as the Gnuplot in Fig. 23. This figure shows a bit different shade in the center areas between the measured points. This different shade suspected to the colour classified by the Gnuplot that could provide the finer-grained levels than the proposed analyzer.
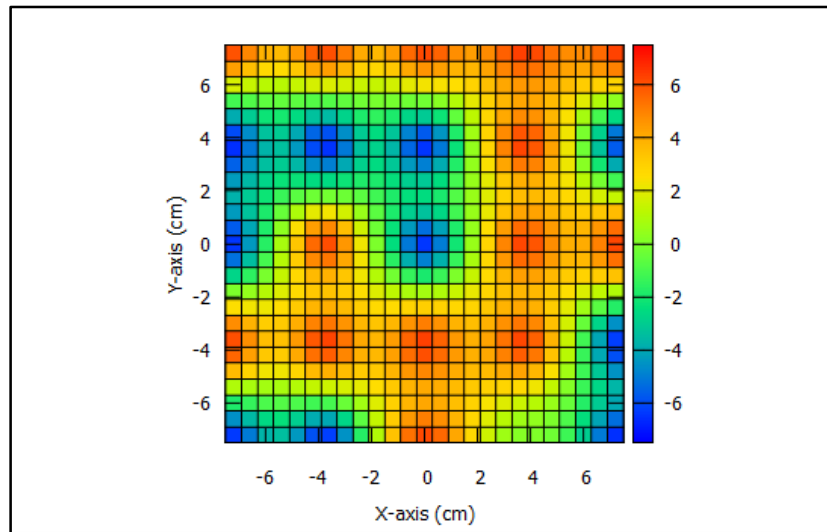
**Figure 23.** The ion balance distribution imaged as the heat map of Fig. 20 refined by Gnuplot, using IDW interpolation with exponent n=1.
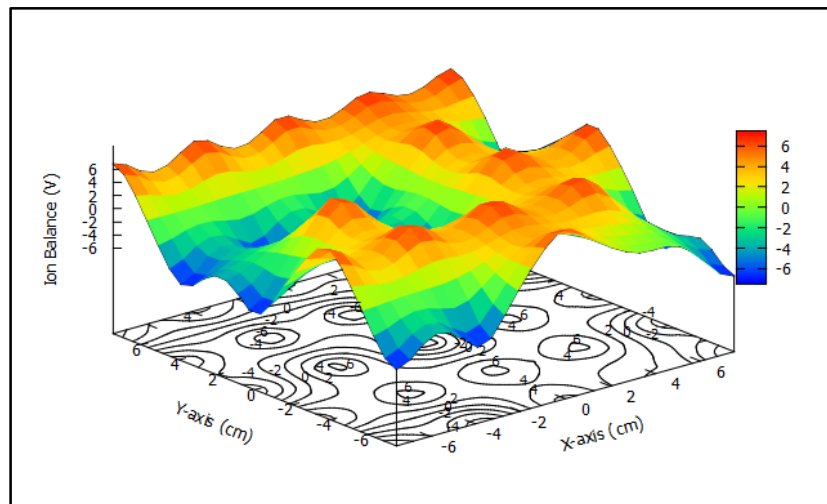


**Figure 24.** The ion balance distribution imaged as the surface and contour plots of Fig. 20 refined by Gnuplot, using IDW interpolation with exponent n=1.

Fig. 24 shows the ion balance distribution imaged as the surface plot with the contour lines. This image emphasizes the different levels at of the interpolated data points between the measured data points. In addition, the spline interpolation was evaluated using the same data points. The heat map in Fig. 25 is closely the same as Fig. 22. Then, the surface plot and contour line plot in Fig. 26 emphasizes with a more reasonable image of the ion balance distribution.
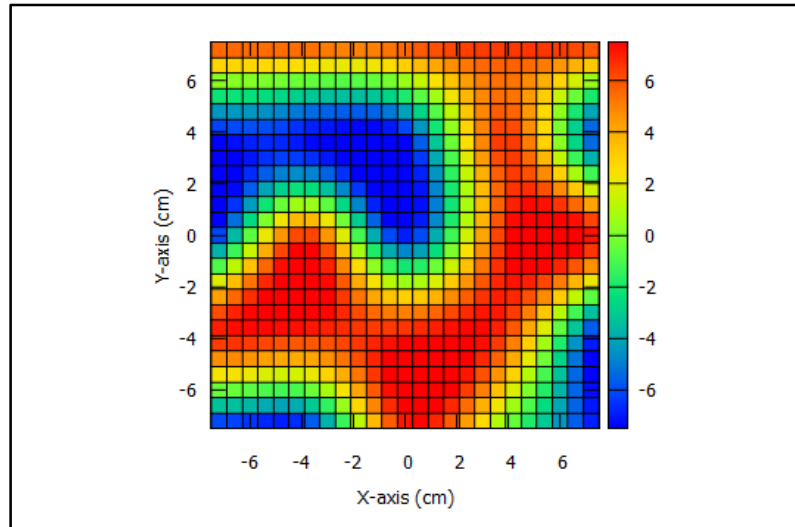
**Figure 25.** The ion balance distribution imaged as the heat map of Fig. 20 refined by Gnuplot, using spline interpolation.
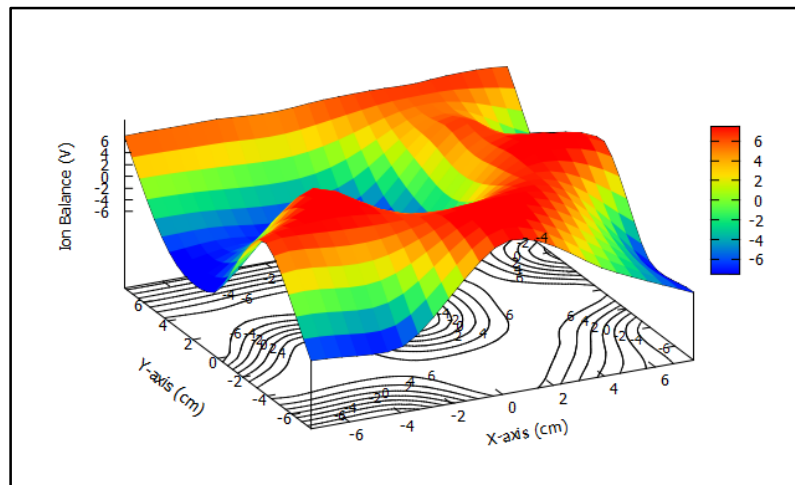


**Figure 26.** The ion balance distribution imaged as the surface and contour plots of Fig. 20 refined by Gnuplot, using spline interpolation.

## 3.4 Results Summary

The proposed analyzer offers the finer-grained assessments of the ion balance than the conventional one due to the partial surfaces analysis and resolution enhancement with IDW interpolation. The plate-averaged readings correlated well and linearly with a conventional analyzer. The overall segmented

plate size matched with the standard CPM which was used as reference. Finally, this proposed analyzer could express the ion distribution profile which is hidden by the large size ion receiving plate.

However, this prototype analyzer has only been built for proof-of-concept of the partial surface ion balance analysis, demonstrating in the laboratory level, and observing a spatial variation in the ion balance distribution. This encourage further studies of stability and reproducibility of such distributions. The user-friendly function, cover and casing are necessary to be designed and optimized for the actual production use.

# CHAPTER 4

# CONCLUSIONS AND REMARKS

Since the prototype analyzer was demonstrated, then this chapter sum-up the results which were reported and discussed in the previous chapter. Finally, the remarks of this thesis are stated at the end of this chapter.

## 4.1 Conclusions

The prototype of the partial surfaces ion balance analyzer has been developed corresponding to the four key processes: conceptual design, feasibility study, detail design and prototype design. The prototype analyzer offers finer-grained assessments of the ion balance than the conventional CPM, due to its multi-plate sensor. The plate-averaged readings correlated well and nearly linear with a standard analyzer. The segmented plate size matched that of the standard measurement which was used as reference. However, strongly varying ion balance distributions over the segmented measurement plates were clear when assessed graphically. The observations highlighted the potential non-uniformity issues with ionized air.

The image resolution was enhanced by the IDW interpolation method. This interpolation did not assess any value out of range of the measured values, while the ion balance distribution was attractive imaged visually, and corresponding to reality. The multi-plate ion balance analyzer has been demonstrated in these initial proof-of-concept tests, and the observed spatial variations in the ion balance distribution encourage further studies of stability and reproducibility of such distributions. If, to the contrary, all sensor plate segments had given similar results, then this study would indicate that there is no need for the high spatial resolution of a multi-plate sensor.

## 4.2 Remarks

This thesis demonstrated the key important method for identifying the ionizer performance in term of ion balance distribution characterizing. The partial surfaces measurement by the developed analyzer could indicate the image of the ion balance distribution clearly. This analyzer suitable for ion balance measurement of the critical electrostatic protected areas which are handling the small footprint of electrostatic discharge sensitive devices such as integrated circuit or head gimbals assembly.

## Reference:

[1]    C. Hafner, J. Smajic and M. Agio, "Numerical Methods for the Electrodynamic Analysis of Nanostructures," in *Nanoclusters and nanostructured surfaces*, 1st Edition, A. Ray, Ed. Stevenson Ranch, CA: American Scientific Publishers, pp. 207-274, 2010.

[2]    H. W. Hart and B. John A, *Engineering Electromagnetics,* 8th Edition, McGraw-Hill, NY, USA, 2012.

[3]    T. Carozzi, A. Eriksson, B. Lundborg, B. Thidé and M. Waldenvik, *Electromagnetic Field Theory,* 2nd Edition, Dover Publications, 31 East 2nd Street Mineola, NY, USA, 2011.

[4]    H. H. Skilling, *Fundamentals of Electric Waves (Translated by Mongkol Dejnakarintra, PhD.),* Chulalongkorn University Press, Chulalongkorn University, Bangkok, Thailand, 2011.

[5]    C. A. Balanis, *Advance Engineering Electromagnetics,* 2nd Edition, John Wiley & Sons, Inc., NJ, USA, 2012.

[6]    *Electrostatic Discharge (ESD) Technology Roadmap–Revised March 2013*, ESD Association, 7900 Turin Road, Bldg. 3, Rome, NY, 2013.

[7]   A. Castellanos, *Electrohydrodynamics,* CISM Courses and Lectures no. 380, Springer-Verlag,Wien, NY, USA, 1998.

[8]   F. W. Peek, *Dielectric Phenomena in High Voltage Engineering,* McGraw-Hill, NY, USA, 1929.

[9]   J. R. Roth, "Aerodynamic Flow Acceleration using Paraelectric and Peristaltic Electrohydrodynamic Effects of a One Atmosphere Uniform Glow Discharge Plasma*," Physics of Plasmas*, vol. 10, pp. 2117-2126, 2003.

[10]   A. Ohsawa, "Modeling of Charge Neutralization by Ionizer," *Journal of Electrostatic*, vol. 63, pp.767-773, 2005.

[11]   A. Ohsawa, "Efficient Charge Neutralization with an AC Corona Ionizer," *Journal of Electrostatic*, vol. 65, pp. 598-606, 2007.

[12]   A. Ohsawa, "2-D Electrohydrodynamic Simulations towards Zero Offset Voltage with Corona Ionisers," *Journal of Electrostatic*, vol. 71, pp. 116-124, 2013.

[13]   A. Ohsawa, "Computer Simulations of Insulator Charge Neutralisations with a Corona Ioniser-Influence of Initial Surface Charge Distribution," *Journal of Electrostatic*, vol. 71, pp. 287-293, 2013.

[14]   N. E. Jewell-Larsen, S. V. Karpov, I. A. Krichtafovitch, V. Jayanty, C. Hsu, and A. V. Mamishev, "Modeling of Corona-induced Electrohydro-dynamic Flow with COMSOL Multiphysics," *Proc. ESA Annual Meeting on Electrostatics 2008*, Paper E1.

[15]   *ANSI ESD STM 3.1-2015: EOS/ESD Association Standard for Protection of Electronic Discharge, Susceptible Items-Ionization, ESD Association*, 7900 Turin Road, Bldg. 3, Rome, NY, 2015.

[16]   *IEC 61340-4-7: ELECTROSTATICS Part 4-7: Standard test methods for specific applications–Ionization*, International Electrotechnical Commission, 2010.

[17] K. Takahashi, M. Sato, T. Ohkubo, T. Fujiwara, and K. Takaki, "2-D Measurement of Charged Particles Diffusing from a Double DC Corona Discharge Ionizer," *IEEE Trans. Plasma Sci.*, vol. 41, no. 8, pp. 1863–1868, Aug. 2013.

[18] A. McCarthy and W. Lukaszek, "A New Wafer Surface Charge Monitor (CHARM)," *Proceedings of the 1989 International Conference on Microelectronic Test Structures*, Edinburgh, Scotland, March 13-14, pp. 153-156, 1989.

[19] W. Lukaszek, E. Quek and W. Dixon, "CHARM2: Towards an Industry-Standard Wafer Surface-Charge Monitor," *Advanced Semiconductor Manufacturing Conference*, 1992.

[20] M. Lee, J. R. Hu, W. Catabay, P. Schoenborn and A. Butkus, "Comparison of CHARM-2 and Surface Potential Measurement to Monitor Plasma Induced Gate Oxide Damage," *Proc. Int. Symp. Plasma Process-Induced Damage*, pp.104 -107, 1999.

[21] R. Rodrigo et al., "CPM Study: Discharge Time and Offset Voltage, Their Relationship to Plate Geometry," *Electrical Overstress/Electrostatic Discharge Symposium Proceedings*, pp. 1-5, 2004.

[22] V. Kraz, "Notes on Maintaining sub-1V Balance of an Ionizer," *Electrical Overstress/Electrostatic Discharge Symposium (EOS/ESD)*, pp. 1-6, 2004.

[23] V. Kraz, S. Cruz, and K. A. Martin, "Method and Device for Controlling Ionization," US Patent, Patent No. US 7,522,402 B2 (2009).

[24] J. Crowley, A. Ignatenko, and L. Levit, "Biased-Plate Characterization of Pulsed DC Ionizers," *Journal of Electrostatics*, vol. 62, pp. 219-230, 2004.

[25] N. Jindapetch, S. Plong-ngooluam, K. Thongpull, K. Chetpattananondh, "A Low Voltage Decay Time Analyzer for Monitoring Ionizers," *Journal of Electrostatics*, vol.70, pp. 489-498, 2012.

[26] P. Secker and J. Chubb, "Instrumentation for Electrostatic Measurements," *Journal of Electrostatics*, vol. 16, pp. 1-19, 1984.

[27] P. Secker, "The Design of Simple Instruments for Measurement of Charge on Insulating Surfaces," *Journal of Electrostatics,* vol. 1, pp. 27-36, 1975.

[28] J. Chubb, "Measurement of Tribo and Corona Charging Features of Materials for Assessment of Risks from Static Electricity," *IEEE Trans. Industry Applications,* vol. 66, no. 6, pp. 1182-1187, 1990.

[29] J. Chubb, "Instrumentation and Standards for Testing Static Control Materials," *IEEE Trans. Industry Applications,* vol. 36, no. 6, pp. 1515-1522, 2000.

[30] B. Benamar, E. Favre, A. Donnot and M.O. Rigo, "Finite Element Solution for Ionized Fields in DC Electrostatic Precipitator," In *Proceeding of COMSOL Users Conference Grenoble*, Grenoble, France, 2007.

[31] *MINITAB Handbook: Update for Release 16*, 6th Edition, Brooks/Cole Publishing Co., Pacific Grove, CA, USA, 2010.

[32] P. K. Janert, *Gnuplot in Action*, 2nd Edition, Manning Publications, New York, USA, 2016.

**APPENDICES**

# A1-3D Computational Simulations of Electrostatic Potential in Partial Surfaces towards the Precision of Ion Balance Analysis

Sayan Plong-ngooluam[1,a], Nattha Jindapetch[2,b], Phairote Wounchoum[2,c], Duangporn Sompongse[1,d]

[1]Western Digital (Thailand) CO., LTD. Bang Pa-In, Phra Nakhon Si Ayutthaya, Thailand

[2]Department of Electrical Engineering, Faculty of Engineering, Prince of Songkla University, Hat Yai, Songkhla, Thailand.

[a]Sayan.Plong-ngoolaum@wdc.com, [b]nattha.s@psu.ac.th, [c]phairote.w@psu.ac.th,[d]Duangporn.Sompongse@wdc.com

**Abstract.** This paper reports a 3-D computational simulation of electrostatic potential uniformity which was affected by various measurement plates. The finite element analysis method was done by COMSOL Multiphysics to model the electrostatic potential behavior. The electrostatic potential from two electrodes in the free space plane was modeled and used as a reference result to compare with the electrostatic potential results of four various measurement plates including the standard 6″×6″ charged plate and its dividing by four, nine and sixteen segments. This investigation revealed the uniformity error of the electrostatic potential from the conventional plate. The precision of ion balance analysis can be improved by the using of a partial surface, i.e. by dividing the conventional plate into many smaller-size plates.

## Introduction

Electrostatic discharge (ESD) became a problem in electronic industry since 1970s [1]. The ESD events were causing of device failures, manufacturing yield losses and system interference. Grounding is a general method for electrostatic discharge protection. It is used to drain the electrical charge to the ground and to make equipotential situation. However, it is less effective to remove the static charges from insulative surfaces or isolated conductive materials. The ionizers are widely used to remove these static charges by providing the opposite polarity ions to neutralize the object surfaces. Therefore, the ion balance analysis guarantees the good-function ionizers.

In order to characterize the ionizer, ANSI/ESD STM3.1-2006 [2] and IEC 61340-4-7 [3] constitute a standard test method (STM) for evaluation and selection of the ionizers. The STM requires the ion balance measurement to identify the balance of positive and negative ions. However, the STM defines the ion balance by the measurement of voltage on a floated 6″×6″ conductive surface. In current situation, the electronics manufactories that produce a miniaturized device such as an integrated circuit or magneto resistive head are requiring the ion balance within +/-1V or even tighter for the safety electrostatic sensitive devices. The sub-1V ion balance environment requires the sufficient resolution and accuracy to measure ionizer balance [4]. The conventional ion receiving plate leads the insufficient resolution of ion balance measurement due to the exposure conductive is too much larger than the handled devices. Then, the miniaturized ion balance analyzer using a 1″×1″ plate was launched to serve the sub-1V ion balance measurement. However, such a miniaturized analyzer does not characterize the full size of the planar surface that is measured by the conventional plate due to their analyzed results are single points at a time.

This paper aims to simulate the electrostatic potential uniformity that has been changed by placing of various measurement plates in the synchronously time. The modeling is guided by the study of ionized fields in DC electrostatic precipitator in [5]. In addition, the partial surfaces that are divided from the conventional plate into 4, 9 and 16 segments are analyzed for validating the feasibility of measurement error reduction by the partial surfaces ion balance analysis.
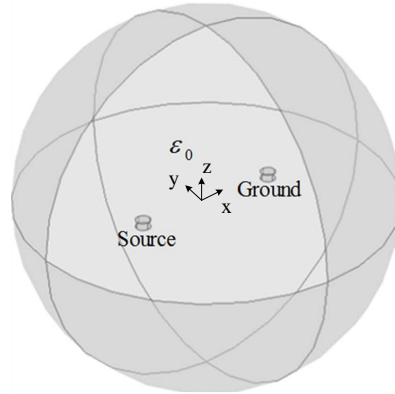
Figure 1. A reference model of electrostatic environment.

**Mathematical Model**

The Gauss's law says that the electric field in any closed surface of a free space is equal to the total charge that is enclosed by that surface [5]. It can be constituted by the divergence theorem as

$$\nabla \cdot \mathbf{E} = \frac{\rho_v}{\varepsilon_0}. \tag{1}$$

Equation (1) is relating to the electric potential as (2).

$$\mathbf{E} = -\nabla V \tag{2}$$

where $\mathbf{E}$ is an electric field, $\rho_v$ is a volume charge density, $\varepsilon_0$ is a permittivity of free space and $V$ is an electric potential. By substituting (2) into (1), we can obtain the Poisson's equation as

$$\nabla^2 V = -\frac{\rho_v}{\varepsilon_0}. \tag{3}$$

If there is no any quantity of charge density in the interested domain, the right hand side of (3) is equal to zero. It becomes a Laplace's equation following (4).

$$\nabla^2 V = 0 \tag{4}$$

From (1), the electric field $\mathbf{E}$ is depended on permittivity of free space $\varepsilon_0$. The vector field $\mathbf{D}$ is an electric displacement or electric flux density that is simplified from the electric field as

$$\mathbf{D} = \varepsilon \mathbf{E}. \tag{5}$$

**Boundary Conditions**

A reference electrostatic environment is modeled in 3-D computation on the COMSOL Multiphysics using the electrostatic module as the geometrical illustration in Fig.1. It is a comprising of two cylindrical electrodes which one centimeter in radius and height. These electrodes are assigned to ground and a voltage source. There are placed in the center of 50 centimeters spherical vacuum environment with 20 centimeters separation distance. The 1000V of electric potential is applied for all boundaries of the source domain. All boundaries of the ground domain are configured as ground. Then, the simulated one millimeter-thick aluminum conductive plates are illustrated in Fig. 2. These plates are placed between the source and the ground. All boundaries are configured as a floating potential with the initial charge of zero coulomb.
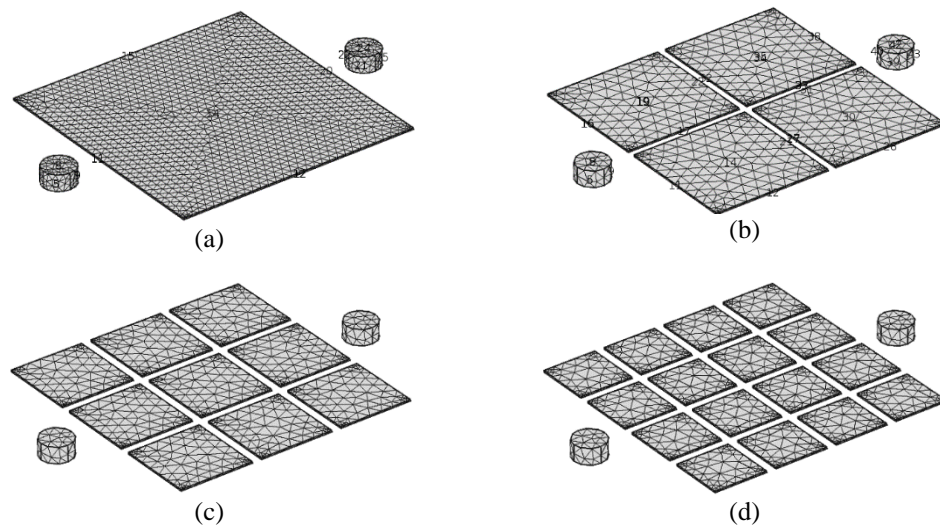
Figure 2. The geometrical meshes of source, ground and conductive plates, (a) A 6″×6″plate, (b) A 4-segment plate, (c) A 9-segment plate and (d) A 16-segment plate.

## Results

The electric flux is illustrated by the steam line over the half cut plane of electric potential in Fig. 3. These results are explaining that electric flux can be induced by the conductive plate and made uniformity changed. The electric flux uniformity has been changed after the conductive plates are placed between the electrodes. The highest change has been observed when the 6″×6″plate has been placed. Then, the changes are reduced after replacing by a 4-segment plate, 9-segment plate and the significant reduction has been observed when a 16-segment plate has been placed. From (5), the electric flux density $\mathbf{D}$ is proportional to the electric field $\mathbf{E}$ on (2) which is relating to electric potential $V$. Thus electric potential $V$ can be induced when the conductive plate has been placed. The planes from Fig.3 can be sheared as a flat sheet at the center in the xy plane and analyzed by a two dimensional surface plots with contours. In addition, the 2-D surface is included for more clearly as shown in Fig. 4. The multiple levels of electrostatic potential are observed over the isosurface plot when the measurement surface is divided. The isosurface plots in Fig.4 explain that the change of electric potential uniformity is highest when the conventional 6″×6″ plate is placed due to the single level of electric potential as shown in Fig. 4(b). It validates the feasibility of the measurement error when this result is compared to the reference result in Fig. 4(a). The multiple levels of electric potential are observed when the plate has been divided to 4-segment, 9-segment and 16-segment plates. This indicates the reduction of the measurement error.

## Conclusions

In this paper, we have investigated the electric potential uniformity that changed after the conductive plates have been placed for the potential measurement. The analytical model has been done by the using of COMSOL Multiphysics in 3-D computation. The modeling results revealed that the electric potential can be changed by the induction of conductive surfaces. These results are validating the feasibility of resolution enhancement of ion balance analysis by the partial surface method. This enhancement suits for the small footprint devices such as single chip, integrated circuit or head gimbals assembly of hard disk drives.

## Acknowledgements

(a) Free space  (b) $6'' \times 6''$ plate  (c) A 4-segment plate

(d) A 9-segment plate  (e) A 16-segment plate
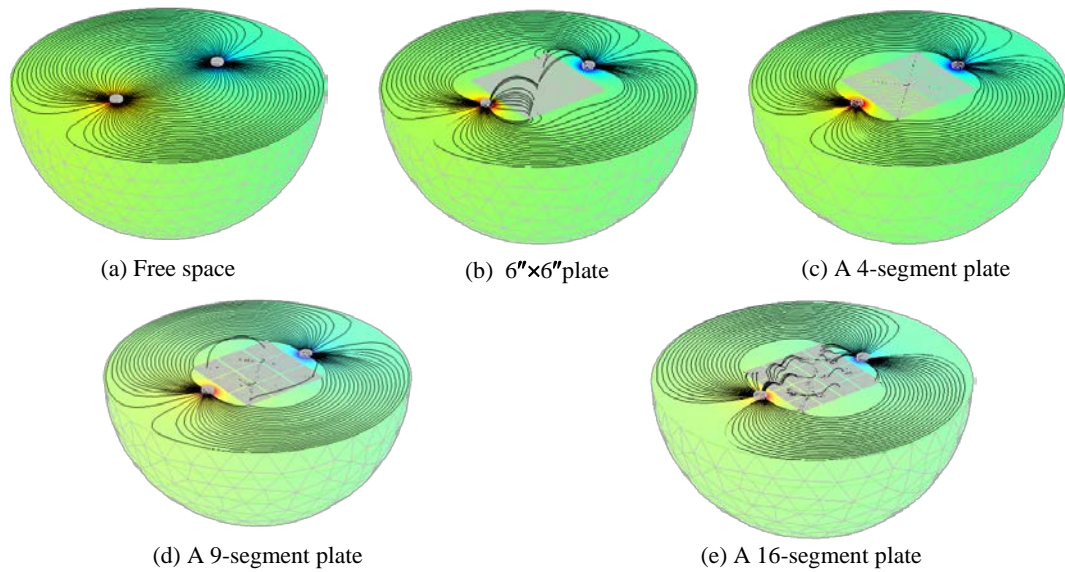
**Figure 3**. The cut planes of electric potential plots with electric flux illustrations in; (a) free space without measurement plate, (b-e) the changes after placing various measurement plates.



(a) Free Space  (b) A $6'' \times 6''$ plate  A 4-segment plate

(d) A 9-segment plate  (e) A 16-segment plate
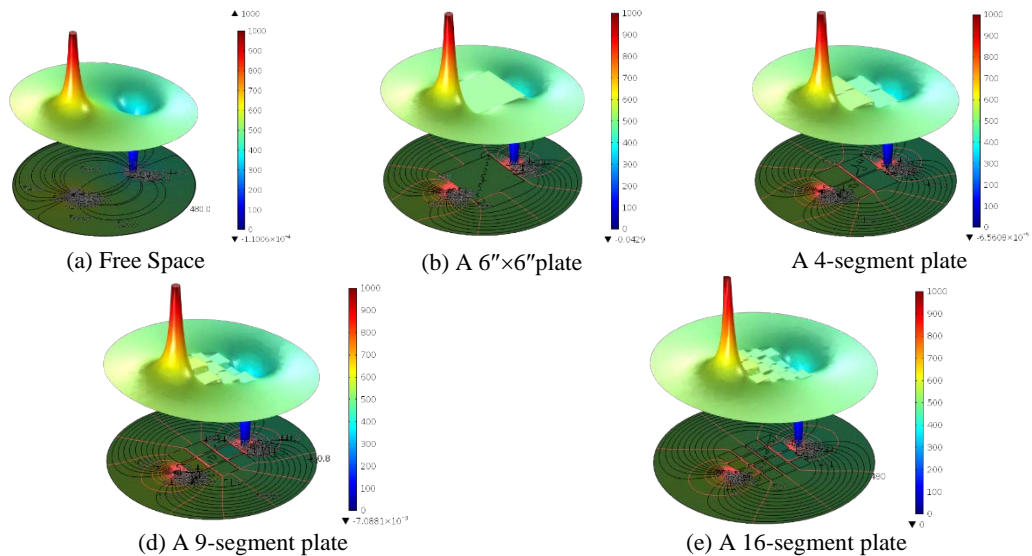
**Figure 4**. The 2-D surface, contour and isosurface of electric potential plots; (a) free space without measurement plate, (b-e) the electrical flux changes after placing various measurement plates.

### References

[1] ESD Association Standards Committee, Electrostatic Discharge (ESD) Technology Roadmap, ESD Association, 2013.

[2] ESD Association Standards Committee, ANSI ESD STM 3.1-2006: The Protection of Electrostatic Discharge Susceptible Items-Ionization, ESD Association, 2006.

[3] IEC technical committee, IEC 61340-4-7: Electrostatics−Part 4-7: Standard test methods for specific applications−Ionization, International Electrotechnical Commission, 2010.

[4] V. Kraz, "Notes on maintaining sub-1V balance of an ionizer," Electrical Overstress Electro-static Discharge Symposium (EOS/ESD), (2004).

[5] B. Benamar, E. Favre, A. Donnot, and M.O. Rigo, "Finite element solution for ionized fields in DC electrostatic precipitator," Proceedings of COMSOL Users Conference Grenoble, (2007) International Conference on Electrical & Electronic Technology 2016.

# A2-Partial measurement of planar surface ion balance analysis

## Sayan Plong-ngooluam[a,b,*], Nattha Jindapetch[b], Phairote Wounchoum[b], Duangporn Sompongse[a]

[a]*Western Digital (Thailand) CO., LTD. Bang Pa-in, Phra Nakhon Si Ayutthaya, 13160, Thailand*
[b]*Department of Electrical Engineering, Faculty of Engineering, Prince of Songkla University, Hat Yai, Songkhla, 90112, Thailand*

**ABSTRACT**

This paper reports the experimental results of the partial surfaces ion balance analysis on the ionized planar surface to identify the fine-grained level of ionizer balance measurement. The standard 6″×6″ charged plate was exposed under the ionized air which was supplied from the DC corona ionizer to measure the ion balance. Then the one square inch charged plate had been used to measure the ion balance in the 36-segment partial measurement points which were ordinary arranged on that planar surface. These 36-segment partial results were analyzed by the statistical software to image the ion balance distribution on that planar surface. The experiment revealed the fined-grained levels could be identified behind the coarsely results which had been measured by the standard charged plate. The surface plot could image the ion balance distribution on that planar surface which was ionized by the ionizer thoroughly. This ion balance imaging could be used to enhance the ionizer performance analysis in term of ion balance and distribution along the ionized surface.

**Introduction**

The electrostatic discharge (ESD) had been a problem in electronics industry because the ESD events could be damaging devices, harming the systems or inducing the particulate contamination on the charged surfaces due to electrostatic forces (ESD Association, 2014). In general, the ground connecting is a simple method for making an equipotential surface to drain out the electrostatic charges to the system ground. However, this method is less effective to remove the electrostatic charges from the insulator surface or conductive particles (Glor, 1985; Robinson *et al.* 2009) due to availability of conduction and conductivity of these objects. To prevent these electrostatic problems, the air ionization is the widely used technique to remove the electrostatic charges from the insulator surfaces or the tiny conductive objects which are unable to connect the ground cable. The air ionizer provides the opposite polarity ions to neutralize the electrostatic charges on the object. It is necessary to measure the balance of these supplied ions because the ionizers could be acting as the electrostatic charges generators while the sourced ions are unbalanced.

The ANSI/ESD STM3.1-2015 (ESD Association, 2015) is a standard test method (STM) for characterizing the ionizer performance. It defines the ion balance as the electrostatic potential value caused by the ion collecting on a floated 6″×6″ conductive plate with 20 pF capacitance. This configuration was agreed with a typical silicon wafer at the time of drafting the standard in the late of 1980s (Rodrigo *et al.,* 2004). However, many electronics manufacturers are working on the small scale, which is handling the tiny devices such as the magneto resistive heads. They are requiring the ion balance within +/-1V or tighter for the safety of electrostatic sensitive (ESDS) devices (Kraz, 2004). They might concern to the precision of ion balance measurement because the actual devices are much smaller than the standard charged plate. The smaller plate reports a less ion balance voltage than a larger plate (Rodrigo *et al.,* 2004). Then the small charged plate analyzers were launched to serve the sub-1V ion balance measurement such as the ionizer controllers on US patents 6,985,346 B2 (Kraz *et al.,* 2006), US 7,522,402 B2 (Kraz *et al.,* 2006) and the biased-plate monitor (Crowley *et al.,* 2004). These analyzers provide alternative methods to identify the ion balance with the miniaturized plates to collect the ions from ionizer and correlate the result to the standard charged plate monitor result described on STM.

However, the ions distribution depends on the drift velocities and the airflow velocities as reported in the electrohydrodynamics theory investigation on the ionizer models (Ohsawa, 2013). The electrostatic potential on each foot-step might not uniform due to the fluid dynamic functions. The modeling (Plong-ngooluam *et al.*, 2015) has mentioned that ion balance measurement precision could be enhanced by the surface dividing. Anyway, this simulated result still need the field measurement in the ionized environment to validate the feasibility of that simulated results.

In this work, the ion balance on the 6″×6″ planar surface was partially analyzed by the miniaturized charged plate, which was ordinary arranged as the same area as the standard charged plate measurement. The partial results were imaged by the surface plot to express the ion balance distribution along the 6″×6″ planar surface which was neutralized by the ionized air from the DC corona ionizer.

**Ion Balance Measurement**

The ionizer is an equipment that provides either positive or negative air ions to neutralize the electrostatic charges on the surface or tiny object. The typical corona ionizer generates the ions by the collision between the neutral molecules and electrons when they are accelerated by an electric field which exceeds the inception level described by on (Ohsawa, 2005). These emitted air ions would attract an object surface and neutralize it. Then, ion balance could be described by the electrostatic potential ($V$) which depends on the positive ion ($n_p$) and negative ion densities ($n_n$) as

$$\nabla^2 V = \frac{-e(n_p - n_n)}{\varepsilon_0},\tag{1}$$

where $e$ is an elementary charge and $\varepsilon_0$ is the permittivity of free space.

The motions of positive ion ($n_p$) and negative ion ($n_n$) in (1) depend on the air velocity as

$$\frac{\partial n_p}{\partial t} + \nabla \cdot (n_p \mathbf{u}_p) - D_p \nabla^2 n_p = -\beta n_p n_n \qquad Positive,\tag{2}$$

$$\frac{\partial n_n}{\partial t} + \nabla \cdot (n_n \mathbf{u}_n) - D_n \nabla^2 n_n = -\beta n_p n_n \qquad Negative,\tag{3}$$

where $\mathbf{u}_p$ and $\mathbf{u}_n$ are air velocities including of positive and negative ion mobilities, $D_p$ and $D_n$ are positive and negative ion diffusion coefficients, and $\beta$ is the ion-ion recombination coefficient.

Since the ion balance is defined by the electrostatic potential value which is caused by an accumulation of positive and negative ions, it can be expressed by the ratio of the total amount of charge ($Q$) which is accumulated on that plate and ion receiving plate capacitance ($C$) as

$$V = \frac{Q}{C}.\tag{4}$$

Assume that charge distribution on the ion receiving surface and electrostatic feild are uniform, the total amount charge ($Q$) can be  defined as

$$Q = \rho_S A,\tag{5}$$

where the $\rho_S$ is the density of charge on the ion receiving surface (*A*). This charge density is the summed result of ion balancing term of (1) which can be defined as

$$\rho_S = e(n_p - n_n) .$$ (6)

By the substitution (5) on (4), the electrostatic potential (*V*) proportionally depends on the ion receiving surface and the charge density as

$$V = \frac{\rho_S A}{C} .$$ (7)

Based on this assumption, it could be concluding that the ion balance which is measured by the smaller surface will be lower than the bigger surface when the ion distribution is uniform and the plate capacitance is fixed conditions. However, the surface charge density on (6) depends on the ion motion (2) and (3) which are concerning to the air velocity. The $6''\times6''$ planar surface with the fixed 20pF capacitance which is constituted by the STM might not represent the suitable grain result which depends on the ion motions.

## Experimental Setup and Analytical Method

This section describes the apparatus such as the ionizer configuration, the $6''\times6''$ charged plate, the arrangement of the $1''\times1''$ charged plate, and the partial measurement evaluation. Moreover, the analytical method is described at the end of this section.

### Apparatus

The charged plate analyzer Trek model 157 with the standard 20pF $6''\times6''$ planar surface plate was used to measure the ion balance as the standard ionizer measurement. Then the partial measurement was performed using the $1''\times1''$ miniaturized plate. With this plate, the total capacitance still fixed at 20pF as same as the standard plate capacitance. The 36-segment partial measurement points were ordinary arranged over the standard $6''\times6''$ planar surface plate as shown in Fig.1. The DC corona ionizer MKS model 5802i was installed over the non-obstructive workstation with a grounded surface. The ionizer was located at the center of the workstation with 60 centimeter in height from the grounded surface. The charged plates were placed at 45 centimeter under the ionizer facing with the 15 centimeter from the grounded surface as describes on the STM.

### Partial Measurement Evaluation

The evaluation was started by adjusting the ionizer balance to -1.0 Volt which was measured by the standard $6''\times6''$ plate. After adjusted the ionizer, the standard $6''\times6''$ plate was moved out then placed the $1''\times1''$ charged plate and measured the ion balance at the arranged points as shown in Fig.1. The measurement was performed from the first segment through the 36th segment sequentially. Then repeat the evaluation with the 0.0 Volt and +1.0 Volt ion balance adjustment.
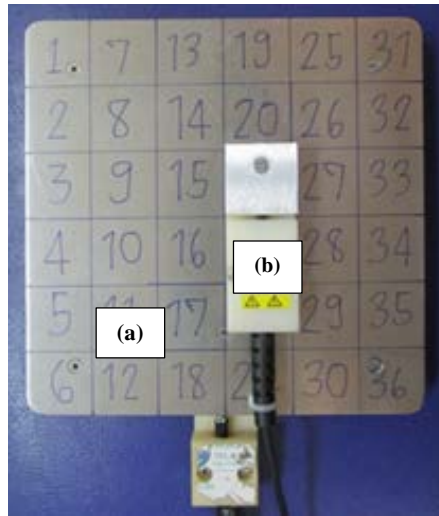
**Fig. 1:** The partial measurement point on the planar surface arranging;
(a) The standard 6″×6″ charged plate.
(b) The 1″×1″ square plate.

*Analytical Method*

The Minitab, a statistical software, provides the wireframe plot to image the relationship between three variables in the x, y and z coordination. In this work, the 36-segment partial measurement results were assigned as response values z which were arranged in the x-y plane according to the plate arrangement in Fig.1. The Minitab also provides the distance method (Ryan *et al.,* 2010) to interpolate the unknown data points between the measured data points. All data points which are interpolated by this method always within the range of measured data points. It works well in a wide range of circumstances. The number of x and y meshes could be determining the resolution of the regular grid. In this experiment, the distance method was using to interpolate the ion balance distribution over the 6″×6″ planar surface with the regular 50×50 mesh from the 6×6 measured data points as the arrangement in Fig. 1. This interpolation is proposed to enhance the fine-grained levels of ion balance results beyond the actual measured results which were measured from the 36-segment partial surface.

**Results and Discussions**

The partial measurement reported the results in the six rows and six columns. The rows are intersections in the y axis and intersections in the x axis. The ion balance distributions have been analyzed and imaged by the wireframe plot with the 50×50 meshes data interpolation using distance method. The partial measurement results of ion balance from the -1.0 Volt ionizer adjustment are summarized in Table 1. The measurement values were varying from -1.0 to -0.4 Volt. These results could be used to image the ion balance distribution as shown in Fig. 2. The image is expressing the fine-grained levels over the 6″×6″ planar surface and vary around -0.5 Volt from the settled point which was adjusted and measured by the standard 6″×6″ charged plate.

TABLE 1 The partial measurement results of ion balance from the ionizer with -1.0 Volt adjustment (unit in Volt).

|     | C1   | C2   | C3   | C4   | C5   | C6   |
| --- | ---- | ---- | ---- | ---- | ---- | ---- |
| R1  | -0.8 | -0.7 | -0.4 | -0.8 | -0.7 | -0.7 |
| R2  | -0.8 | -0.7 | -0.6 | -0.8 | -0.9 | -0.8 |
| R3  | -0.9 | -0.8 | -0.5 | -0.8 | -0.9 | -0.6 |
| R4  | -0.6 | -0.8 | -0.7 | -0.8 | -0.8 | -0.8 |
| R5  | -0.7 | -0.7 | -0.7 | -0.8 | -0.7 | -1.0 |
| R6  | -0.7 | -0.7 | -0.7 | -0.7 | -0.8 | -0.9 |

The partial measurement results of ion balance from the 0.0 Volt ionizer adjustment are summarized in Table 2. The measurement values were varying from -0.3 to 0.3 Volt. This result proves that the performance of ionizer under test is capable with the sub 1V ion balance control workstation requirement because all data points are within the range of +/-1 Volt. The ion balance distribution image of the 0.0 Volt ionizer adjustment is shown in Fig. 3. It expresses the fine-grained levels which vary around +/-0.3 Volt from the settled point. However, the minimum and the maximum points are not locating in the same positions as the ion balance image in Fig. 2. The suspicion might be the variation of the turbulence of the air that was driven by the fan unit which was install in the ionizer. This turbulence could affect to the ions mobility mechanisms in the ions transport region, regarding to the electrohydrodynamics theory which is the interactive mechanism between the electric fields and the surrounding fluid.
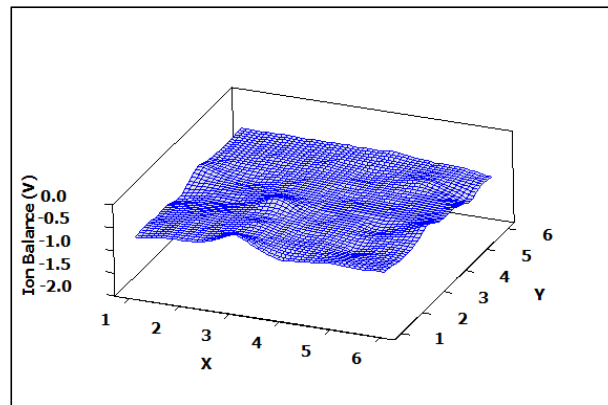


Fig. 2: The ion balance distribution image with -1.0 Volt ionizer adjustment.

TABLE 2 The partial measurement results of ion balance from the ionizer with 0.0 Volt adjustment (unit in Volt).

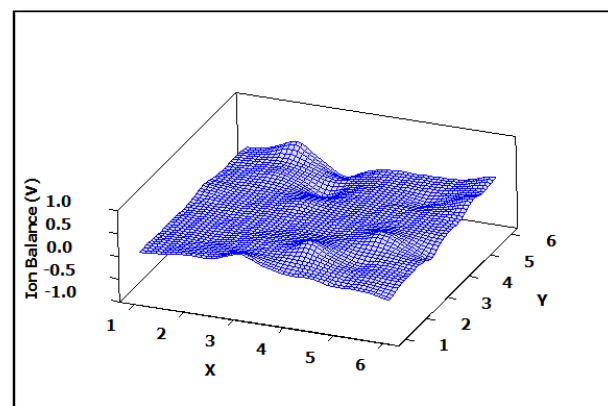|    | C1  | C2  | C3   | C4  | C5   | C6   |
|----|-----|-----|------|-----|------|------|
| R1 | 0.0 | 0.1 | 0.3  | 0.0 | -0.1 | -0.2 |
| R2 | 0.0 | 0.0 | 0.1  | 0.3 | -0.1 | -0.1 |
| R3 | 0.0 | 0.0 | 0.0  | 0.0 | 0.2  | -0.2 |
| R4 | 0.1 | 0.0 | 0.1  | 0.0 | 0.0  | 0.0  |
| R5 | 0.0 | 0.1 | -0.3 | 0.0 | -0.1 | 0.2  |
| R6 | 0.0 | 0.3 | -0.3 | 0.0 | 0.0  | 0.2  |



Fig. 3: The ion balance distribution image with 0.0 Volt ionizer adjustment.

The partial measurement results of ion balance from the 1.0 Volt ionizer adjustment are summarized

in Table 3. The measurement values were varying from 0.5 to 1.7 Volt. The ion balance distribution image is illustrated by the wireframe plot as shown in Fig. 4. The fine-grained levels of ion balance are expressing over the 6″×6″ planar surface as same as the ion balance distribution images from the -1.0 Volt and the 0.0 Volt adjustments. Based on these results, the ion balance were distributed over the 6″×6″ planar surface with +/-0.5 Volt variation. It validated the ionizer capability which needs for the workstation which requires to control the ion balance within +/-1Volt because these fine-grained levels results could be identified by the partial measurement technique. The ion balance results on the regular 50×50 mesh of the wireframe plots were consisting of measurement data points and interpolated data points. These data points were plotted at the at the x-y intersections of the mesh.

TABLE 3 The partial measurement results of ion balance from the ionizer with 1.0 Volt adjustment (unit in Volt).

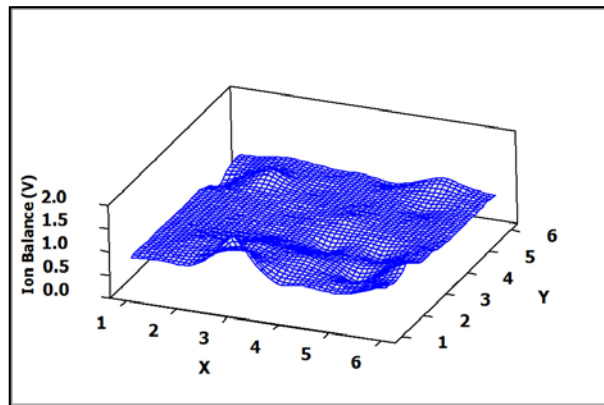|     | C1  | C2  | C3  | C4  | C5  | C6  |
| --- | --- | --- | --- | --- | --- | --- |
| R1  | 0.8 | 1.6 | 0.7 | 0.7 | 0.7 | 1.0 |
| R2  | 0.8 | 1.6 | 0.7 | 0.9 | 0.5 | 1.1 |
| R3  | 0.8 | 0.7 | 0.7 | 0.5 | 0.5 | 0.8 |
| R4  | 0.8 | 0.8 | 0.1 | 0.8 | 0.7 | 0.7 |
| R5  | 0.5 | 1.0 | 0.7 | 0.7 | 0.6 | 0.7 |
| R6  | 0.7 | 0.8 | 0.7 | 0.6 | 1.1 | 0.7 |



Fig. 4: The ion balance distribution image with 1.0 Volt ionizer adjustment.

## Conclusions

The experimental results validated that the partial surface measurement could identify the fine-grained levels of ion balance measurement result which could not be identified by the standard charged plate measurement. The results show the variation of the voltage levels on different areas of the planar surface. In the other word, the different area has the different voltage. The ion balance results measured by the large planar surfaces are losing such fine-grained voltage levels on different areas of the planar surface because the given result is the summation of all ions which are collected from the whole surface.

These partial measurement results also identify the ionized air uniformity over the 6″×6″ planar surface which is subjected to be neutralized. It could enhance the ion balance measurement precision in term of ions distribution characterization. Moreover, this partial measurement also provides the method of the suitable plate improvement for the ion balance measurement of electrostatic protective areas which are handling the tiny electrostatic discharge sensitive devices such as integrated circuits or the head gimbals assembly.

**Acknowledgements**

**REFERENCES**

ESD Association (2014). *Electrostatic discharge (ESD) technology roadmap-revised,* 7900 Turin Road, Bldg. 3, Rome, NY.

M. Glor (1985). Hazards due to electrostatic charging of powders, *Journal Electrostatics,* 16, 175-191.

K. Robinson, R. Brearey, and J. Szafraniec (2009). Sheet sticking caused by charge flow in a buried conducting layer. *Journal of Electrostatics,* 67(5), 781-788.

ESD Association (2015). *ANSI ESD STM 3.1-2015, The Protection of Electrostatic Discharge Susceptible Items-Ionization.* 7900 Turin Road, Bldg. 3, Rome, NY.

R. Rodrigo et al. (2004). CPM study: Discharge time and offset voltage, their relationship to plate geometry. *Electrical Overstress/Electrostatic Discharge Symposium 2004,* Grapevine, TX, 1-5.

V. Kraz (2004). Notes on maintaining sub-1V balance of an ionizer. *Electrical Overstress/Electrostatic Discharge Symposium 2004*, Grapevine, TX, 1-6.

V. Kraz, S. Cruz, and K. A. Martin (2006). *US Patent No. US 6,985,346 B2.* Washington, DC: U.S. Patent and Trademark Office.

V. Kraz, S. Cruz, and K. A. Martin (2009). *US Patent No. US 7,522,402 B2.* Washington, DC: U.S. Patent and Trademark Office.

J. Crowley, A. Ignatenko, and L. Levit (2004). Biased-plate characterization of pulsed DC ionizers. *Journal of Electrostatics,* 62, 219-230.

A. Ohsawa (2005). Modeling of charge neutralization by ionizer. *Journal of Electrostatics,* 63, 767-773.

A. Ohsawa (2013). 2-D electrohydrodynamic simulations towards zero offset voltage with corona ionisers. *Journal of Electrostatics*, 71, 116-124.

S. Plong-Ngooluam, N. Jindapetch, P. Wounchoum, and D. Sompongse (2015). 3-D Computational Simulations of Electrostatic Potential in Partial Surfaces towards the Precision of Ion Balance Analysis. *Applied Mechanics and Materials,* 781, 308-311.

B. F. Ryan, B. L. Joiner and J. D. Cryer (2010). *MINITAB Handbook: Update for Release 16, 6th Edition.* Brooks/Cole Publishing Co., Pacific Grove, CA, USA.

# A3-A Feasibility Study of Ion Balance Measurement by Partial Surfaces

Sayan Plong-ngooluam[a,b]1, Nattha Jindapetch[b]

Phairote Wounchoum[b], Duangporn Sompongse[a]

[a]*Western Digital (Thailand) CO., LTD. Bang Pa-In, Phra Nakhon Si Ayutthaya, 13160, Thailand*
[b]*Department of Electrical Engineering, Faculty of Engineering, Prince of Songkla University, Hat Yai, Songkhla, 90112, Thailand*

**Abstract**

This paper reports a feasibility study of the ion balance measurement by the partial surfaces. The partial surfaces were exposed under the DC corona ionizer which could be varied ion balance. The appearance of electrostatic potential, which is caused by the imbalance of positive and negative ions, was measured by the high impedance electrostatic voltmeter. The result from these partial surfaces was compared with the standard test method which is using the $6'' \times 6''$ charged plate. The average voltages of all segments of the partial surfaces are correlated to the electrostatic potential values which were measured by the standard $6'' \times 6''$ charged plate. Moreover, the partial surfaces offer the fine-grained level of results. It validates that the precision of the ion balance measurement can be improved by the partial surfaces.

## Introduction

Since 1970s, the electrostatic discharge (ESD) had been a problem in electronic industry [1]. The ESD events were damaging devices, harming the systems. Moreover, an electrostatic charges can be inducing the product contamination on the charged surfaces due to electrostatic forces. The ground connecting is a general method for making an equipotential surface to prevent the ESD event. However, this method is less effective to remove the static charges on the insulator. The ionization is widely used to remove the static charges from insulator surfaces. This method provides the opposite polarity ions to neutralize the electrostatic charges on the object surfaces.

The standard test method (STM) to measure the ionizer is based on ANSI/ESD STM3.1-2006 [2] and IEC 61340-4-7 [3]. The STM requires the ion balance and decay time measurement based on the standard charged plate monitor (CPM). This measurement is insufficient resolution because the charged plate is much larger than a miniaturized device such as an integrated circuit or a magneto resistive head [6]. Some of these devices are requiring the ion balance within +/-1V or even tighter to prevent the ESD damage. The sub-1V ion balance controlled area requires the sufficient resolution to identify the ionizer balance [4]. The miniaturized ion balance analyzer using the $1'' \times 1''$ plate was launched to serve that requirement. However, this analyzer does not characterize the full surface area that is measured by the standard CPM and analyzed results are reported as single points at a time. Then the partial surfaces have been studied [6]. The electrostatic finite element analysis (FEA) of the 4-segment, 9-segment 16-segment partial surfaces and the standard CPM were analyzed. The single level of electrostatic potential was observed on the standard CPM model. On the other hand, the multi-levels are observed on the partial surface models. It concluded that the ion balance measurement resolution could be enhanced by this technique.

This paper aims to study the feasibility of the resolution enhancement by the partial surface technique which is described on [6]. The 25-segment partial surfaces have been assembled over the square 6″×6″ area with the insulative base. It is put below the DC corona ionizer which is used as the adjustable ion source. The apparent voltage on each plate is measured by the high impedance electrostatic voltmeter. The experimental results can prove the feasibility of the partial surfaces ion balance analyzer.

**Ionizer Measurement**

The electrostatic charges on the surface of insulators or isolated conductors can be neutralized by the opposite air ions. Ionizer is designed to supply the positive and or negative air ions to the object to be neutralized. The typically is the DC corona ionizer. The ions are generated by the collision between the neutral molecules and electrons when they are accelerated by an electric field which exceeds the inception level. The inception voltage calculation is described on Ohsawa's model [5].

In order to characterize the ionizer, a CPM is used to measure the ionizer's performance [2], [3]. The standard CPM need the 6″×6″ floated conductive plate to collect the ions in ionized air which is supplied from the ionizer. The ion balance is defined from the accumulation of positive and negative ions on that plate. It can be monitored by the electrostatic voltmeter. When the plate capacitance is fixed in the range of 20 pF, the appeared voltage can be defined by the ratio of the charge on that plate and its capacitance as (1).

$$V = \frac{Q}{C},$$

(1)

where $V$ is the voltage on the plate with respect to ground, Q is the charge on the plate in coulombs, and C is the plate capacitance with respect to ground.

However, these accumulated charges could be rapidly discharged through the voltmeter then resulting in zero volt. To maintain the existed charges on that conductive plate, the measuring of the electric field from the plate using a non-contacting electrostatic voltmeter are preferred to prevent the charge drainage from that plate.

Nowadays, the electronics manufacturers are producing a miniaturized devices which is quite smaller than the standard CPM. It is concerning the insufficient resolution and accuracy to measure ionizer balance because the standard CPM is larger than the handled devices as the describing on [4]. Then the modeling [6] had validated that the resolution of ion balance measurement can be enhanced by partial surfaces method which divides the standard plate in to 4, 9 and 16 segments. The highest segments plate provides the best resolution. However, that feasibility has been analyzed by using the computer simulation. It requires actual measurement evaluation to validate the feasibility before build the prototype of partial surfaces ion balance analyzer.
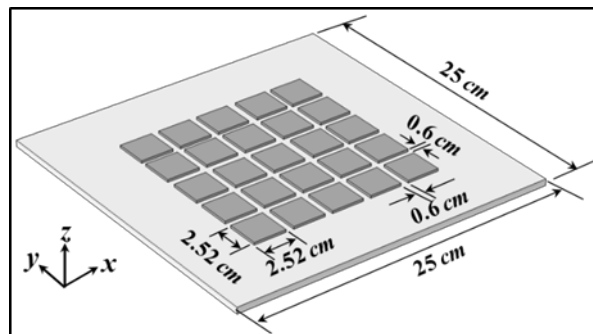


Fig. 1: The illustration of 25-segment partial surfaces.

**Ion Balance Measurement by Partial Surfaces**

The 25-segment partial surfaces have been assembled as the geometrical illustration in Fig. 1. The plate is made of 25 pieces of aluminum sheets which are 2.52 cm in width, 2.52 cm in depth and 0.2 cm of thickness. These aluminum sheets are assembled on the acrylic base which is 25 cm in width, 25 cm in depth and 0.5 cm of thickness. The arrangement of these aluminum sheets are in the center of acrylic base with the 0.6 cm spacing. The coverage area is the square 6″×6″ which is the same as the coverage of standard CPM.

The ion source was evaluated by using of the MKS model 5802i, DC corona ionizer. The Trek's charged plate monitor model 157 with the standard CPM was used to measure the ion balance while the ionizer adjustment. The appeared voltage on the aluminum sheets were probed by the Trek's model 822HH electrostatic voltmeter. This voltmeter provides input resistance higher than 1.0E+14 ohms and input capacitance less than 1.0E-14 farad. The ionizer was installed at 45 cm from the grounded surface as shown in Fig.2. The partial surfaces plates were placed under the ionizer facing with the 15 cm from the grounded surface as describes on the STM.

The evaluation was started by adjusting the ionizer offset to -10 Volt which was read by the Trek model 157 with the standard CPM. After adjusted, then took that plate out and replaced by the 25-segment partial surfaces. The Trek model 822HH was used to probe the voltage on each partial surfaces and recorded the results. Then repeated these processes and steps with the 2 Volt of ionizer offset increment until +10 Volt. The average voltage of 25-segment partial surfaces was used to compare with the results from the standard CPM. The appeared voltage from the partial surfaces at zero volt ion balance adjustment were illustrated in the 3D surface plot. The statistical software, Minitab was used to approximate the new data points from known data points. The distance method with the $2^{nd}$ distance power has been used to interpolate with 25×25 meshes in the *x-y* plane.

**Results and Discussions**

The correlation results is expressed by the scattering plot shown in Fig. 3(a). The linear equation is comprising of 0.90 coefficient, 0.27 Volt intercept and 0.99 of $R^2$. It means that the average voltage from the partial surfaces plate is correlating to standard CPM result. Because the coefficient is closing to the unity, the intercept is closing to zero and the perfect $R^2$. The 3D surface plot of the voltage from 25-segment partial surfaces measured with the zero-volt ionizer adjustment is shown in Fig. 3(b). The approximated range is ±2 Volt along the square 6″×6″ area. It is expressing the fine-grained level of the measurement results which are averaged then resulted as zero-volt.
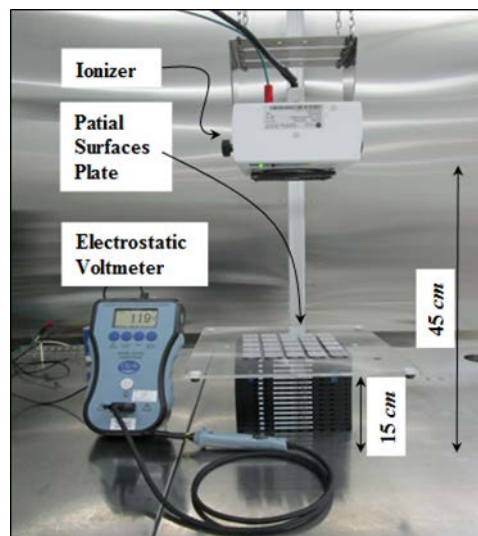


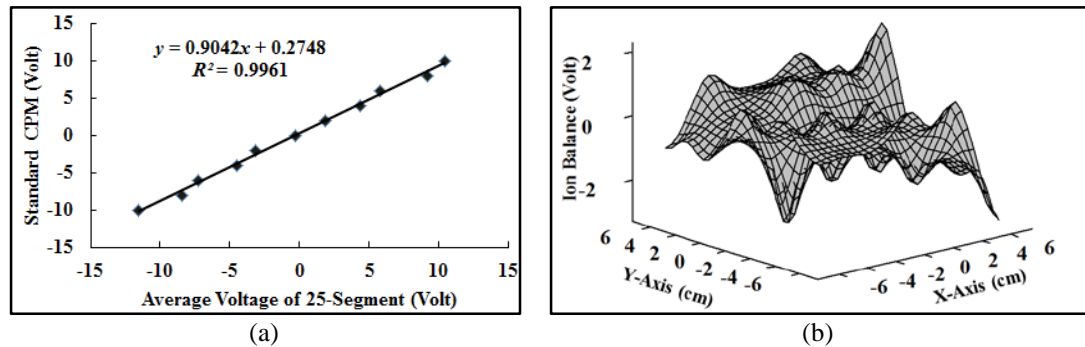Fig. 2: The 25-segment partial surfaces measurement setup.

Fig. 3: The ion balance analysis results from the 25-segent partial surfaces, (a) average voltage versus the standard CPM results, (b) 3D surface plot of appeared voltage with zero-volt adjustment.

**Conclusions**

The feasibility study results prove that ion balance measurement result from partial surfaces is correlating to the result from conventional charged plate monitor. Moreover, the partial surfaces also offer the fine-grained levels of ion balance measurement along the coverage area. It means that the ion balance measurement resolution can be enhanced by the partial surfaces method as tangible. It suits for ion balance measurement on the electrostatic protective areas which are handling the small footprint of electrostatic discharge sensitive devices such as integrated circuit or head gimbals assembly.

**Acknowledgements**

**References**

1. Electrostatic Discharge (ESD) Technology Roadmap-Revised, ESD Association, 7900 Turin Road, Bldg. 3, Rome, NY,(2014).
2. ANSI ESD STM 3.1-2006, The Protection of Electrostatic Discharge Susceptible Items-Ionization, ESD Association, (2006).
3. IEC 61340-4-7: ELECTROSTATICS Part 4-7: Standard Test Methods for Specific Applications Ionization, International Electrotechnical Commission, (2010).
4. V. Kraz, Notes on Maintaining Sub-1V Balance of an Ionizer, Electrical Overstress/Electrostatic Discharge Symposium (EOS/ESD),(2004).
5. A. Ohsawa, Modeling of Charge Neutralization by Ionizer, Journal of Electrostatics 63, (2005) 767-773.
6. S. Plong-Ngooluam, N. Jindapetch, P. Wounchoum, and D. Sompongse, 3-D Computational Simulations of Electrostatic Potential in Partial Surfaces towards the Precision of Ion Balance Analysis, Applied Mechanics and Materials 781, (2015), 308-311.

# A4-A Finite Element Analysis of Multiple Ion Receiving Plates for Ionizer Balance Monitoring

S. Plong-ngooluam[a,2], N. Jindapetch[b], P. Wounchoum[b], D. Sompongse[a]

[a]Western Digital (Thailand) Company Limited, 140 Moo 2, BangPa-in Industrial Estate, Klongjig, Bangpa-in, Ayutthaya, 13160, Thailand
[b]Department of Electrical Engineering, Faculty of Engineering, Prince of Songkla University, Hat Yai, Songkhla, 90112, Thailand

**Abstract**

This paper reports a finite element analysis of multiple ion receiving plates to investigate the optimum number of plates for achieving fine-grained resolution in ionizer balance measurement. Both square and circular plates, also subdivided into 4, 9, 16, 25, and 36 segment plates, were modeled in an electrostatic field. The potential distribution of each model was further analyzed by simple linear regression to assess the measurement resolution. The results indicate that the segmented plates provide improved measurement resolution.

*Keywords:* electrostatic potential, finite element analysis, ion balance analyzer, ion receiving plate

## 1. Introduction

Ionizers are necessary to eliminate undesirable charges in the production lines of electrostatic discharge (ESD) sensitive devices [1]. The charge separation and accumulation models [2] were extended by Robinson et al. to identify electric charges present in manufacturing processes, and to provide methods to eliminate the undesirable charges [3]. Grounding is a general method to dissipate electrostatic charges to the ground and to achieve equipotential conditions. However, it is not effective against static charges on insulating surfaces or in isolated conductive particles [3-5]. Instead, air ionization is used to remove these static charges by providing the opposite polarity ions to attract the static charges on the object surfaces until the static charges are neutralized.

For measuring such ionizing performance, ANSI/ESD STM3.1 [6] provides the standard test method (STM) for ionizer evaluation and selection. This STM requires a charged plate monitor (CPM) for ion balance measurement to identify the equilibrium of positive and negative ions. This

---

[2] Corresponding author.Tel.: +66 35278772/875233406.
*Email address:* Sayan.Plong-ngooluam@wdc.com (S. Plong-ngooluam)

characteristic is defined by the voltage induced on a standard charged plate, which is a floated 15 cm×15 cm square shaped conductive surface. The size of this plate agreed with a typical silicon wafer at the time of drafting the standard, in the late 1980s [7]. However, the current electronics manufacturers are comparatively tiny devices, such as integrated circuits or magnetoresistive heads. These devices are sensitive to ESD damage at low voltage levels, so the ionizer balance must be less than ±1V or even better [8]. The sub-1V ion balance environment requires sufficient resolution and accuracy in determining the ion balance of an ionizer [9]. The standard charged plate has insufficient resolution in ion balance measurement, because the measurement plate is larger than the devices to be treated. Therefore miniaturized ion balance analyzers were launched to serve the sub-1V measurements, such as the ionizer controller in US patents US 6,985,346 B2 [10], US 7,522,402 B2 [11], and the biased-plate monitor [12]. However, these analyzers do not characterize the ion balance over a 15 cm×15 cm area as the conventional plate does. Their results only represent a single point at a time. Such point measurements are insufficient because the ion distribution in the transport region depends on drift and airflow velocities, as in the Ohsawa's ionizer models [13– 15] that are based on electrohydrodynamics. The ions are distributed according to their spatial motility, which depends on air velocity, ion mobility, diffusion, and ion-ion recombination factors. The wafer surface charge monitor (CHARM) [16] offered the ability to measure the charging characteristics on the wafer surface by using multiple charge collection plates. Then, simulations in [17] were used to investigate smooth changes in the electrostatic potential distribution as measured by multiple plates. The results indicated that measurement errors could be reduced by using multiple plates. However, those simulations did not resolve fully the subdivision to multiple plates. Shape and number of segments should be investigated to determine a reasonable number of segments based on measurement performance and practicality. The experimental results in [18] validated the hypothesis that ion balance measurement resolution could be improved by using multiple plates. The multiple plate measurement results could resolve the ion balance distribution at a fine-grained level not possible with the standard CPM. Moreover, the experiment also revealed good correlation between the average over multiple plates and the standard CPM results. Furthermore, a feasibility study [19] evaluated measurements of ionized air with multiple ion-receiving plates. The eventual voltage on each plate was measured by a commercial electrostatic voltmeter. The results proved that multiple ion receiving plates offered fine-grained spatial resolution and the average voltage correlated well with the results from standard CPM.

In this work, the electrostatic behavior of multiple plates was analyzed by the finite element method and statistical analysis, to determine the changes of the electrostatic potential in the quantitative results. Simple linear regression (SLR) was used to estimate the gain and offset errors, while the goodness of fit indicates the confidence level of the linear regression models. Furthermore, circular and square shaped plates were modeled and compared, to investigate shape

effects. The results help to select suitable plates for improving the resolution of ionizer balance measurements.

## 2. Ion Receiving Plate and Its Curvature Effect

This section describes the relationship of electrostatic field and electrostatic potential, the characteristics of conductive surfaces when they are used as ion receiving plates in ion balance measurements, and curvature effects on the accuracy of the ion balance measurement.

2.1 *Electrostatic Field, Flux, Potential and their Relationship*

The Gauss's law [18] explains that the electrostatic field through any closed surface of a free space is equal to the total charge which is enclosed by that surface. By the divergence theorem, this requires locally that

$$\nabla \cdot \mathbf{E} = \frac{\rho_v}{\varepsilon_0},\tag{1}$$

where $\mathbf{E}$ is electrostatic field, $\rho_v$ is volume charge density, $\varepsilon_0$ is the permittivity of a free space.

The electrostatic field E is related to the electrostatic potential V by

$$\mathbf{E} = -\nabla V.\tag{2}$$

Since, the electrostatic field $\mathbf{E}$ in (2) depends on the permittivity of free space, the vector field $\mathbf{D}$ is electrostatic displacement or electrostatic flux density defined by

$$\mathbf{D} = \varepsilon_0\mathbf{E}.\tag{3}$$

This electrostatic flux $\mathbf{D}$ is properly scaled for the flow of electrostatic field through a given area. It is proportional to the number of electrostatic field lines through a surface element, as shown in Fig 1.

2.2 *Ion Receiving Plate*

The conductive surface $S$ which is orthogonally exposed to an electrostatic field $\mathbf{E}$ is able to collect the charge $Q$. This collected charge is directly proportional to the electrostatic field tangential to such surface $E_s$ as

$$Q = \varepsilon_0\varepsilon_r E_S S,\tag{4}$$

where $\varepsilon_r$ is the relative permittivity of the environment around the receiving surface $S$.

The electrostatic potential $V$ on this surface is directly proportional to the quantity of that $Q$ but inversely proportional to capacitance $C$ as

$$V = \frac{Q}{C}.$$ (5)

The measurement of this electrostatic potential has been used as the charge induced meter for observing the electrostatic field [8, 27–30]. In the ion balance measurement, the charge $Q$ is accumulated from positive and negative ions, when this surface is exposed to ionized air. It is then called an ion receiving plate. In this situation, the charge $Q$ on the ion receiving plate is the integral of the neutralizing current $i_n(t)$ and proportional to the voltage $V$ across the plate as

$$V = \frac{1}{C} \int_{t_0}^{t} i_n(t) dt + V_0 ,$$ (6)

where $V_0$ is the initial voltage of the ion receiving plate.

The neutralizing current $i_n(t)$ is the flow rate of the charge $Q$ as is contributed by the positive and the negative ions. Their motions in the transport region [15] are given by

$$i_n(t) = -e \int_v (n_p \mathbf{v}_p - n_n \mathbf{v}_n - n_p \mathbf{v}_p - D_p \nabla n_p + D_n \nabla n_n) \cdot \mathbf{e}_L dv ,$$ (7)

where $e$ is the elementary charge, $v$ is the system volume, $n_p$ and $n_n$ are the positive and negative ion densities, respectively. Here, $\mathbf{v}_p$ and $\mathbf{v}_n$ are positive and negative ion velocities composed of the air and the drift velocities. $D_p$ and $D_n$ are the positive and the negative ion diffusion coefficients, respectively. $\mathbf{e}_L$ is the Laplace field when unit voltage is applied to the plate.

2.3 *Curvature Effect*

The charge $Q$ on the conductor surface, which is not necessary to be closed, is obtained by integrating the surface density $\rho_s$ over all differential surface elements $dS$ as Z

$$Q = \int_S \rho_S dS .$$ (8)

where $\rho_S$ is the surface charge density.

The surface charge density in (8) is non-uniform because the surface charges are distributed to create an equipotential surface or equivalently to eliminate the electric field tangential to the surface $E_s$ by their distribution. Thus the surface charge density $\rho_s$ is described by

$$\rho_s = \varepsilon_0 E_s.$$ (9)

The surface charges near a convex edge of the conductor are denser than elsewhere on the surface. Then, the electrostatic field density and the electric flux are maximal, as in region A of Fig.1. On the other hand, the electrostatic field and the electric flux are minimal at concave edges as in region B of Fig.1. This phenomenon has been applied to corner detection as described in [22]. Thus the conductor shape by its edge curvature affects variations of the electric field along the interface region [23] between the conductor surface and the free space. It needs further consideration in the case of multiple sensing surfaces, as in the multiple plate analyzer or in the wafer surface charge monitor.

## 3. Analysis Method

This section describes the analytical methods to investigate the plates, in order to improve the ion balance measurement resolution. The used tools are simulations of the ion receiving plates and linear regression analysis.

### 3.1 Simulations of Ion Receiving Plates

This electrostatic field has been modeled by using the Electrostatic module in the COMSOL Multiphysics similarly as in [17], which followed the guidance in Benamar's DC electrostatic precipitator modeling [21]. The free space environment was modeled as spherical volume with 50 cm diameter. The outer surface of this sphere was a zero charge boundary ($\mathbf{n}\cdot\mathbf{D}$=0). The electrostatic field was formed by two cylindrical electrodes, named source and ground, which were one centimeter in radius and height. All boundaries of the source electrode were configured to 1000 V electrostatic potential and all boundaries of the ground electrode were configured to ground (0 V). These electrodes were placed at the center of the spherical volume of free space with 20 cm separation as shown in Fig.2. In centimeter units, the source and the ground were located at (-10, 0, -0.5) and (10, 0, -0.5), respectively. The electrostatic field $\mathbf{E}$ in (2) depends on the electrostatic potential difference between these two electrodes. The free space model was studied at this point to simulate the original electrostatic field without any measurement plate. The electrostatic potential of this model was used as reference data to compare with the cases with measurement plate. The ion receiving plates were modeled using one millimeter thick conductive sheets placed between these electrodes. The center of these plates was located at the (0, 0, -0.5) position. All boundaries of these plates had floating potential with zero initial charge ($Q_0 = 0$).

For the single plate models, the square plate and the circular plate had equal areas. The square plate was 15 cm×15 cm, which is the same size as the standard CPM. The circular plate had 16.9 cm diameter.

For the multiple plate models, the 4, 9, 16, 25 and 36-segment square plates were simulated. These sub-plates were regularly arranged to 15 cm×15 cm array with 6 millimeter gaps between the plates, as shown in Fig.2. The sizes of the 4, 9, 16, 25, and 36-segment square shaped sub-plates were 7.25 cm×7.25 cm, 4.60 cm×4.60 cm, 3.30 cm×3.30 cm, 2.52 cm×2.52 cm and 2.00 cm×2.00 cm, respectively. Similarly, the 4, 9, 16, 25, and 36-segment circular plates were simulated. The diameter of each circular sub-plate was the same as the width of its counterpart square plate. For example, the diameter of each sub-plate in the 4-segment circular plate was 7.25 cm, equaling the width of the 4-segment square sub-plates.

The whole domain was cut at the center ($z$=0), and this cut surface was analyzed in two dimensions. The electrostatic potential data points on these surfaces were exported to a spreadsheet across a specified range with constant increments in the $x$-and $y$-coordinates. The data points represented the square area from corner (-7.5, -7.5) to (7.5, 7.5) in cm, with 0.5 cm per step (see the X marks in Fig.3). Any points out of the conductor domains or out of this coverage area were neglected.

*3.2 Simple Linear Regression Analysis*

Linear regression is a statistical method to model relationships between variables from a discrete collection of data points [24]. The explanatory variables are used to describe the response variables. In simple linear regression (SLR), only one explanatory variable $x$ is used to describe the response variable $y$ as

$$y = mx + c + e_i, \tag{10}$$

where $c$ is the $y$–intercept, $m$ is the slope or the regression coefficient of $x$, and $e_i$ the noise term accounting for mismatch of model and given data.

The goodness of fit describes how well the model can reproduce the given data [25]. The goodness of fit of an SLR model is indicated by the $R^2$ value defined by

$$R^2 = 1 - \frac{SS_{res}}{SS_{tot}}, \tag{11}$$

where $SS_{res}$ is the residual sum of squares and $SS_{tot}$ is the total sum of squares [26].

The $R^2$ value is nonnegative and less than or equal to 1. $R^2$=0 means that the model is not at all useful. On the other hand, $R^2$=1 would indicate perfect fit to the data. The relationship of the response and the explanatory variable can be visualized in an $xy$ scatter plot, along with the least squares fitted regression line representing predicted responses at each explanatory value.

In this work, the SLR was used to analyze the variance between the reference model and the measurement models with the zero noise ($e_i$=0) to qualitatively assess correlations. The reference model was the simulated electrostatic field in free space without measurement plates. The measurement models were the electrostatic fields simulated with measurement plates. The physical meaning of SLR analysis is to assess the measurement quality in terms of gain and offset errors. The regression coefficient represents the gain error and the *y*-intercept represented the offset error. An ideal result would have unity gain with zero offset. In other words, the measurement itself disturbs the measured ion balance, and the amount of that disturbance is assessed by simulating cases without and with that disturbance.

## 4. Results and Discussions

The finite element analysis results were assessed in the *xy* plane at *z*=0 cm. The electrostatic potential of the free space model without conductive plate is shown in Fig.4 by a contour and surface plot. The electrostatic contour lines were linearly distributed with 500 V at the center, as expected by symmetry. Then the single plates were simulated, placed at the center between the electrodes. The 500 V equipotential level covers the conductive plate and takes its shape. The electrostatic potential with the 15 cm×15 cm square plate is shown in Fig.5, and the potential with the 16.9 cm circular plate is shown in Fig.6.

In the multiple plate models, each conductive plate could have its own equipotential level. These fine-grained levels of electrostatic potential are observed in Fig.7 for the 36-segment square plate model and in Fig.8 for the 36-segment circular plate model. While these plots indicate that the multiple plate measurement can provide the finer-grain results, with better spatial resolution than a single plate, they do not indicate significant differences caused by the shape of the sub-plates.

For the SLR analysis, the electrostatic potential of the free space model in Fig.4 was discretely sampled on a grid and used as the explanatory variable (*x*), and the electrostatic potentials from the measurement models were similarly used as the response variables (*y*). A scatter plot relating the free space and the single 15 cm×15 cm square plate models is shown in Fig.9. Both $R^2$ and the gain were close to zero with 499.83 V offset. Since the *y*-value is practically constant 500 V over the conductive plate, the constant offset leaves nothing to be explained by *x*. The single circular plate expectedly gave similar results, seen in Fig.10. These results agree with the experiments in [7], which concluded that the shape of a single plate does not affect the ion balance measurement results. The SLR analysis of the multiple plate models gave significant differences. The number of electrostatic potential levels increased with the number of segments or sub-plates. The 4-segment square plate gave $R^2$ 0.757 with gain 0.520 and 240.05 V offset. The 9-segment square plate gave 0.870 for $R^2$, 0.752 for gain, and 123.68 V offset. The 16-segment square plate gave 0.923 for $R^2$, 0.841 for gain, and 79.32 V offset. The 25-segment square plate gave 0.948 for $R^2$, 0.885 for gain,

and 57.12 V offset. The electrostatic potentials of the free space model and the 36-segment square plate model are compared in Fig.11. The linear regression fit gave 0.968 for $R^2$, 0.939 for gain, and 30.26 V offset. With the same segment numbers, the circular plates gave better results. The 36-segment circular plate gave 0.981 for $R^2$, 0.960 for gain, and 20.10 V offset. The electrostatic potentials of the free space model and the 36-segment circular plates are compared in Fig.12.

Table 1 summarizes the SLR results indicating that the offset error decreased exponentially as the number of mutually similar segments increased. These results prove that the multiple plate measurement can enhance the spatial resolution, with accurate results, when compared with a single plate measurement. In general, the minimum acceptance of $R^2$ is 0.9. Thus, the 16-segment square plate and the 9-segment circular plate were minimums accepted.

In addition, the significant difference between use of square or circular plates indicates that the electrostatic field uniformity could be distorted by edge curvature effects as the square shape has a high curvature at its corners. These corners could provide high electrostatic flux densities and create electrostatic field strength variations in the overall measurement area. However, the gaps between the segments could also affect results by increasing stray capacitance in the overall plate. These aspects may be further investigated in the future.

Table 1: Summarization of SLR analysis results.

| Measurement Plate | Parameters | | |
|---|---|---|---|
| | $R^2$ | Gain | Offset error (V) |
| 15 cm×15 cm (Square) | <0.01 | <0.01 | 499.83 |
| 4-Segment (Square) | 0.757 | 0.520 | 240.05 |
| 9-Segment (Square) | 0.870 | 0.752 | 123.68 |
| 16-Segment (Square) | 0.923 | 0.841 | 79.32 |
| 25-Segment (Square) | 0.948 | 0.885 | 57.12 |
| 36-Segment (Square) | 0.968 | 0.939 | 30.26 |
| 16.9 cm (Circular) | <0.01 | <0.01 | 500.17 |
| 4-Segment (Circular) | 0.762 | 0.589 | 205.28 |
| 9-Segment (Circular) | 0.912 | 0.838 | 80.79 |
| 16-Segment (Circular) | 0.942 | 0.856 | 71.88 |
| 25-Segment (Circular) | 0.968 | 0.929 | 35.18 |
| 36-Segment (Circular) | 0.981 | 0.960 | 20.10 |

## 5. Conclusions and Future Works

Multiple plates can be applied in the measurement of ion balance, in which case their electrostatic potentials could be due to charges induced by the electrostatic field or due to the ions received from an ionizer.

Finite element analysis revealed that the electrostatic potential uniformity could be induced by the conductive plates. Linear regression analysis of potentials on multiple plates revealed that the sub-plates can faithfully follow the electric field that would prevail if undisturbed by the measurement, especially in case of finely segmented plate. Circular sub-plates allowed good linear fits of simulated measurements and undisturbed field.

As finer subdivision of the measurement plate further improves the spatial resolution, the number of plates in a multiple plate measurement should be maximized within practical limits.

## 6. Acknowledgements

## References

[1] Electrostatic discharge (ESD) technology roadmap-revised, ESD Association, 7900 Turin Road, Bldg. 3, Rome, NY, 2014.

[2] M. Glor, Hazards due to electrostatic charging of powders, J. Electrostatics 16 (1985) 175-191.

[3] K. Robinson and W. Durkin, Electrostatic issues in roll-to-roll manufacturing operations, IEEE Trans. Ind. Appl. 4 (6) (2010) 2172-2178.

[4] K. Robinson, Charge relaxation due to surface conduction on an insulating sheet near a grounded conducting plane, IEEE Trans. Ind. Appl. 40 (5) (2004) 1231-1238.

[5] A. F. Diaz and R. M. Felix-Navarro, A semi-quantitative tribo-electric series for polymeric materials: the influence of chemical structure and properties, J. Electrostatics 62 (2004) 277-290.

[6] ANSI ESD STM 3.1-2015, The Protection of Electrostatic Discharge Susceptible Items-Ionization, ESD Association, 2015.

[7] R. Rodrigo, D. Bellmore, J. Diep, T. Jarrett, N. Jonassen, C. Newberg, D. Parkin, D. Pritchard, J. Salisbury, A. Steinman, and J. Turangan, CPM study: discharge time and offset voltage, their relationship to plate geometry, 26th Electrical Overstress/Electrostatic Discharge Symposium, Grapevine, 2004.

[8] N. Jindapetch, S. Plong-ngooluam, K. Thongpull, K. Chetpattananondh, A Low Voltage Decay Time Analyzer for Monitoring Ionizers, J. Electrostatics 70 (2012) 489-498.

[9] V. Kraz, Notes on maintaining sub-1V balance of an ionizer, Electrical Overstress/Electrostatic Discharge Symposium (EOS/ESD), 2004.

[10] V. Kraz, S. Cruz, and K. A. Martin, Method and device for controlling ionization,US Patent, Patent No. US 6,985,346 B2 (2006).

[11] V. Kraz, S. Cruz, and K. A. Martin, Method and device for controlling ionization,US Patent, Patent No. US 7,522,402 B2 (2009).

[12] J. Crowley, A. Ignatenko, and L. Levit, Biased-plate characterization of pulsed DC ionizers, J. Electrostatics 62 (2004) 219-230.

[13] A. Ohsawa, Modeling of charge neutralization by ionizer, J. Electrostatics 63 (2005) 767-773.

[14] A. Ohsawa, Efficient charge neutralization with an ac corona ionizer, J. Electrostatics, 65 (2007) 598-606.

[15] A. Ohsawa, 2-D electrohydrodynamic simulations towards zero offset voltage with corona ionisers, J. Electrostatics, 71 (2013) 116-124.

[16] A. McCarthy and W. Lukaszek, A New Wafer Surface Charge Monitor (CHARM), Proceedings of the 1989 IEEE International Conference on Microelectronic Test Structures, Edinburgh, Scotland, March 13-14, 1989, pp. 153-156.

[17] S. Plong-Ngooluam, N. Jindapetch, P. Wounchoum, D. Sompongse, 3-D Computational Simulations of Electrostatic Potential in Partial Surfaces towards the Precision of Ion Balance Analysis, Applied Mechanics and Materials 781 (2015) 308-311.

[18] S. Plong-Ngooluam, N. Jindapetch, P. Wounchoum, and D. Sompongse, Partial Measurement of Planar Surface Ion Balance Analysis, Pertanika J. Science and Technology, 2016, to be published.

[19] Sayan Plong-ngooluam, Nattha Jindapetch, Phairote Wounchoum, Duangporn Sompongse, A Feasibility Study of Ion Balance Measurement by Partial Surfaces, Procedia Computer Science 86 (2016) 164-167.

[20] H. W. Hayt and J. A. Buck, Engineering Electromagnetics, 8th Edition, McGraw-Hill, NY, USA, 2012.

[21] B. Benamar, E. Favre, A. Donnot, and M.O. Rigo, Finite element solution for ionized fields in DC electrostatic precipitator, Proceeding of COMSOL Users Conference 2007, Grenoble, 2007.

[22] G. H. Abdel-Hamid and Y.H. Yang, Electrostatic field-based detection of corners of planar curves, Proceedings of the 1993 Canadian Conference on Electrical and Computer Engineering, Vancouver, 1993, pp. 767-770.

[23] S. Yuferev, L. Di Rienzo, and N. Ida, Surface impedance boundary conditions of high order of approximation for the finite integration technique, J.ACES 22 (2007) 53-59.

[24] R. Payne, A Guide to Regression, Nonlinear and Generalized Linear Models in GenStat, 15th Edition, VSN Int., Hertfordshire, 2012.

[25] S. Weisberg, Applied Linear Regression, 3rd Edition, John Wiley & Sons, Inc., Hoboken, NJ, USA, 2005.

[26] J. Rawlings, S. Pantula and D. Dickey, Applied Regression Analysis: A Research Tool-Second Edition, Springer, NY, USA, 2001.

[27] P. Secker and J. Chubb, Instrumentation for electrostatic measurements, J. Electrostatics 16 (1984) 1-19.

[28] P. Secker, The design of simple instruments for measurement of charge on insulating surfaces, J. Electrostatics 1 (1975) 27-36.

[29] J. Chubb, Measurement of tribo and corona charging features of materials for assessment of risks from static electricity, IEEE Trans. Ind. Appl. 66 (6) (1990) 1182-1187.

[30] J. Chubb, Instrumentation and standards for testing static control materials, IEEE Trans. Ind. Appl. 36 (6) (2000) 1515-1522.
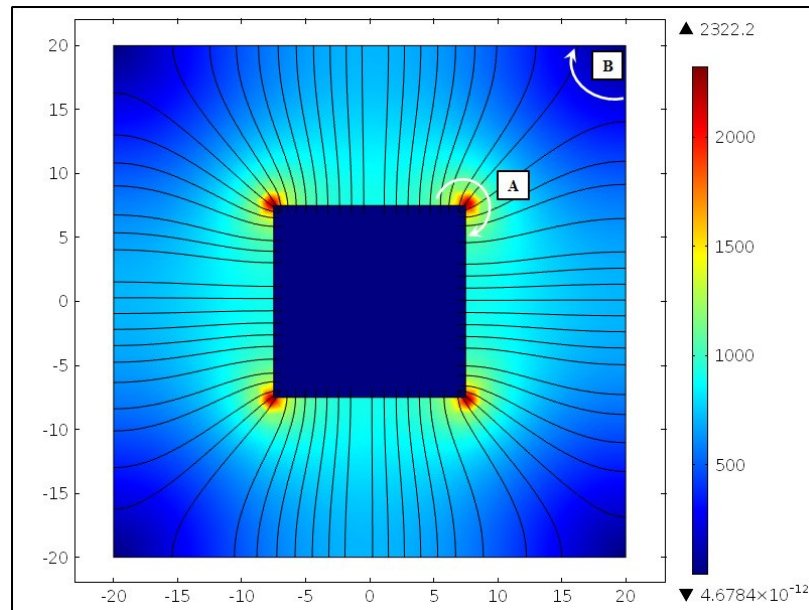
Figure 1: The electrostatic field in Volt/meter units. The electrostatic field was maximal at the convex corner (A) of a conductive plate, and minimal at the concave corner (B).
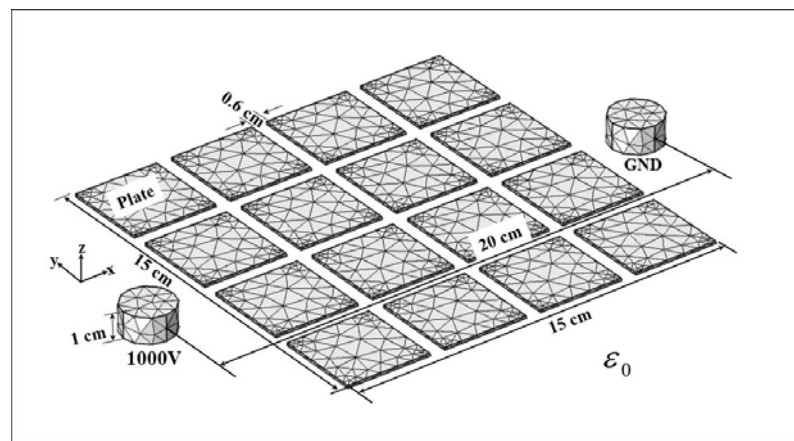


Figure 2: Example of geometrical meshing of the source, the ground, and the conductive plates.
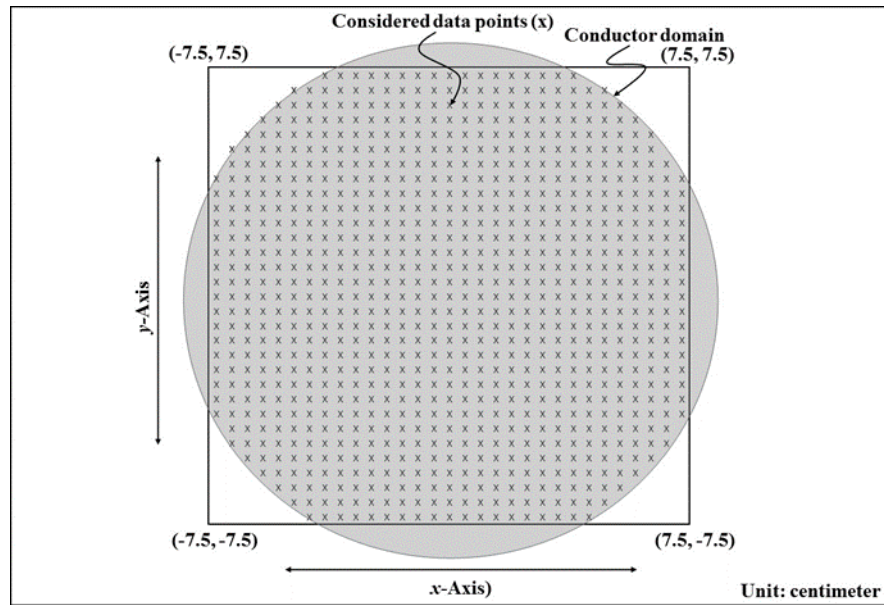
Figure 3: The points sampled from the conductor domain to obtain discrete data for simple linear regression analysis.
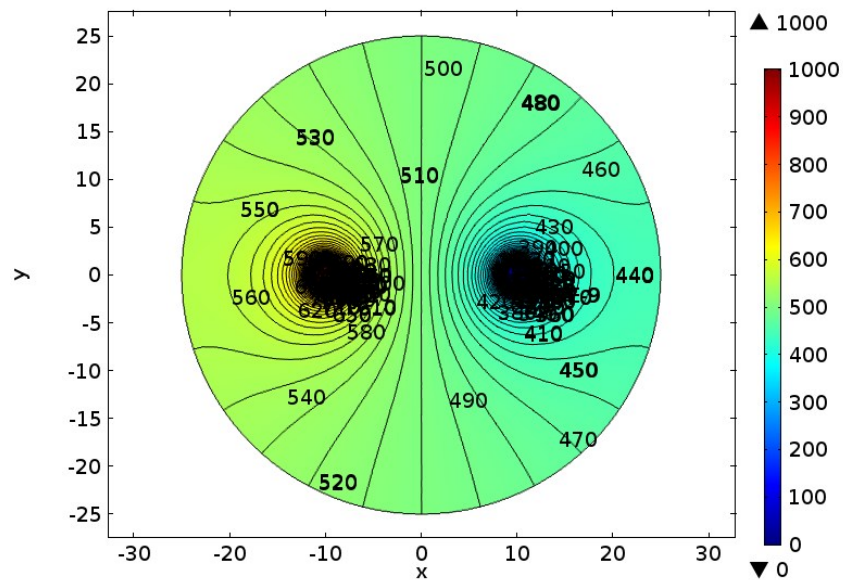


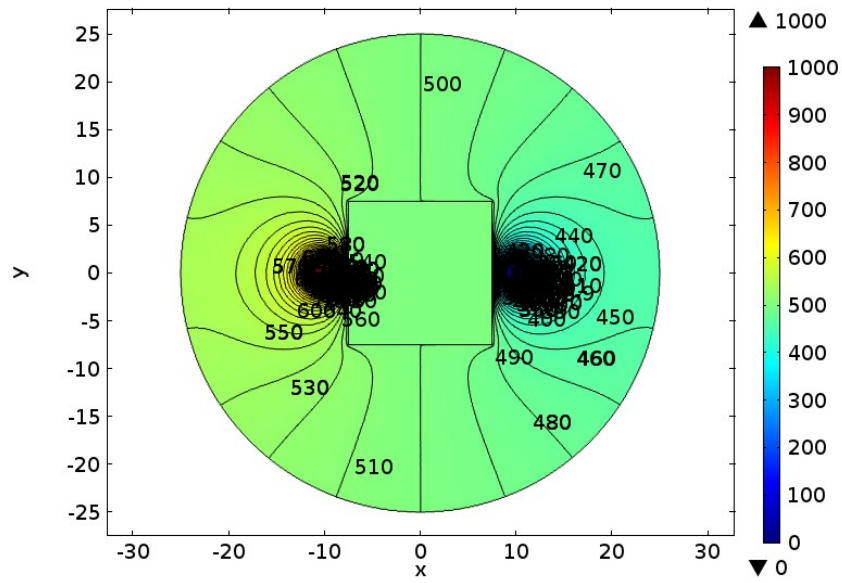Figure 4: Surface plot of the electrostatic potential with level contours for the free space model.

Figure 5: Surface plot of the electrostatic potential with level contours for the 15 cm15 cm square plate model.
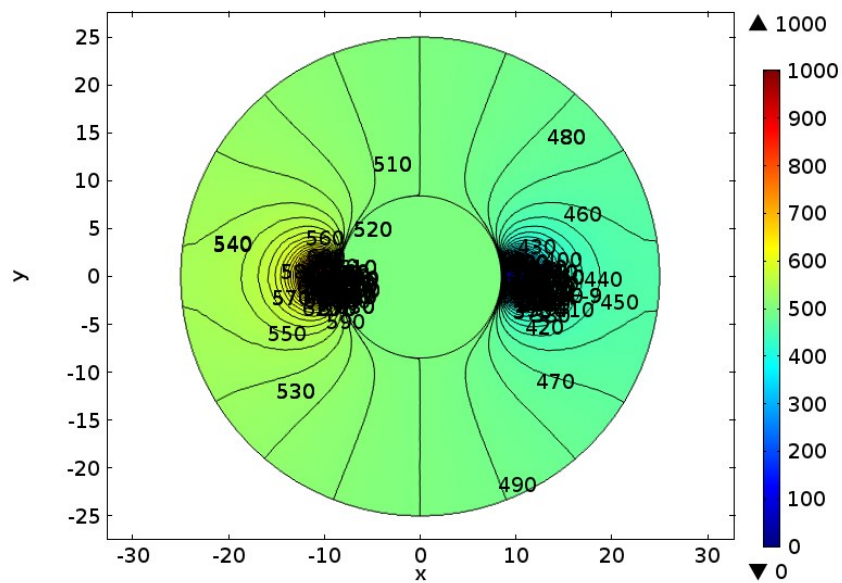


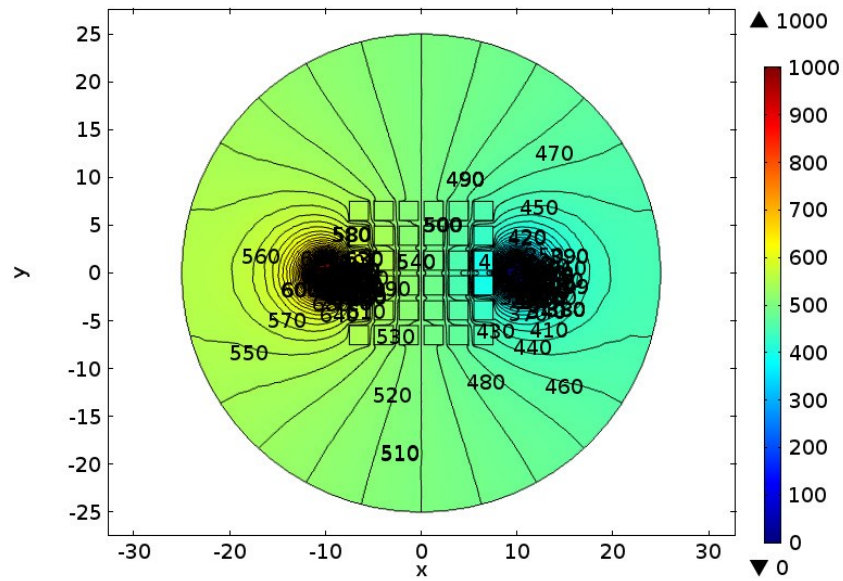Figure 6: Surface plot of the electrostatic potential with level contours for the 16.9 cm circular plate model.

Figure 7: Surface plot of the electrostatic potential with level contours for the 36-segment square plate model.
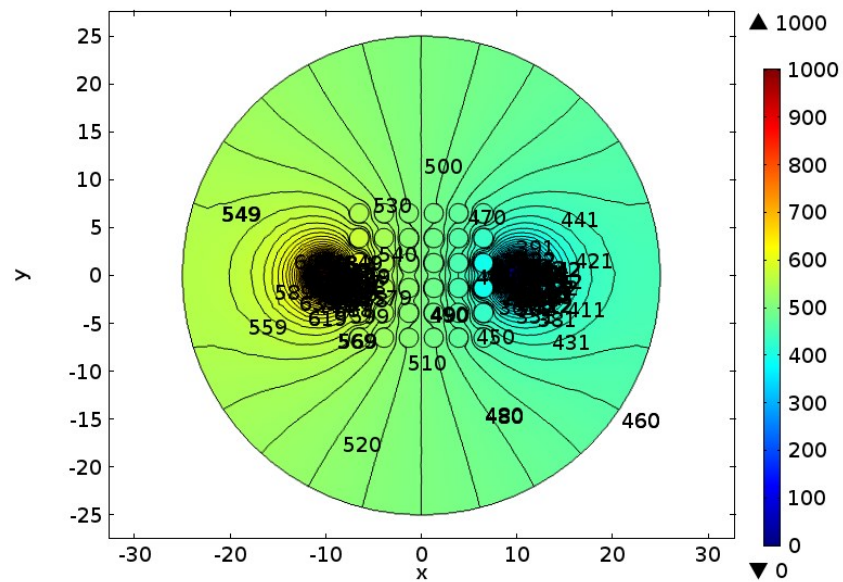


Figure 8: Surface plot of the electrostatic potential with level contours for the 36-segment circular plate model.
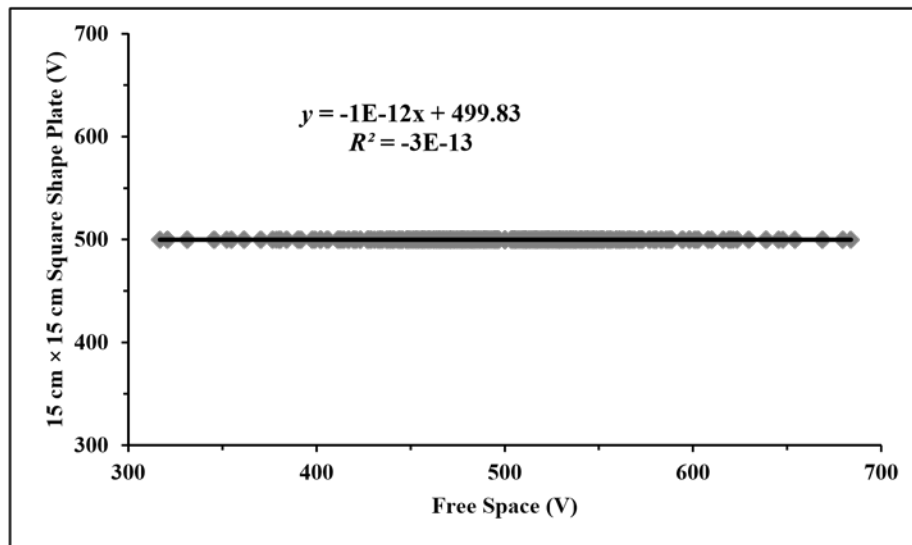
Figure 9: Scatter plot of electrostatic potential on the 15 cm15 cm square plate model versus the potential in free space undisturbed by measurement.
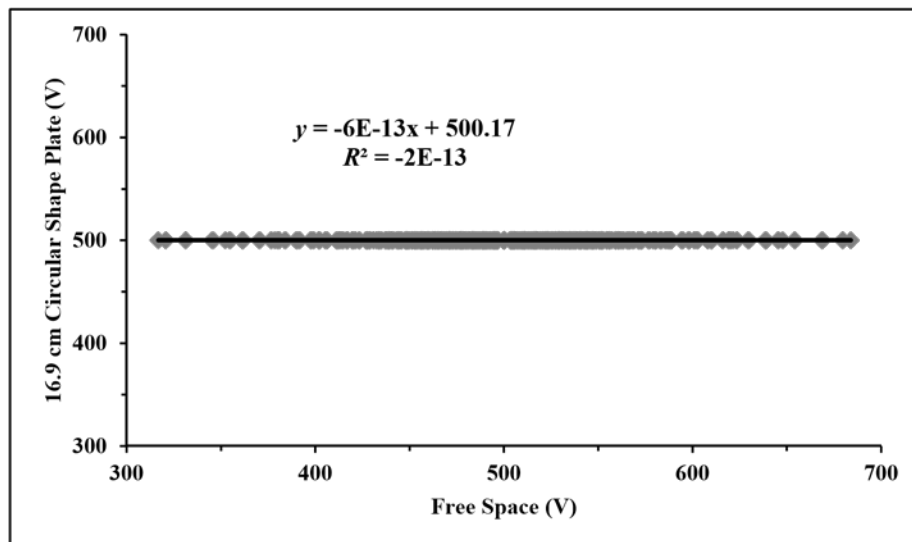


Figure 10: Scatter plot of electrostatic potential on the 16.9 cm circular plate model versus the potential in free space undisturbed by measurement.
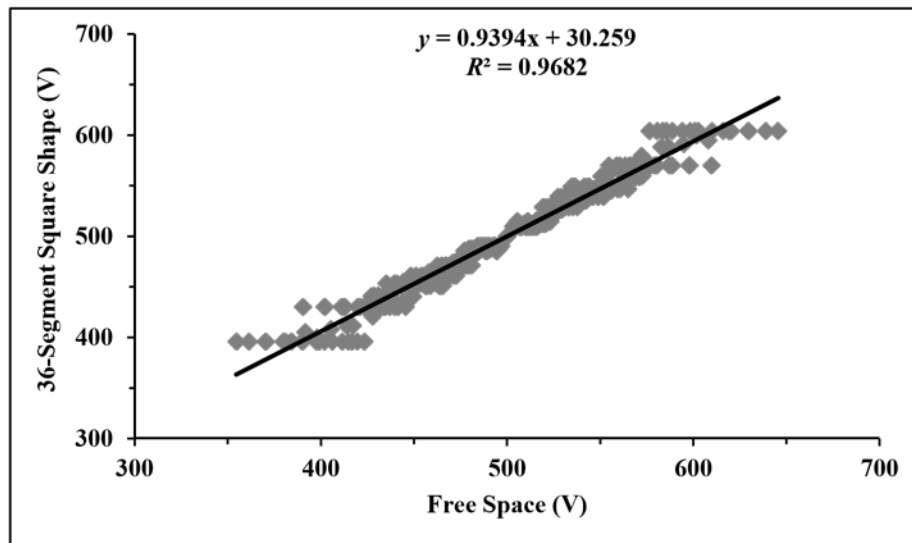
Figure 11: The scattering plot of electrostatic potential from 36-segment square shape plate model versus the free space model.
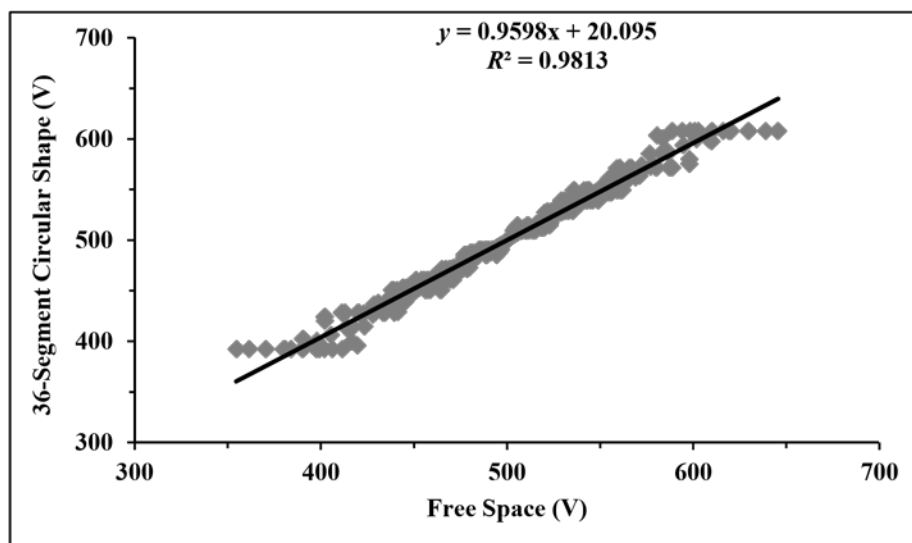


Figure 12: Scatter plot of electrostatic potential on the 36-segment circular plate model versus the potential in free space undisturbed by measurement.

# A5-A Proof-of-concept Study Demonstrating a Multi-Plate Ion Balance Analyzer

S. Plong-ngooluam[a,b,*], N. Jindapetch[b], P. Wounchoum[b], D. Sompongse[a]

[a]*Western Digital (Thailand) Company Limited 140 Moo 2, Bang Pa-in Industrial Estate, Klongjig, Bang Pa-in, Phra Nakhon Si Ayutthaya, 13160, Thailand*
[b]*Department of Electrical Engineering, Faculty of Engineering, Prince of Songkla University, Hat Yai, Songkhla, 90112, Thailand*

## Abstract

This paper demonstrates a multi-plate ion balance analyzer with inverse distance weighted interpolation for characterizing ionizer performance. The proposed analyzer design uses ultra-high input impedance charge induced meter to measure the electrostatic potential of multiple ion receiving plates. An embedded microcontroller processes the multi-channel analog signals synchronously and presents the results on a graphical display. Data interpolation enables high resolution results from the multi-plate measurements. This developed analyzer is suitable for ion balance characterization in small footprint devices sensitive to electrostatic discharges, such as a single-chip integrated circuit, or the head gimbals assembly of a hard disk drive.

*Keywords:*  multi-plate, ion balance, inverse distance weighting, ionizer

*Corresponding author. Tel.: +66 (0) 35 278 772; fax: +66 (0)35 278 050.
*Email address:* Sayan.Plong-ngoolaum@wdc.com (S. Plong-ngooluam)

## 1. Introduction

The ESD events damage devices and harm the systems, and an electrostatic charge can also induce particulate contamination of the charged surfaces due to electrostatic forces [2]. Also the micro-electromechanical system (MEMS) can be disturbed by electrostatic charges [6, 7]. Therefore, understanding the behavior of charges on MEMS devices is necessary to design and control such devices and their fabrication process.

Grounding is the simple method that eliminates the electrostatic charges and prevents ESD, but it can leave electrostatic charges on insulator surfaces. Therefore, ionizers are used to cancel electrostatic charges by emitted ions of opposite polarity, and to neutralize exposed surfaces. However, if the ionizer emits imbalanced ions, it could generate electrostatic charges instead of neutralizing them. Therefore, it is necessary to measure the ion balance of an ionizer. ANSI/ESD STM3.1-2015 [3] is the standard test method (STM) for ion balance measurement of an ionizer. The STM requires the $6''\times6''$ charged plate monitor (CPM) to measure the ion balance. This measurement lacks desired resolution because the charged plate is much larger than some targeted devices such as an integrated circuit or a magneto resistive head. Such devices require an ion balance within ±1 V, or even tighter, to prevent the ESD damage.

The ion balance control to sub-1V deviations requires the ionizer to be balanced with sufficient resolution [4]. Small sized ion balance analyzers have been launched to serve these requirements, such as the ionizer controller in US patent number US 7,522,402 B2 [9], and biased-plate monitor [10]. However, these alternatives report on a single point at a time, but cannot determine the ion balance of an area of interest, which is the purpose of the STM.

The measurement of electrostatic potential using multiple plates was simulated in [13]. The results revealed that the measurement resolution could be enhanced by this concept. The multiple plates measurement concept has thereafter been validated experimentally [14]. A 25-segment conductive plate

was exposed to ionized air, and its electrostatic potential was measured with a high-resistance electrostatic voltmeter. The fine-grained charge levels of the conductive plates corroborated the general concept. However, each result was collected from measurements done at different times. So, further validation of the concept is needed to demonstrate observing the ion balance distribution over a $6''\times6''$ surface.

Aside from the physical plates, numerical interpolation can estimate results within the range of actually measured data points. A widely used and simple interpolation method is inverse distance weighting (IDW)[15]. Generally, the IDW is used to estimate a spatial distribution within a focal area, and has been used in studies of climate change, in rainfall mapping, and in distribution estimates of pollution levels.

Therefore, this paper aimed to report a new ion balance measurement method, using the multi-plate sensor, which could measure the ion balance on the multiple segment plate as synchronously, and to illustrate the fine-grained results. Moreover, IDW interpolation was used to estimate values at points within the range of the measured points. This interpolation enhanced the resolution of ion balance distribution on the measured surface.

## 2. Related Prior Works

This section reviews prior work related to ion balance measurement and inverse distance weighting interpolation. The development of the multi-plate ion balance analyzer, partly based on this review, is described subsequently.

### 2.1. Ionizer and Ion Balance

The electrostatic charges on the insulator surfaces or the tiny isolated conductors can be neutralized by the ionizer [3]. The typical ionizer generates the ions by the corona discharge technique [5]. The ions are generated by the collisions between neutral molecules and electrons accelerated to ionization levels by an electric field, and these ions produced at the corona discharge could

be carried by the air flow to the object to be neutralized, where their transportation depends on the air flow velocity, ion drift velocity and ion-ion recombination [8]. Thus, the electrostatic potential $V$ depends on the balanced result between the positive and the negative ions as

$$\nabla^2 V = \frac{-e(n_p - n_n)}{\varepsilon_0},$$ (1)

where $n_p$ and $n_n$ are positive and negative ion densities, respectively, $e$ is the elementary charge, and $\varepsilon_0$ is the permittivity of free space.

### 2.2. Charged Plate Monitor

In order to characterize the ionizer, a CPM is used to measure the ionizer's performance [3]. The CPM uses the $6''\times6''$ floated conductive plate to collect the ions in the ionized air supplied by the ionizer. The ion balance is assessed from the electrostatic potential caused by accumulation of the ions on that conductive plate within 1 minute of operation. Since the plate is geometrically fixed, the electrostatic potential $V$ is in fixed ratio to the charge $Q$ determined by the capacitance $C$ as

$$Q = \frac{V}{C}.$$ (2)

The electrostatic charges stored in the small capacitance plate could be discharged through a generic voltmeter, which would rapidly deplete the charge. To maintain the accumulated charge, an electrostatic field measurement with a non-contact electrostatic voltmeter is preferred. This prevent the drainage of the charge. For example, the micro mechanical electrostatic field sensor was developed to measure the surface potential in MEMS device fabrication process [6, 7]. A cantilever-like bending beam could detect the electrostatic force without contacting to the object surface. In the free space, the force $\mathbf{F}$ relates to the electrostatic field $\mathbf{E}$ as

$$\mathbf{F} = \varepsilon_0 \mathbf{E}^2 A,$$ (3)

where $A$ is the sensing surface. Then the electrostatic potential $V$ is related to the electrostatic field $\mathbf{E}$ by

$$\mathbf{E} = -\nabla V. \tag{4}$$

Nowadays, the modern ultra-high impedance amplifiers can contact the charged surface with only low current drainage [12, 19{22] such as LMC6001, OPA128 and LMC6081. These amplifiers provide a very low input capacitance and an ultra-high resistance. They could meet the STM requirement of plate isolation exceeding $1.0 \times 10^{14}$ ohms and $2.0 \times 10^{-11}$ farad input capacitance. These amplifiers are used here, instead of the non-contact voltmeter, to measure the electrostatic potential for ion balance analysis.

## 2.3. Inverse Distance Weighting Interpolation

IDW interpolation is a specific type of weighted average for interpolating values sampled at spatial point locations to a neighbourhood of this point cloud [16-18]. It uses the distances from a target location to sampled locations, at which data values have been measured, to provide an estimated value at the target location. At the location $j$, the estimated data point $Z_j$ is obtained from the distance $d_{ji}$ to location $i$ of known data point $Z_i$ as

$$Z_j = \frac{\sum_{i=1}^{N} \frac{Z_i}{d_{ji}^n}}{\sum_{i=1}^{N} \frac{1}{d_{ji}^n}}, \tag{5}$$

where the exponent $n$ can be selected; often used exponents are 1, 2 or 3.

The IDW is an easy-to-understand and practical interpolation method for implementation as illustrated in Fig.1. However, it never gives estimates above the maximum or below the minimum of the samples values, because the estimates are weighted averages of the sampled points. The IDW is sensitive to the sampling, and can give circular or transient curve patterns around solitary sampling points. Furthermore, the IDW is specifically designed for interpolation and will perform poorly as extrapolation method.

### 3. A Multiple Plates Ion Balance Analyzer Design

This section describes the conceptual design of the multi-plate ion balance analyzer. Its multi-plate sensor will be described, the analyzer is represented here by a block diagram, and the implementation of IDW interpolation is briefly discussed.

### 3.1. The Multi-Plate Sensor

The ion receiving plate is a bare conductor, made of stainless steel sheet, and equipped with a driven shield layer. The ion receiving plate and driven shield are separated by an insulator as recommended in [3]. The voltage follower amplifier is configured as a charge induced meter, which was introduced in [12], as the conceptual circuit in Fig.2. The ultra-high input impedance amplifier is used for transimpedance the ion receiving plate. This amplifier made of the ultra-low input current operational amplifier which provides input resistance higher than $1.0 \times 10^{14}$ ohms with the input capacitance less than $3.0 \times 10^{-12}$ farad. Then, the output of this amplifier can be probed by a generic voltage measurement tool, such as a voltmeter or an oscilloscope. The driven shield is electrically connected to the output of an amplifier. It makes ion the receiving plate independent of ground due to the dominant driven shield. Regarding to the contact plate configuration described in STM, the plate capacitance is effectively replaced by the $2.0 \times 10^{-11}$ farad capacitor $C_i$, which is electrically wired between the non-inverting pin and ground. The one mega-ohm input resistor Ri is provided for protecting the against high currents to the non-inverting input of the amplifier.

Since the analyzer is designed for sub-1V ion balance measurements, a simple amplifier circuit with the range of ±7.5 V can meet these requirements. Moreover, it increases the measurement resolution while the range is reduced.

The charge induced meter, ion receiving plate, driven shield and insulators are all embedded as a single ion balance sensor module. Figure 3 illustrates the multi-

layer stacking of that ion balance sensor. The construction uses a double-sided printed circuit board (PCB) with the 1.6 millimeter thickness FR-4 substrate. The electronic components and electrical conductors are on the bottom side of the PCB, while the driven shield is located on the top side. The ion receiving plate is installed over the driven shield, separated by a 0.1 millimeter thickness mica sheet.

The number of plates in the multi-plate system was decided based partly on the manual labor required in fabrication, done in-house. We wanted approximately $1''×1''$ sized sensors for sufficient spatial resolution to identify components or electric wiring issues. Six millimeter spacing between the plates was required by the mounting screws, and was used as the plate-to-plate spacing. The eventual multi-plate sensor had 25 segments as illustrated in Fig.4. The driven shields were 25.2 millimeter side squares and were arranged to cover a square $6''×6''$ area, same total area as in the standard CPM. A zeroing switch is provided to drain the charges from the plates and capacitors before the next measurement [3].

*3.2. Block Diagram of the Multi-Plate Ion Balance Analyzer*

The block diagram of the ion balance analyzer is shown in Fig.5. The multi-plate ion balance assembly unit (1) provides 25 segments of conductive plate, with 25 channels from ultra-high impedance buffer amplifiers. The signals output by the charge induced meters need to be conditioned by signal conditioners (2), from ±7.5 V to the 0-5 V range, which is the input voltage range of the digital converter (ADC). Then signals are sampled and held by the sample-hold units (3) to ensure that they are synchronously converted, although the microcontroller (4) reads sequentially. The signals are multiplexed from 25 to 5 lines due to the limited ADC input channels of the microcontroller. The microcontroller (4) is the central processing unit performing user interfacing, data sampling, multiplexing,

interpolating, recording and reporting the measurement results. The graphical LCD output (5) reports the analysis results.

### 3.3 Standard Charged Plate Monitor Measurement

The 25-segment multi-plate sensor has similar total square $6''\times6''$ surface as the standard CPM. The "whole surface voltage" can be defined as the average voltage of all segment outputs from the multi-plate ion balance sensor. This approach has been validated experimentally in [14].

The standard charge plate monitor measurement is started by closing the active zeroing switch, opening it, and then starting the one minute timer. After the timed period, the signals are sampled and held synchronously. Then the microcontroller reads the signals via a multiplexer, executes the averaging and reports the numerical result. Moreover, the microcontroller also displays the electrostatic potential surface as an image, a color map of the ion balance levels on segments of the $6''\times6''$ composite square, and example of which is shown in Fig.6.

### 3.4. Multi-Plate Ion Balance Measurement Operating Procedure

The multi-plate measurement is executed by temporarily closing the zeroing switch, opening it, starting the one minute timer, holding synchronously sampled signals, and reading the signals, similarly as in the standard charged plate operation. However, now the signals are reported for individual plate segments. The surface image is also displayed, possibly partly, depending on the electrostatic potentials on the segmented plate. Each data point from the multi-plate ion balance measurement consists of 5×5 cell values, which are arranged as illustrated in Fig.7. These measured values can further be interpolated to estimate the potentials at a higher resolution along the plate.

*3.5. Implementation of Inverse Distance Weighted Interpolation*

To enhance the image resolution, the discrete data points from the multi-plate sensor can be used with interpolation to refine the ion balance distribution image. However, the interpolated data should be within the range of these measured data. The IDW scheme of interpolation is used here, because it is simple and always gives estimates within the range of measured data. The resolution was refined to 25×25 by interpolation, on the square 6″×6″ surface, as illustrated in Fig.8. Now 7×7 pixels on the LCD represented 6×6 millimeter squares on the measured surface. The measured data are assigned to edges of the refined grid, as well as inside it, to avoid extrapolation and enforce only interpolation. The grid of given values now has spacing of six cells in the rows and the columns. The blank cells in Fig.8 are to be interpolated by equation (5), and we chose to use $n = 1$ for the comfortable of microcontroller coding. With the same reason, a linear interpolation of the nearest two points is used for the proof-of-concept study.

The measured data points $Z_i$ are the 25 values from the multi-plate sensor, filled in the cells which are at the column 0, 6, 12, 18 and 24, which are in the row A, G, M, S and Y as shown in Fig.8. The interpolation was started in the rows with measured data points using the nearest measured data points to calculate the estimates for each blank cell. For example, the cell A1 was interpolated from cell A0 with one cell distance, and from A6 with five cell distance. In the same manner, the cell A2 had distance two from A0 and distance 4 from A6. This processing is shown in equations (6) and (7).

$$A1 = \frac{\dfrac{A0}{1} + \dfrac{A6}{5}}{\dfrac{1}{1} + \dfrac{1}{5}}, A2 = \frac{\dfrac{A0}{2} + \dfrac{A6}{4}}{\dfrac{1}{2} + \dfrac{1}{4}}, A3 = \frac{\dfrac{A0}{3} + \dfrac{A6}{3}}{\dfrac{1}{3} + \dfrac{1}{3}}, \ldots \qquad (6)$$

$$G1 = \frac{\dfrac{G0}{1} + \dfrac{G6}{5}}{\dfrac{1}{1} + \dfrac{1}{5}}, G2 = \frac{\dfrac{G0}{2} + \dfrac{G6}{4}}{\dfrac{1}{2} + \dfrac{1}{4}}, G3 = \frac{\dfrac{G0}{3} + \dfrac{G6}{3}}{\dfrac{1}{3} + \dfrac{1}{3}}, \ldots \qquad (7)$$

After all cells in the rows A, G, M, S and Y are filled, the remaining blanks in the other rows can be interpolated in the same manner, now each within its own column. This is as in equations (8) and (9).

$$B0 = \frac{\dfrac{A0}{1}+\dfrac{G0}{5}}{\dfrac{1}{1}+\dfrac{1}{5}}, B1 = \frac{\dfrac{A1}{1}+\dfrac{G1}{5}}{\dfrac{1}{1}+\dfrac{1}{5}}, B2 = \frac{\dfrac{A2}{1}+\dfrac{G2}{5}}{\dfrac{1}{1}+\dfrac{1}{5}},... \tag{8}$$

$$C0 = \frac{\dfrac{A0}{2}+\dfrac{G0}{4}}{\dfrac{1}{2}+\dfrac{1}{4}}, C1 = \frac{\dfrac{A1}{2}+\dfrac{G1}{4}}{\dfrac{1}{2}+\dfrac{1}{4}}, C2 = \frac{\dfrac{A2}{2}+\dfrac{G2}{4}}{\dfrac{1}{2}+\dfrac{1}{4}},... \tag{9}$$

Since the interpolated cells are weighted averages from the sampled points, the ion balance distribution image will be smoother and finer-grained. However, their values may be inaccurate, because the range of interpolated data points are always within the range of measured data.

## 4. Results and Discussions

This section assesses the experimental results from operating the multi-plate ion balance analyzer as described in the previous section. The constructed laboratory prototype of the proposed analyzer is shown in the photo of Fig.9. It was tested in standard CPM analysis and in multi-plate ion balance analysis, and the data interpolation was demonstrated.

### 4.1. The Laboratory Prototype of Proposed Analyzer

A photo of the proposed multi-plate laboratory prototype is shown in Fig.9. The multi-plate ion balance sensor was installed on top side so it can receive ions from an ionizer, for the ion balance measurement. However, this prototype analyzer has only been used for proof-of-concept evaluation so far. A cover or casing is necessary for actual production use.

*4.2 Charged Plate Monitor Simulation and Correlation*

The analyzer prototype was tested using of the MKS bench top ionizer model 5802i. A Treks charged plate monitor model 157 with the standard CPM was used to measure the ion balance, as the standard reference. The ionizer was installed at 60 cm from the grounded surface, and the measurement plates were placed under the ionizer facing each other with 15 cm gap, as shown in Fig.10.

In test runs the ion balance was adjusted, and each time it was first measured by the CPM and then re-measured by the prototype analyzer.

Initially, the ion balance results without any adjustment were 0.6 V from the standard CPM and 0.82 V from the prototype multi-plate analyzer, as shown in Fig.11. When the ionizer balance was adjusted in range from -7 to +7 V, the prototype and reference measurements correlated well with good linearity, as shown in Fig.12. The slope is closed to unit with 0.2 V offset, and 0.9975 coefficient of determination $R^2$.

*4.3. Multiple Plates Ion Balance Analysis*

The multi-plate ion balance analysis revealed finer-grained information regarding the ion balance. In the initial test, for which the standard CPM reported 0.6 V, the multi-plate measurement gave variations across the plate segments, as shown in Fig.13. Despite the wide range of values from highly negative to highly positive, the average value was closely similar to the standard CPM result used as reference measurement.

*4.4. Inverse Distance Weighting Interpolation*

From the 25-segment data records provided by the multi-plate ion balance analysis, the interpolation done with equations (6-9) provides images like that shown in Fig.14. The continuous interpolation enhanced the resolution to a finer grained image. However, whatever interpolation method is used, it will not remove the large voltage variations in the multi-plate measurement: by default,

interpolation adds numerical estimates while keeping the original measured values.

It remains to be seen if the type of distribution seen in Fig.14 is reproducible or created by some sort of randomly seeded instability. If it is reproducible, then the gross scale ion balance can be quite misleading, and the uniformity of ion balance will require attention.

*4.5. Ionizer Measurement Results Analysis*

The results in subsection 4.3 and 4.4 indicated that the ionizer under evaluation could distribute the non-uniformity of ion balance through the surface to be neutralized. This non-uniformity could not be identified in subsection 4.2 which correlated to the standard CPM result. These results explain that ionizer under test did not capable for the sub-1 V ion balance control for the ESDS devices which is one inch or smaller footprint. This ionizer may need the further investigation to understand the cause of non-uniformity ion balance distribution.

## 5. Conclusions and Future Works

The proposed analyzer offers finer-grained assessments of the ion balance than conventional, due to its multi-plate sensor. Its plate-averaged readings correlated well and nearly linearly with a conventional analyzer. The overall segmented plate size matches that of standard measurements, used here as reference. However, strongly varying ion balance distributions over the segmented measurement plate were clear when assessed graphically. The observations highlight potential non-uniformity issues with ionized air.

The image resolution was enhanced with a simple interpolation method. However, it has not been assessed to what extent the enhancement, while visually attractive, corresponds to reality.

In any case, the multi-plate ion balance analyzer has been demonstrated in these initial proof-of-concept tests, and the observed spatial variations in ion balance distribution encourage further studies of stability and reproducibility of such distributions. If, to the contrary, all sensor plate segments had given similar results, then this study would indicate that there is no need for the higher spatial resolution of a multi-plate sensor.

In the future work, this analyzer may needs to evaluate the electrostatic field induction measurement for comparing with the distribution made by the data interpolation after the chassis and cover are properly shielded. The gaps between the sensing plates could be resulting in the mutual capacitances which can affect the values of the measured potentials. This suspicion also needs to be investigated in the future.

## Acknowledgments

## References

[1] Electrostatic discharge (ESD) technology roadmap-revised, ESD Association, 7900 Turin Road, Bldg. 3, Rome, NY, (2014).

[2] K. Robinson, R. Brearey, J. Szafraniec, Sheet sticking caused by charge flow in a buried conducting layer, Journal of Electrostatics, 67 (5) (2009) 781-788.

[3] ANSI ESD STM 3.1-2015, The Protection of Electrostatic Discharge Susceptible Items-Ionization, ESD Association, (2015).

[4]  V. Kraz, Notes on maintaining sub-1V balance of an ionizer, Electrical Overstress/Electrostatic Discharge Symposium (EOS/ESD), (2004).

[5]  Y. P. Raizer, Gas Discharge Physics, Springer, Berlin, 1991.

[6]  M. Hanf, W. Dtzel, Micromechanical electrostatic field sensor for the characterization of charges in MEMS devices, Sensors and Actuators A: Physical, 115 (23) (2004) 280-285.

[7]  A. Roncin, C. Shafai, D.R. Swatek, Electric field sensor using electrostatic force deflection of a micro-spring supported membrane, Sensors and Actuators A: Physical, 123-124 (2005) 179-184.

[8]  A. Ohsawa, Modeling of charge neutralization by ionizer, Journal of Electrostatics, 63 (2005) 767-773.

[9]  V. Kraz, S. Cruz, and K. A. Martin,Method and device for controlling ionization, US Patent, Patent No. US 7,522,402 B2 (2009).

[10] J. Crowley, A. Ignatenko, and L. Levit, Biased-plate characterization of pulsed DC ionizers, Journal of Electrostatics, 62 (2004) 219-230.

[11] A. Pandey, J. Kieres, M. Noras, Verification of non-contacting surface electric potential measurement model using contacting electrostatic voltmeter, Journal of Electrostatics, 67 (23) (2009) 453-456.

[12] N. Jindapetch, S. Plong-ngooluam, K. Thongpull, K. Chetpattananondh, A Low Voltage Decay Time Analyzer for Monitoring Ionizers, Journal of Electrostatics, 70 (2012) 489-498.

[13] S. Plong-Ngooluam, N. Jindapetch, P. Wounchoum, D. Sompongse, 3-D Computational Simulations of Electrostatic Potential in Partial Surfaces towards the Precision of Ion Balance Analysis, Applied Mechanics and Materials, 781 (2015) 308-311.

[14] Sayan Plong-ngooluam and Nattha Jindapetch and Phairote Wounchoum and Duangporn Sompongse, A Feasibility Study of Ion Balance Measurement by Partial Surfaces, Procedia Computer Science, 86 (2016) 164-167.

[15] Gunnink J.L., and Burrough P.A., Interactive spatial analysis of soil attribute patterns using exploratory data analysis (EDA) and GIS.In: Masser I., Salge F.(Eds). Spatial Analytical Perspectives on GIS.Taylor and Francis, New York, 1996, pp. 87-99.

[16] Shepard D., A two-dimensional interpolation function for irregularlyspaced data. In Proceedings of the 1968 23rd ACM national conference (ACM'68). ACM, New York, NY, USA, (1968) 517-524.

[17] Franke, R., Scattered Data Interpolation: Tests of Some Method. Mathematics of Computation, 38(157) (1982) 181-200.

[18] Diodato N., and Ceccarelli M., Interpolation processes using multivariate geostatistics for mapping of climatological precipitation mean in the Sannio Mountains. Earth Surf. Process. Landforms, 30 (2005) 259-268.

[19] P. Secker, The design of simple instruments for measurement of charge on insulating surfaces, Journal of Electrostatics 1 (1975) 27-36.

[20] P. Secker and J. Chubb, Instrumentation for electrostatic measurements, Journal of Electrostatics 16 (1984) 1-19.

[21] J. Chubb, Instrumentation and standards for testing static control materials, IEEE Trans. Industry Applications 26(6) (1990) 1182-1187.

[22] J. Chubb, Measurement of tribo and corona charging features of materials for assessment of risks from static electricity, IEEE Trans. Industry Applications 36(6) (2000) 1515-1522.

[23] H. W. Hayt and J. A. Buck, Engineering Electromagnetics, 8th Edition, McGraw-Hill, NY, USA, 2012.

[24] B. F. Ryan, B. L. Joiner and J. D. Cryer, MINITAB Handbook: Update for Release 16, 6th Edition, Brooks/Cole Publishing Co., Pacific Grove, CA, USA, 2010.
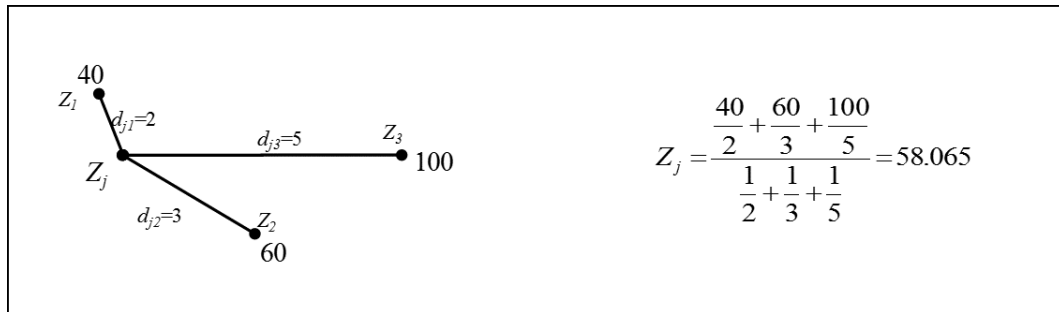
Figure 1: An example of interpolation by inverse distance weighting with exponent choice $n$=1.
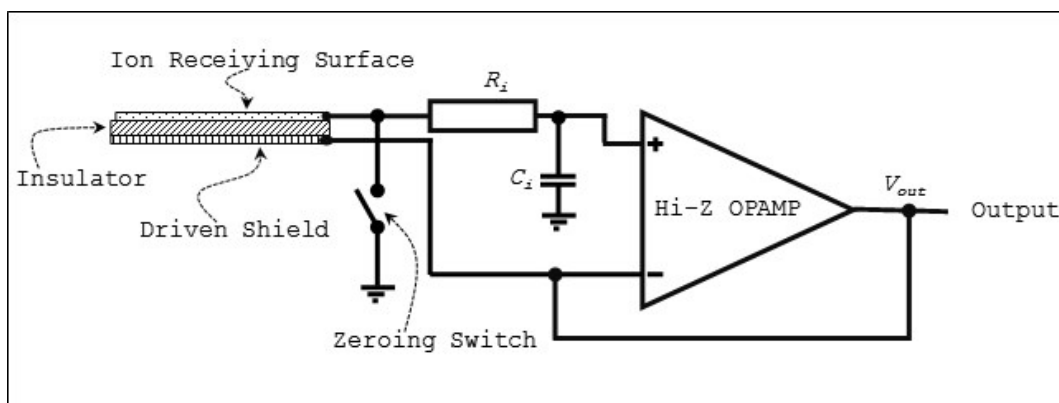


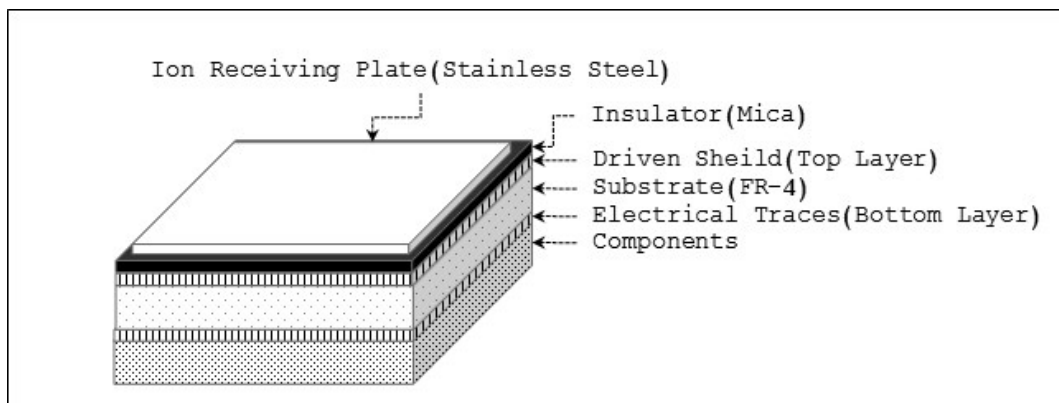Figure 2: The electrostatic potential measurement using the charge induced meter concept.



Figure 3: The multi-layer stacking of ion balance sensor module.
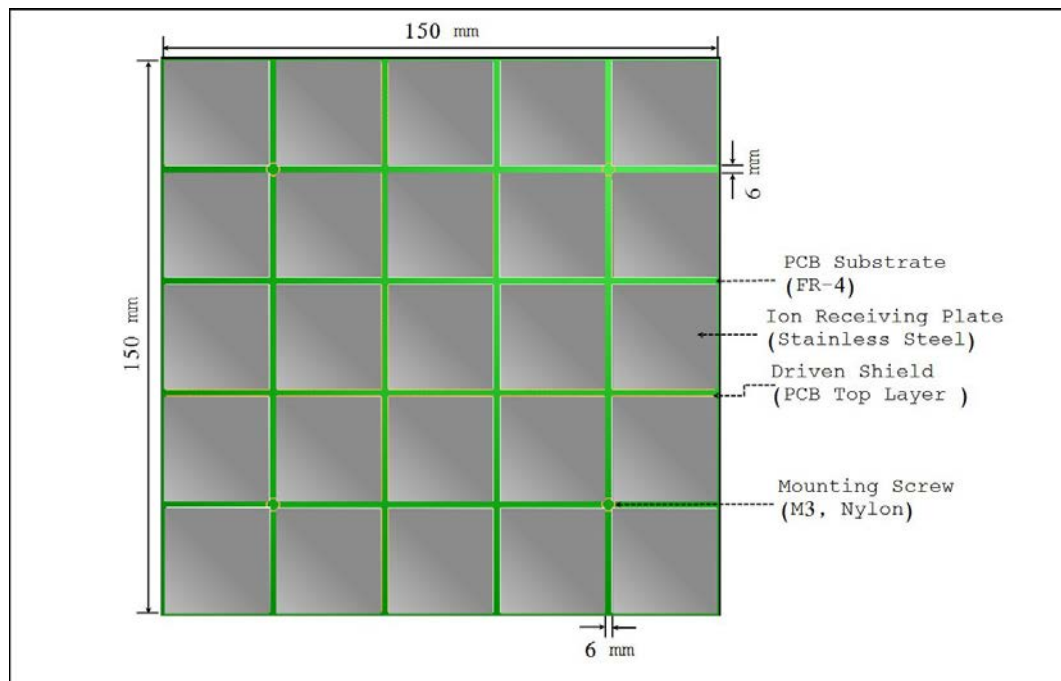
Figure 4: Schematic top view of the multi-plate ion balance sensor, composed by tiling sensors shown in Figure 3.
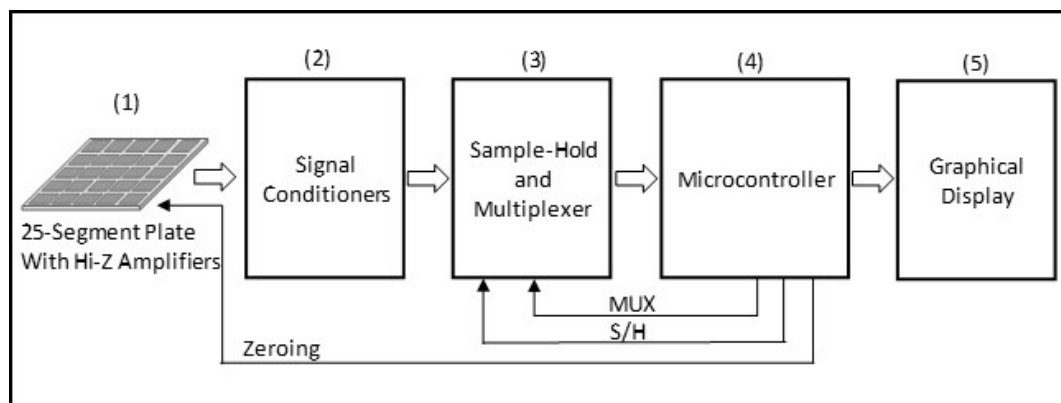


Figure 5: Block diagram of signal processing in the multi-plate ion balance analyzer.
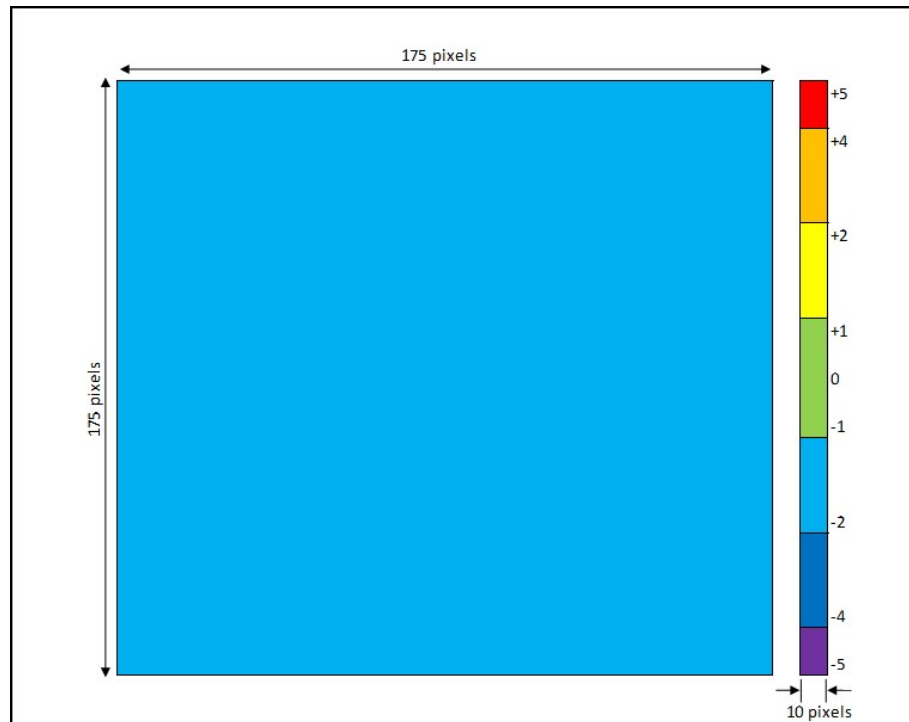
Figure 6: The ion balance on the 6″ ×6″ charged plate is graphically visualized as a heat map, here showing uniform charge level.
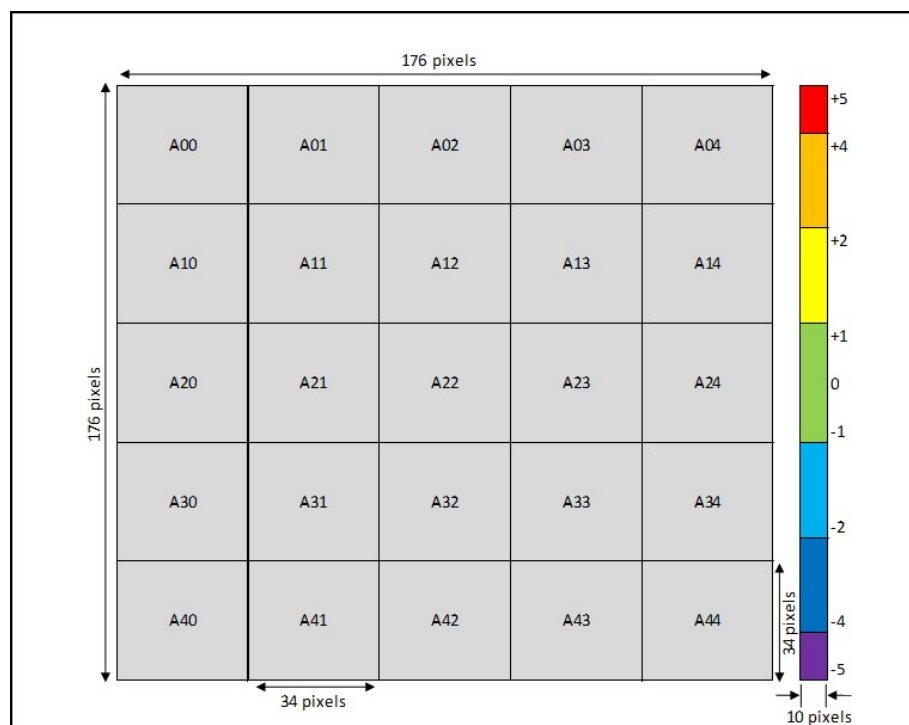


Figure 7: Details of how the graphics representing the 5×5 plate segments were rendered on-screen to the user of the prototype.
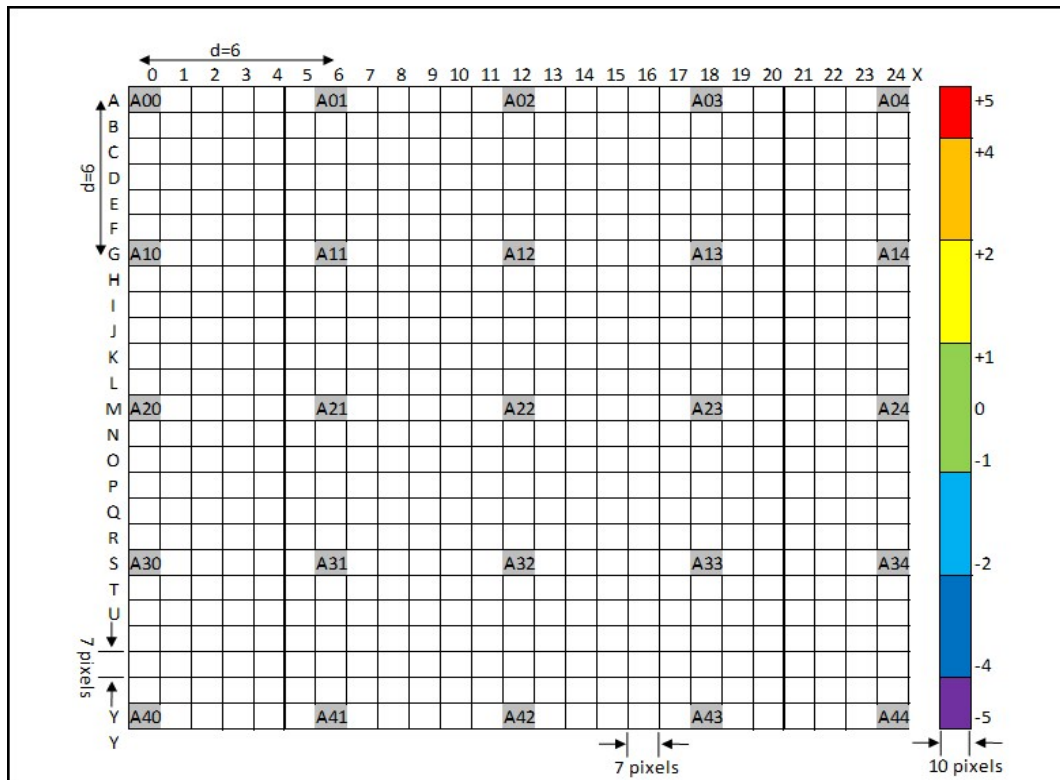
Figure 8: The measured values were placed on a grid like shown by the grey cells, and the estimates for the blank cells were interpolated as detailed in the text.
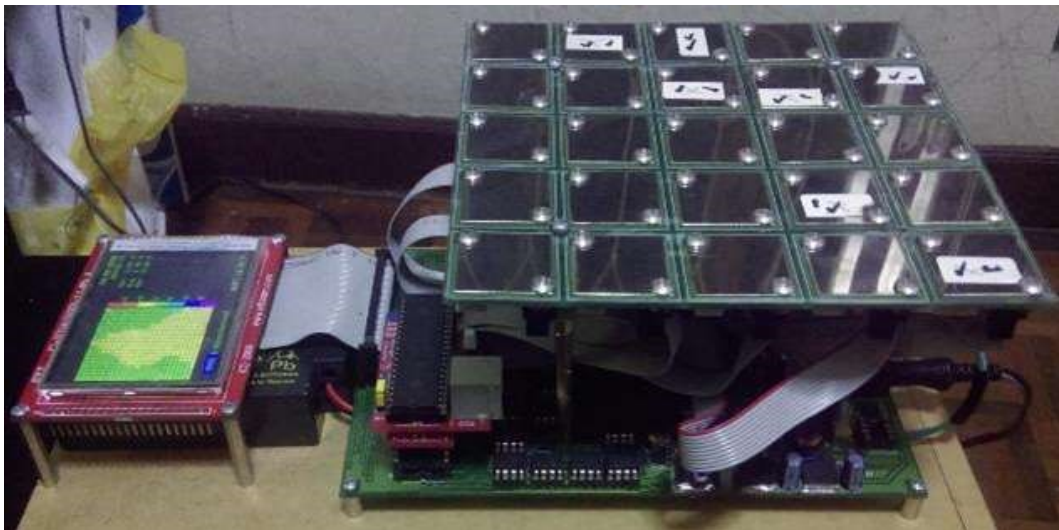


Figure 9: Photo of the laboratory prototype used in this proof-of-concept study of a multi-plate ion balance analyzer.
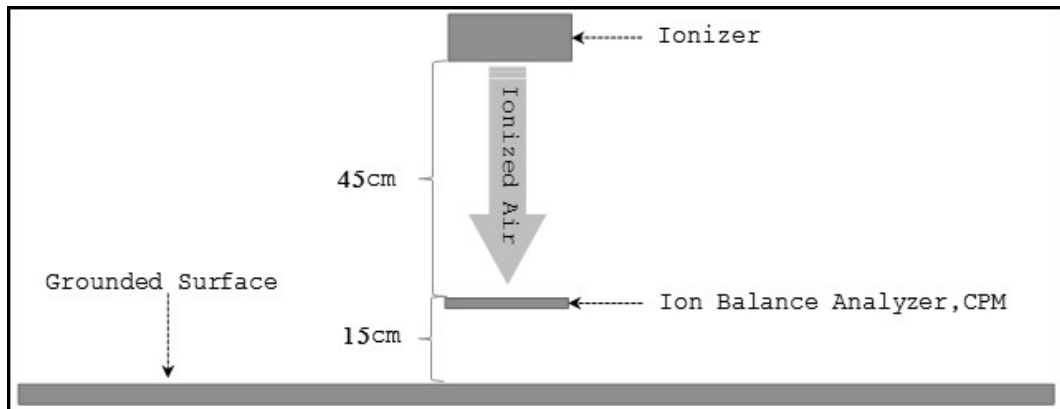
Figure 10: Display of average charge when prototype is used to simulate the conventional single plate measurement.
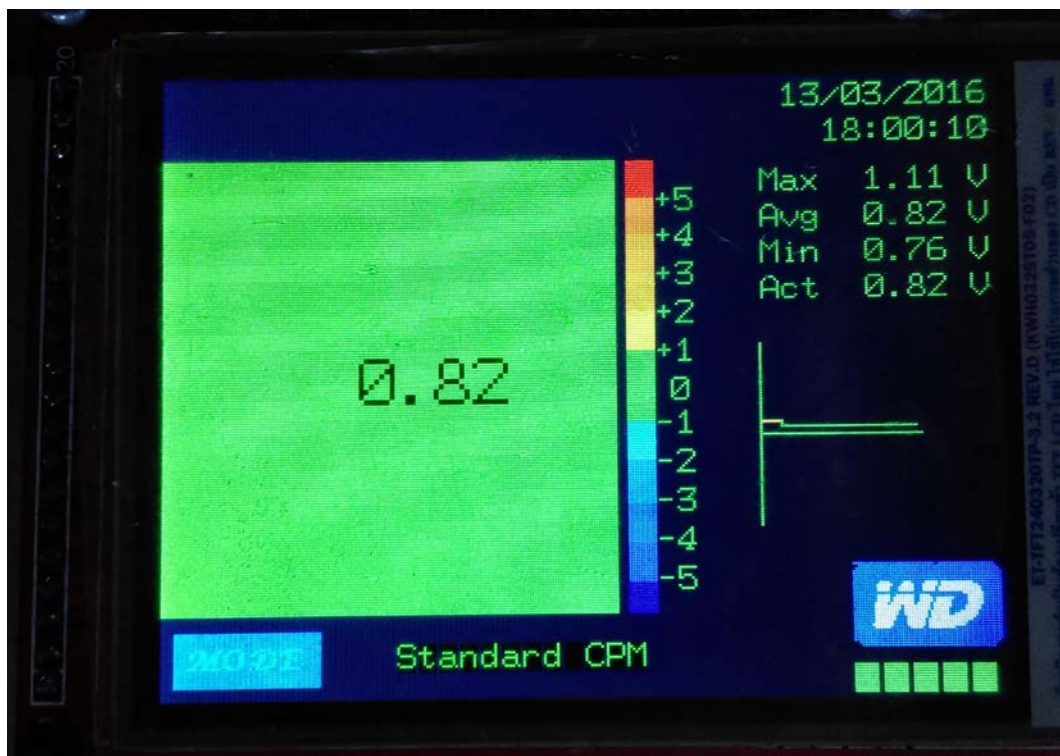


Figure 11: Display of average charge when prototype is used to simulate the conventional single plate measurement.
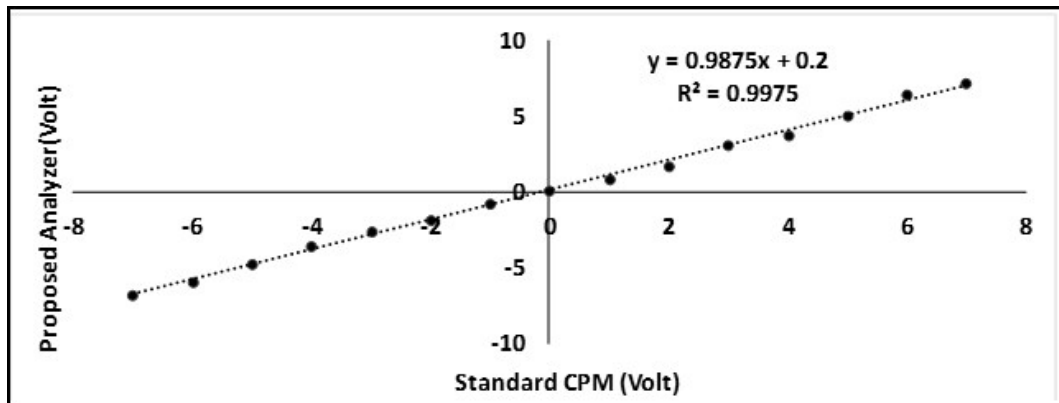
Figure 12: The correlation between the prototype analyzer (average over plate segments) and the standard charged plate monitor (CPM ) used as a reference measurement.
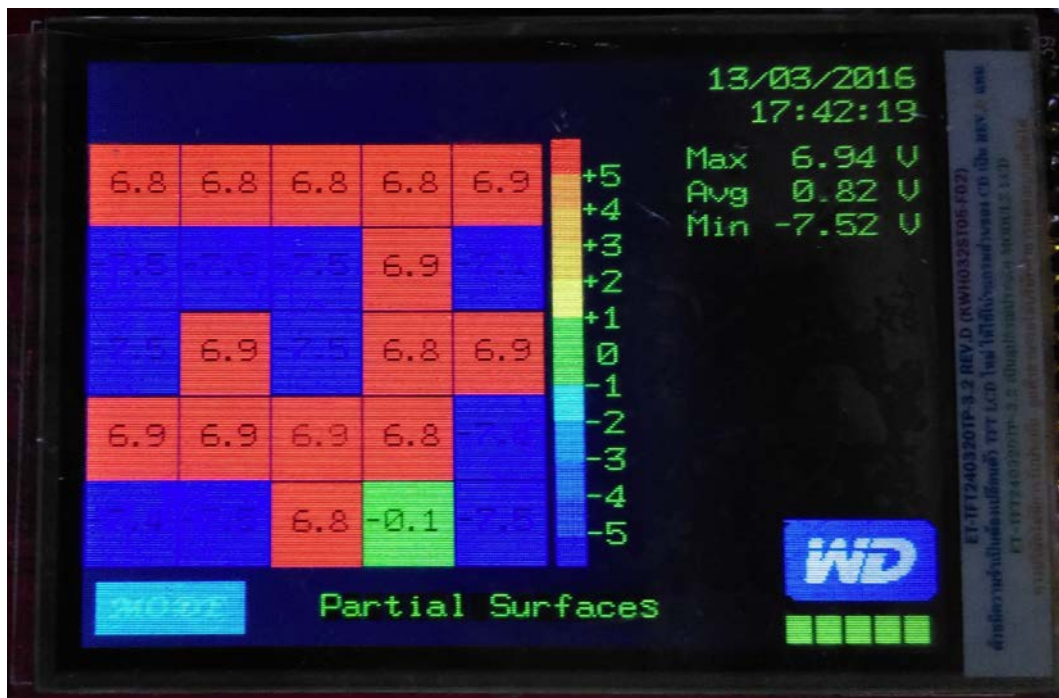


Figure 13: The ion balance showed large non-uniformity when viewed at the resolution of the segmented sensor plate.
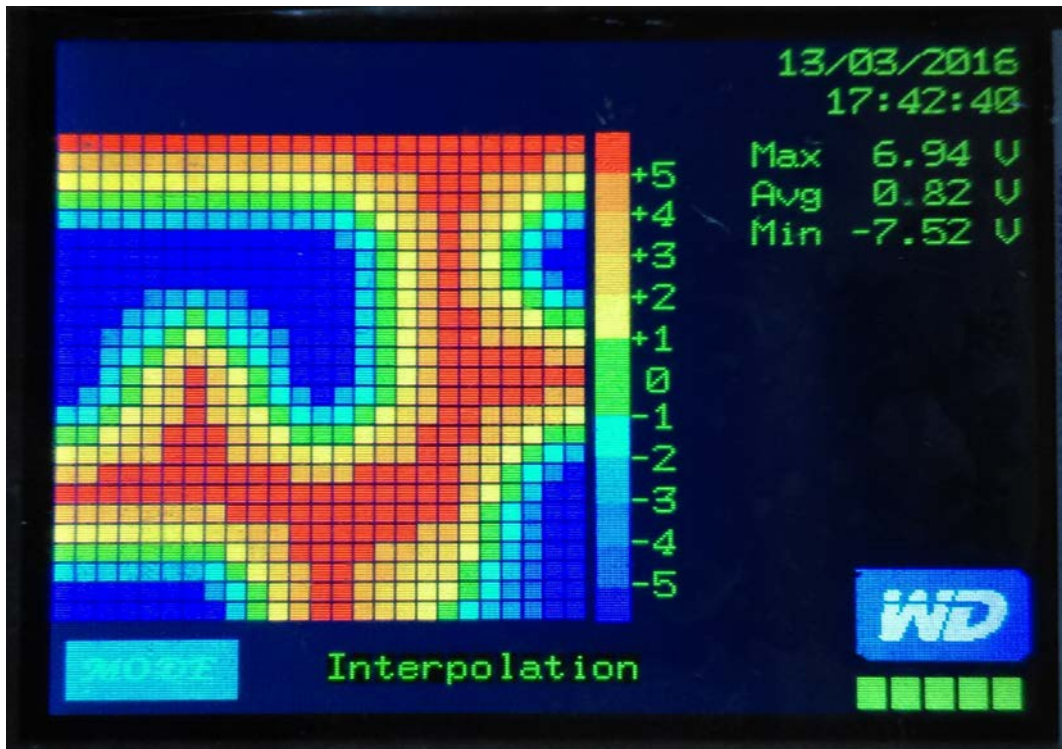
Figure 14: The previous coarse heat map of Figure 13 after refining by interpolation.

# VITAE

**Name**           Mr. Sayan Plong-ngooluam

**Student ID**      5610130008

**Educational Attainment**

| Degree | Name of Institution | Year of Graduation |
|---|---|---|
| Bachelor of Industrial Technology (Power Electronics Technology) | KMUT North Bangkok | 1999 |
| Master of Engineering (Hard Disk Drive Engineering) | Khon Kaen University | 2011 |

**Scholarship Awards during Enrolment**

**Work – Position and Address**

Principal Engineer, Technical Support Engineering Department, Western Digital (Thailand) CO., LTD., Bang Pa-in, Phra Nakhon Si Ayutthaya, 13160, Thailand.

**List of Publication and Proceeding**
**International Journals**

S. Plong-Ngooluam, N. Jindapetch, P. Wounchoum, and D. Sompongse, "A Proof-of-concept Study Demonstrating a Multi-Plate Ion Balance Analyzer," *Sensors and Actuators A: Physical*, vol. 257, pp. 118-124, 2017.

S. Plong-Ngooluam, N. Jindapetch, P. Wounchoum, and D. Sompongse, "A Finite Element Analysis of Multiple Ion Receiving Plates for Ionizer Balance Monitoring," *Journal of Electrostatics*, vol. 86, pp. 50-58, 2017.

S. Plong-Ngooluam, N. Jindapetch, P. Wounchoum, and D. Sompongse, "Partial Measurement of Planar Surface Ion Balance Analysis," *Pertanika Journal of Science and Technology*, 2017, to be published (Accepted).

Sayan Plong-ngooluam, Nattha Jindapetch, Phairote Wounchoum, Duangporn Sompongse, "A Feasibility Study of Ion Balance Measurement by Partial Surfaces," *Procedia Computer Science*, vol. 86, pp.164-167, 2016.

S. Plong-Ngooluam, N. Jindapetch, P. Wounchoum, and D. Sompongse, "3-D Computational Simulations of Electrostatic Potential in Partial Surfaces towards the Precision of Ion Balance Analysis," *Applied Mechanics and Materials,* vol. 781, pp.308-311, 2015.

**International Conferences**
S. Plong-ngooluam, N. Jindapetch, P. Wounchoum and D. Sompongse, "Partial Measurement of Planar Surface Ion Balance Analysis," *ICEETech 2016*, Univeriti Putra Malaysia, Putra Jaya, Malaysia, August 2016.

S. Plong-ngooluam, N. Jindapetch, P. Wounchoum and D. Sompongse, "A Feasibility Study of Ion Balance Measurement by Partial Surfaces*,"* *iEECON 2016*, Chiang Mai, Thailand, March 2016.

S. Plong-ngooluam, N. Jindapetch, P. Wounchoum and D. Sompongse, "3-D Computational Simulations of Electrostatic Potential in Partial Surfaces towards the Precision of Ion Balance Analysis," *iEECON 2015*, Phuket, Thailand, March 2015.

**National Conference**
การพัฒนาหน่วยวิเคราะห์ความสมดุลย์ของอิออนบนพื้นผิวย่อย, งานประชุมทางวิชาการโครงการพัฒนานักวิจัยและงานวิจัยเพื่ออุตสาหกรรม ครั้งที่ 1.– RRI Congress 2015, ศูนย์นิทรรศการและการประชุมไบเทค วันที่ 22 กรกฎาคม พ.ศ. 2558

**Book Chapter**
Nattha JINDAPETCH, Kittikhun THONGPULL, Sayan PLONG-NGOOLUAM and Pornchai RAKPONGSIRI, "ELECTROSTATIC DISCHARGE INSPECTION TECHNOLOGIES," *Visual Inspection Technology in Hard Disc Drive Industry,* Pasisarn Muneesawang and Suchart Yammen (Eds.), pp. 199 - 221, John Wiley & Sons Inc., April 2015.